Technical Report

Adelaide Coastal Waters Study

Stage 2 *Research Program 2003 - 2005*

Technical Report No. 8   July 2005

Physical oceanographic studies of Adelaide coastal waters using high resolution modeling, in-situ observations and satellite techniques

Sub Task 4 - Draft Final Technical Report

Physical oceanographic studies of Adelaide coastal waters using high resolution modeling, in-situ observations and satellite techniques

Sub Task 4 - Draft Final Technical Report

Authors

Charitha Pattiaratchi and Rhys Jones

Centre for Water Research
University of Western Australia
Nedlands,
Western Australia, 6907

Disclaimer

This report has been prepared by consultants for the Environment Protection Authority (EPA) and the views expressed do not necessarily reflect those of the EPA. The EPA cannot guarantee the accuracy of the report, and does not accept liability for any loss or damage incurred as a result of relying on its accuracy.

Reference

This report can be cited as:

Pattiaratchi C. and R. Jones (2005). *"Physical and oceanographic studies of Adelaide coastal waters using high resolution modeling, in-situ observations and satellite techniques – PPM 2 Sub Task 4 Draft Final Technical Report".* ACWS Technical Report No. 8 prepared for the Adelaide Coastal Waters Study Steering Committee. Centre for Water Research, University of Western Australia, Nedlands WA 6907. July 2005.

Acknowledgement

Executive Summary

Along the Adelaide coastal waters, freshwater discharges from rivers and storm water occur directly onto the nearshore zone. Observations of discoloured water trapped within the nearshore have been reported through aerial photographs and visual observations. However, few quantitative measurements of the dispersion characteristics, which control the alongshore and cross-shore transport of these discharges, have been undertaken globally and none from the Adelaide region. A field study using surf zone drifters developed by the Centre for Water Research, The University of Western Australia, was undertaken to determine the dispersion characteristics of the Adelaide coastal waters. In addition, as the nearshore waves are mainly wind driven, field measurements of directional waves along the Adelaide coastal waters were also undertaken.

The directional wave data results indicated that offshore Brighton Beach during the measurement period (3 September 2004 to 16 October 2004), the mean and maximum wave heights were 0.5 m and 1.7 m, respectively, and the wave period ranged from 3 to 12 seconds. Here, the lower periods coincided with storm events while the longer periods were associated with 'calm' periods when swell was dominant. The wave direction indicated that the predominant wave direction, both swell and locally generated waves, was from the southwest, between 230° and 250°. It also indicated that only southwesterly wind had an influence on the generation of storm waves.

The drifters were deployed on Henley Beach, near the Torrens River outflow, under contrasting seasonal conditions between 1 and 3 September 2004 and from 20 to 23 March 2005. Data obtained from these deployments were used to estimate the apparent dispersion coefficient K as well as the cross-shore and longshore dispersion coefficients K_x and K_y, respectively. During the September deployments, under low-energy conditions, the apparent dispersion coefficient was estimated as K = 0.11 m²s^{-1} within a 95% confidence interval of ±0.08 m²s^{-1}, and the March experiments yielded values of K = 0.12±0.07 m²s^{-1}.

Dispersion coefficients were also calculated for 1 m averaged bins of standard deviation, allowing the analysis of the dispersion's scale dependence. Dispersion rates were found to correlate strongly with the 4/3 power law and were compared to the results of Okubo (1974), where an offset, of an order of magnitude, was noted. This was attributed to the effects of increased shear dispersion close to the coast, as noted by List et al. (1990).

The lower values of dispersion coefficients, in comparison with other studies (mainly from offshore regions), indicated that dispersion in the nearshore zone along the Adelaide coastal waters was restricted due to a combination of low-energy conditions and the surf zone and shoreline bounding effects. This resulted in discharges through rivers and storm water drains being trapped and confined to a narrow zone of relatively low cross-shore horizontal mixing close to the shore, as observed in aerial photographs.

CONTENTS

LIST OF FIGURES

LIST OF TABLES

1 Introduction

1.1 Adelaide Coastal Waters Study

This report forms subtask 4 of the project 'PPM2: Physical oceanographic studies of Adelaide coastal waters using high-resolution modeling, in-situ observations and satellite techniques of the Adelaide Coastal Waters Study (ACWS)'. ACWS was designed to investigate the factors affecting the Adelaide coastal region, in particular, the anthropogenic or natural processes that may have resulted in seagrass loss along the Adelaide coastal waters (CSIRO, 2004a). The study area is defined as the offshore region (extending up to 20 km from the shoreline) between Port Gawler and Sellicks Beach area. The key objective of the ACWS is 'to develop knowledge and tools to enable sustainable management of Adelaide's coastal waters by identifying causes of ecosystem modifications and quantifying the actions required to halt and reverse the degradation' (CSIRO, 2004b). The areas of specific focus and research include:

1) The quantification of contaminant inputs from point sources such as stormwater drains and river outflows, submarine groundwater discharges and inputs from atmospheric sources.

2) The assessment of the impact of these inputs on seagrass ecosystems and other key biota within Adelaide's coastal waters. This is a key motivation for the study of mixing and dispersion within the ACWS as the impact of coastal discharges on the predominantly offshore seagrass beds is dependent on the efficiency of transport and dispersive mechanisms.

3) Monitoring of marine and coastal features using remote sensing technology and the interpretation of changes since the 1940s in response to natural and anthropological stimuli. This will focus specifically on changes in the extent of seagrass beds and morphological variations resulting from sediment supply fluctuations.

4) A complete sediment transport budget will be developed addressing the sources, sinks, and fate of sediments in the coastal littoral zone.

5) Oceanographic studies of currents within the Gulf of St Vincent using modeling, in-situ observations, and satellite imagery. Specifically, this research area addresses coastal and seafloor morphology along with contaminant transport.

6) The development of a cost-effective environmental monitoring strategy, addressing all of the key research areas for implementation and integration with existing monitoring programs.

Along the Adelaide coastal waters, freshwater discharges from rivers and storm water occur directly onto the nearshore zone. Observations of discoloured water trapped within the nearshore have been reported through aerial photographs and visual observations. Based on these factors, the aim of sub task 4 of the ACWS was to '*determine the influences of near-shore regions on coastal hydrodynamics and the implications for the study's modeling and monitoring requirements*'. This was undertaken by performing field studies of nearshore mixing and dispersion within the ACWS region. Only a few quantitative measurements of nearshore dispersion characteristics control the alongshore and cross-shore transport of discharges directly onto the nearshore zone globally and none from the ACWS region. A field study using surf zone drifters developed by the Centre for Water Research, The University of Western Australia, was undertaken to determine the dispersion characteristics

of the Adelaide coastal waters (Johnson, 2003a). In addition, as the nearshore waves are mainly wind driven, field measurements of directional waves along the Adelaide coastal waters were also undertaken.

1.1.1   Motivation for Current Study

The primary motivation for the assessment of mixing and dispersion rates within the study area was to allow the quantification of transport and dilution of land based outflows into the study region. Coastal waters have multiple freshwater sources including river runoff, submarine groundwater discharge, wastewater discharge, and the atmosphere; however, in terms of volume, the flow of rivers, which includes storm water runoff, is the largest single source (CSIRO, 2004a). The mean average discharges of selected rivers within the ACWS region are collated in Table 1.1 along with their respective catchment areas.

Table 1.1: Mean annual discharge, catchment area, and runoff for selected rivers in the ACWS study area (Storm water data audit, v1.3, Draft, 2004).

	Effective catchment area (km^2)	Mean annual flow (GL)	Catchment Yield (ML/km^2 = mm)
Gawler River to sea[1]	883	10.3	11.7
Smith Creek[2]	205.6	5.2	25.3
Barker Inlet[2]	407.8	10.3	25.3
River Torrens[3]	218.5	22.4	102.6
Patawalonga[3]	212.4	19.7	92.6
Holdfast drains[2]	8.8	2.1	239.1
Field River[1]	36.2	2.8	77.3
Christies Creek[1]	37.8	8.1	214.3
L. Onkaparinga[4]	138.7	9.5	68.5
O. Estuary[2]	28.2	5.6	197.5
Southern Creeks[5]	244.9	2.3	9.5

Table 1.1 shows that the run-off through a given area is not directly dependent on the catchment area, with larger catchments not necessarily resulting in larger catchment yields. The Torrens River represents a catchment area of 218.5 km² below the Kangaroo Creek reservoir and has the highest mean annual flow of 22.4 GL. This is more than double that of the Gawler River (10.3GL), which has an effective catchment area of 883 km²—~4 times larger. This discrepancy arises from the nature of the catchment. Whereas the Gawler catchment is largely rural, the Torrens catchment is highly urbanised. Within these urbanised areas, runoff is enhanced because of the existence of extensive and efficient drainage systems as well as large areas of sealed surfaces, such as roads and rooftops, into which water is not able to percolate (Steffensen, 1985). In addition, the time between rain falling and increases in discharges being observed is longer within rural catchments as the water does not drain as efficiently; the consequence of this is that the discharge observed within urban catchments increases rapidly following rainfall, hence inputting a large volume of water within a short period of time. This rapid inflow has the capacity to alter significantly local seawater salinity levels as well as transport large contaminant loads (Steffensen, 1985). In particular, the re-routing of the Torrens River outflow to the coastline through Breakout Creek has created a significant new discharge site where previously no low salinity water had been entering the system.

The water that enters the coastal environment, from these discharges as well as from wastewater treatment facilities and submarine groundwater discharge, has been found to contain many contaminants. These contaminants include nutrients such as nitrogen and phosphorus as well as inorganic substances, suspended sediments and heavy metals, such as lead, copper, cadmium, zinc, and iron (Steffensen, 1985; Stormwater Data Audit, 2004). Furthermore, samples obtained from rivers within the metropolitan region since 1978 have been found to contain the herbicides Lindane, Dachtal, Simazine, and Atrazine as well as the insecticide Dieldrin.

Seagrass beds are an important part of the marine ecosystem within the Gulf of St Vincent and have been declining rapidly in area since the 1940s with a shift in species composition towards algal seaweed such as *Giffordia*, a known indicator of water quality decline (CSIRO, 2004). The biological impact of the various contaminants present in coastal discharges is not well understood and is a major focus of the ACWS. By measuring the dominant oceanographic processes, including dispersion, within the Adelaide coastal region, it is possible to quantify the transport of nearshore waters into the offshore region, the seagrass habitat, and hence determine whether coastal discharges and associated contaminants are a possible cause of seagrass decline.

2   Literature Review

1.2 Study Area

2.1.1 Geographical and Historical Overview

Adelaide is located on the west coast of the Gulf of St Vincent. The Gulf is a semi-enclosed water body approximately 170 km in length, from 34°S to 35°30'S, by 60 km in width at its maximum dimensions. It is relatively shallow, with maximum depths rarely exceeding 40 m (South Australian Coastal Protection Board SACPB[a], 1993).
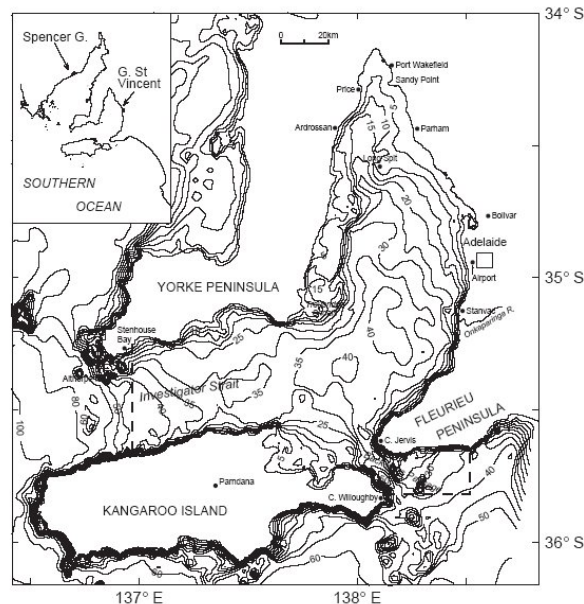
Figure 2.1: Bathymetry of the Gulf of St Vincent, South Australia (de Silva Samarasinghea et al., 2003).

At the time of European settlement the metropolitan coastline was dominated by a continuous sand dune ridge sequence that extended from Seacliff in the south to Outer Harbor. This dune system's width averaged between 200 and 300 m in the southern region between Seacliff and Largs and was largely continuous, interrupted only by the Patawalonga River at Glenelg. In the north, the nature of the dune system changed and was characterised by two or three parallel dune faces each measuring 70 to 100 m in width and separated by narrow swales (SACPB[a], 1993). These prograded barrier systems were formed during periods in which sand accretion from external sources outweighed comparatively small losses due to longshore transport. Along the metropolitan coastline, the dune system's height averaged between 10 and 12 m above mean sea level (MSL); however, the highest point in the dune system occurred around Brighton, where dunes were recorded to an elevation of 15 m (SACPB[a], 1993).

Since European settlement the nature of the Adelaide coastline has changed dramatically. In addition to the diversion of the Torrens River to Breakout Creek, there has been extensive coastal strip development, particularly during the post-war period 1945 to 1965, to the point where only original dune formation relics remain (SACPB[a], 1993). The stabilising effect of this development has effectively eliminated much of the supply of sand into the nearshore region with the effect of accelerating erosion.

2.1.2 Breakout Creek and Henley Beach

Field studies using surf zone drifters, which were tracked using the satellite-based global positioning system (GPS), were conducted on Henley Beach near Breakout Creek (Figure 2.2)—the Torrens River outflow point into Holdfast Bay. Breakout Creek is an artificial waterway that the South Australian Government constructed in 1937 to divert the course of the Torrens River (SACPB[a], 1993). Prior to the concrete-lined channel and weir construction, the Torrens River drained into a series of wetlands located to the east of the barrier dune system. These wetlands then drained naturally to the north primarily through the Port River system and to the south via the Patawalonga. The Breakout Creek outflow construction was deemed necessary to alleviate the flooding of these wetlands, which regularly isolated the coastal communities of Grange and Henley (SACPB[a], 1993). The effect of this diversion was that the natural process of filtering the river discharge through the wetland system was bypassed, leading to the direct discharge of stormwater and associated contaminants into the marine environment.

Figure 2.2: Aerial view of Breakout Creek noting the weir and the northerly flow of the creek across the beachface (Adelaide Coastal Waters Study, 2004).

The outflow from Breakout Creek is highly seasonal with the majority of outflow occurring during the winter months; 80–95% of annual outflow occurs between June and November compared with 5% between December and February (Steffensen, 1985). It represents the coastal discharge of the largest watercourse within the metropolitan area and drains a significant catchment area. The catchment can be divided into two distinct zones: the upper zone, which covers approximately 400 km² and is mostly covered by natural vegetation, and the lower zone, which is just 80 km², but is heavily urbanised. As much as 70% of the rainfall from this lower zone is directly discharged through the river system (Steffensen, 1985). The Kangaroo Creek Reservoir, constructed in 1969, restricts the flow from the upper section; however, occasional overflows occur, resulting in large volumes of stormwater discharging to the ocean (Steffensen, 1985). The total annual discharge through Breakout Creek displays a high level of variation. The annual outflow during the period 1978 to 1983 ranged between 20,000 ML in 1980 and 83,000 ML in 1981, and the maximum instantaneous discharge rate of 167m³s[-1] was recorded in 1979 (Steffensen, 1985).

Sediment transport along Henley Beach is congruous with its regional setting; longshore sediment transport is predominantly northward and driven by obliquely incident wind conditions. Sediment supply to the north of Breakout Creek is dependent on the level of bypassing of sediment that occurs around the outlet stream. Typically, northerly littoral transport of sand is not interrupted by the Torrens discharge; however, during peak flows sand can accumulate on the river mouth's southern side (Deans and Smith, 1999). The natural bypassing of the river mouth by coastal sediments is assisted by realigning the Torrens outflow path at approximately yearly intervals. This is conducted by trenching across the southern beach face and trucking small volumes of sand to the north of the outlet stream (Deans and Smith, 1999).

2.1.3 Hydrodynamic and Meteorological Setting

The tidal range along the Adelaide coastline is 2.4 m and is taken as the range between the Mean High Water Springs and the Indian Spring Low Water Level (Deans and Smith, 1999). This tidal range can be classed as a mesotidal variation (2 m<2.4 m<4 m); however, this represents the maximum variation over a spring tidal range; as such, the 'normal' tidal range that exists for the cycle majority's is lower than this range and can be classed as microtidal (<2 m). The amplification of tidal ranges within the semi-enclosed Gulf of St Vincent (represented in Figure 2.3) is primarily due to convergence effects.
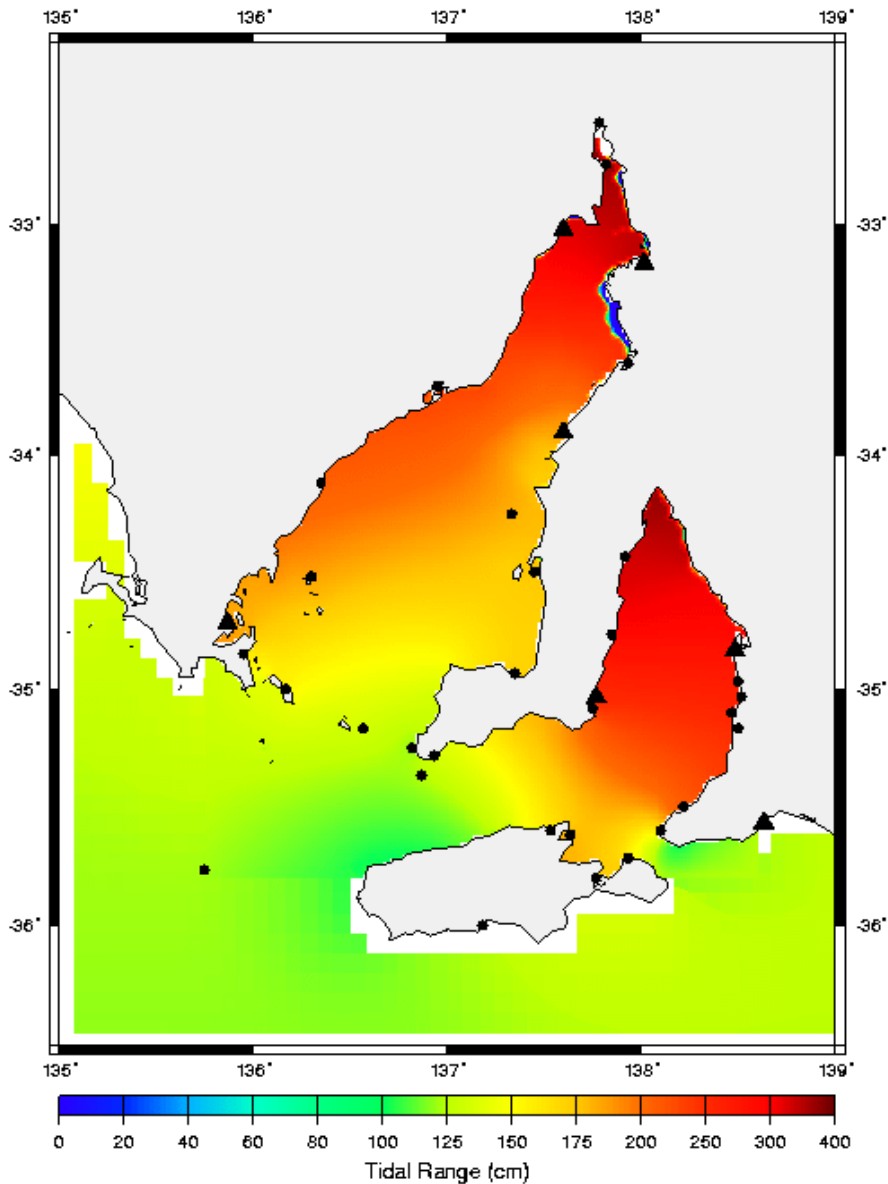
Figure 2.3: Modeled tidal range within the Gulf of St Vincent (right) and the Spencer Gulf (left) showing the amplification of the tidal range within the shallow Gulf areas, isolated from the open ocean (National Tidal Center, 2004).

The tidal regime's form can be determined by calculating the tidal form factor.

$$F = \left(\frac{H_{K_1} + H_{O_1}}{H_{M_2} + H_{S_2}} \right)$$

(1)

When Equation 1 and the values contained in Table 2.1 were used, the value of F for Outer Harbour, and hence the Adelaide metropolitan beaches, was 0.416. This corresponded to a tidal regime of mixed, mainly semidiurnal tides. Within the Gulf of St Vincent, the primary tidal constituents are the principal lunar component M_2 and the principal solar component S_2. These constituents are semidiurnal—meaning they produce only one tide per day—with periods of 12 hours 25 minutes and exactly 12 hours, respectively. As a result of this difference, every 14.77 days they are in opposition and effectively cancel each other

(Grzechnik, 2000). During the periods where the semi diurnal M_2 and S_2 constituents are out of phase by 90 degrees ('neap' tides), tidal fluctuations are driven predominantly by the luni-solar diurnal component K_1 values and the principal lunar diurnal component O_1. As K_1 and O_1 are both diurnal components, it is during these neap periods that the tidal cycle's form changes from semi-diurnal to diurnal, leading to the mixed, mainly semidiurnal tidal classification. At equinoxes, the tide's diurnal components also cancel each other out, producing a period of almost constant water level lasting for several days (Grzechnik, 2000). Matthew Flinders first observed this skipping of the tidal cycle in the Gulf of St Vincent; it was named the 'dodge' tide—a term unique to South Australia.

Table 2.1: Tidal constituent data, Outer Harbor, Gulf of St Vincent. (Adapted from Grzechnik, 2000.)

Tidal Observation Station	Tidal Constituent (amplitudes)			
	O_1 (m)	K_1 (m)	M_2 (m)	S^2 (m)
Outer Harbour	0.17	0.25	0.51	0.51

Wave Climate

The waves generated by local winds are low to medium energy owing to the limited fetch length within the Gulf of St Vincent. However, significant wave energy is able to penetrate into the Gulf from the Southern Ocean (Hemer and Bye, 1999). The Southern Ocean is highly energetic, and the swell produced within it to the southwest of Australia has been recorded as the largest of any in the world's oceans (Chelton et al., 1981; cited in Hemer and Bye, 1999). Provis and Steedman (1985) undertook offshore wave climate monitoring at seven sites between the 1150 m and 75 m depth contours over a period of six months from May to October, 1984. Significant wave heights over 10 m were recorded during a June storm event, in addition to several occurrences of significant wave heights greater than 5 m (Provis and Steedman, 1985; cited in Hemer and Bye, 1999). The significant wave period appeared to be independent of the significant wave height and remained relatively constant during the measurement period at around 15 s. The wave spectra that are created in the Southern Ocean and are incident on the South Australian coastline do not display distinct wind sea and swell peaks except in periods of extremely low swell. The spectra are described as being unimodal and are due to the coastline's close proximity to the swell source not allowing sufficient travel time for the wave field to develop into bimodal spectra (Young and Gorman, 1995).

Hemer and Bye (1999) modeled the wave climate of the semi-enclosed coastal waters of South Australia using the SWAN (Simulating WAves Nearshore) wave model. SWAN is a directional spectral wave model, which incorporates many wave propagation processes including refraction effects due to bottom friction and currents, blocking and opposing by currents, shoaling, and effects due to obstacles. SWAN also accounts for wind generation of wave energy and dissipation effects, which include the dissipation of wave energy due to wind-induced white capping, depth-induced wave breaking, and bottom friction (SWAN, 2004). The major limitation of the SWAN model is it does not consider diffraction effects, which means it is not suitable for locations in which the change in wave height is significant over a short length scale relative to the wavelength (SWAN, 2004). In the version of SWAN utilised by Hemer and Bye (1999), reflection effects around obstacles were not accounted for, making SWAN unsuitable for steep beach face environments; however, these reflection effects were included in subsequent SWAN versions. Hemer and Bye (1999) compared the results obtained from SWAN with those obtained from other models—the Bureau of Meteorology Southern Ocean Wave Model, WAM—as well as physical measurements.

Following this comparison, they were able to conclude that the SWAN and WAM models could be successfully linked to provide reliable swell prediction formulae for the sheltered areas of South Australia's coastline.

Results obtained from running the SWAN model suggested that the direction of swell propagation from the Southern Ocean was critical in determining the extent of intrusion into the Gulf of St Vincent. Kangaroo Island is located in the mouth of the Gulf of St Vincent, which is connected to the Southern Ocean to the north by Investigator Strait, and to the south via Backstairs Passage (Figure 2.1). The island provides a significant level of blockage to the wave energy propagating towards the Gulf, and large wave heights are commonly observed off its coast. Most of the wave energy that enters the Gulf comes from a south westerly bearing (~230°), which allows largely unimpeded passage through Investigator Strait. As the water depth decreases, the waves refract and 'wrap' into the strait, becoming more perpendicular to the depth contours (Hemer and Bye, 1999). Despite substantial refraction occurring within the Investigator Straight—to the extent that the direction of propagation changes by a complete 180° on the north shore of Kangaroo Island—the dominant direction of wave propagation into the Gulf is northerly. However, a significant level of spreading does occur, dissipating the wave energy over a larger area.

Hemer and Bye (1999) developed an equation to predict the wave energy at various locations within the coastal seas of South Australia, including the Gulf of St Vincent and the Spencer Gulf:

$$NWH = a_4 D_0^4 + a_3 D_0^3 + a_2 D_0^2 + a_1 D_0 + a_0 \tag{2}$$

The constants a_{0-4} values are dependent on the location under analysis; the value of D_0 represents the direction from which the incident waves are propagating. The normalised wave height returned is a function of the wave height (H) at the location being analysed divided by the offshore wave height (H_0). By finding the normalised wave height rather than the absolute wave height, Equation 2 remains valid for any offshore wave height. The coefficients a_0 to a_4 values are shown in Table 2.2 for a location offshore from Adelaide in a water depth of approximately 10 m. The wave heights calculated using Equation 1, and an offshore wave height of 3.5 m over a variety of incident wave directions, are shown in Table 2.3.

Table 2.2: The coefficients of equation 4 derived by Hemer and Bye (1999).

	a_4 $(x10^{-9})$	a_3 $(x10^{-6})$	a_2 $(x10^{-3})$	a_1 $(x10^{-1})$	a_0
Coefficients	5.8435	-4.8575	1.4918	-1.9994	9.9339

Table 2.3: Wave heights calculated in 10 m water depth offshore from Adelaide using Equation 5 and the coefficient values in Table 2.2.

	Wave Propagation Direction		
	230°	260°	160°
Wave Height (m)	0.59	0.63	0.34

This data shows a substantial decline in the onshore wave height for all propagation directions as well as a significant variation between propagation directions. This is illustrated by the fact that the predicted swell was twice as large at the specified site if the direction of approach was from the southwest through Investigator Strait than if the direction of approach was from the southeast and was largely blocked by Kangaroo Island (Hemer and Bye, 1999).

Modeled Wave Conditions

Nearshore wave modeling of the Gulf of St Vincent has recently been conducted using SWAN as part of Adelaide Coastal Waters Study Task 2. The results from this work allowed the derivation of the mean wave conditions over the entire year, based on data recorded during 2003, as well as the calculation of mean conditions for the months in which drifters were deployed.

Figure 2.7 represents the mean wave conditions over the entire year. It is evident the primary source of wave energy propagation into the Gulf was through the Investigator Strait. The wave energy propagated in an easterly direction into the Gulf, diminishing in height relative to the distance of propagation. The areas of greatest sheltering were located in the lee of Kangaroo Island and at the Gulf's head, approximately 160 km north of opening. Significant levels of wave energy were incident upon the Gulf's western coast; however, the level of intensity decreased in the northerly direction, resulting in relatively limited conditions occurring offshore from Adelaide. At the study site, wave conditions were further reduced through the dissipation in wave energy experienced as the swell moved into shallower water close to the coast. As such, the mean wave height incident upon the study site over the duration of the year was less then 0.5 m.

The seasonal variation in the prevailing wave conditions was significant and is represented in Figure 2.8. During September (Inset A), the level of wave energy propagation into the Gulf was large because of the higher energy wave conditions in the Southern Ocean, which are experienced through the winter and early spring owing to the passage of high-energy storm fronts through a subtropical ridge of high pressure located to the south of Australia (Petrusevics, 2004). In contrast, the amount of swell energy present in the Gulf during March was relatively low, as during the summer months, the subtropical high pressure ridge that contains the storms responsible for the high-energy conditions during winter moves farther southwards (Petrusevics, 2004). The same general propagation characteristics within the Gulf apply throughout the year; however, the key input parameter—the incident wave energy through the Gulf of St Vincent—heavily influences the extent and magnitude of the wave energy propagation. During September, the average wave height at the study site was observed to be of the order of 0.8–1 m; during March, it was significantly less than 0.5 m. The directional components varied significantly, with westerly waves dominating the study site during winter and southwesterly waves dominating during summer. This directional variability can be attributed in part to the prevailing wind conditions, which vary between seasons and are incorporated in the SWAN model.
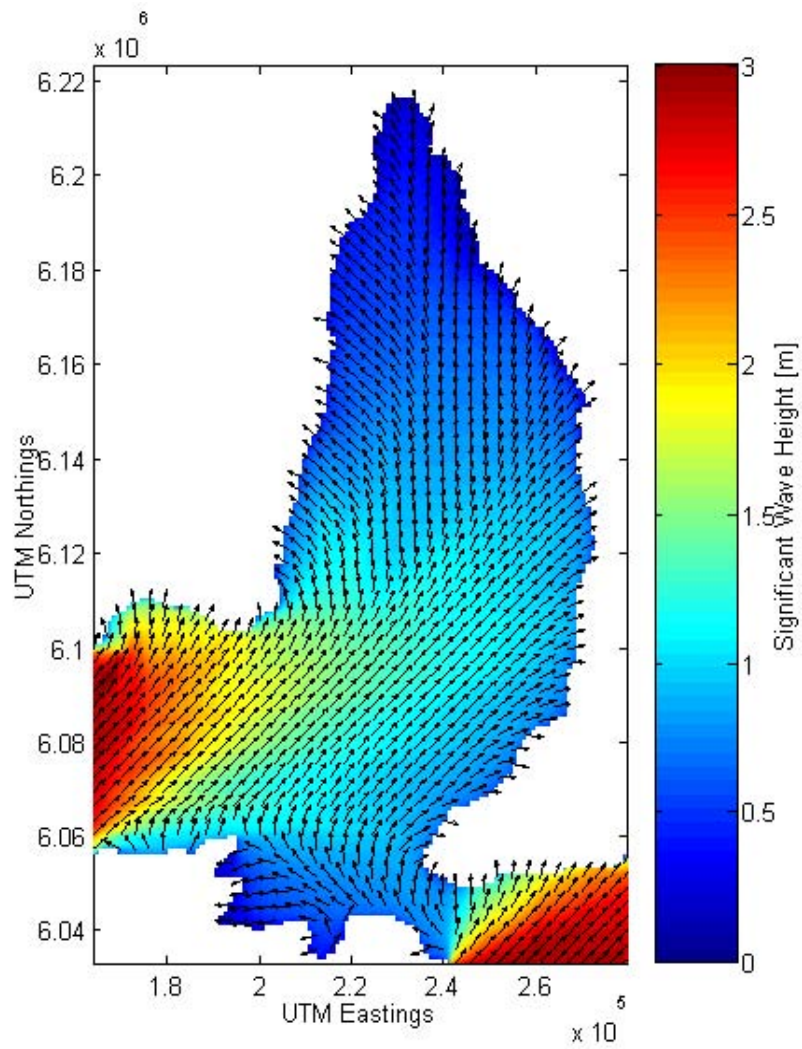
Figure 2.4: Mean swell conditions in the Gulf of St Vincent over the entire year, calculated using SWAN wave modeling software.
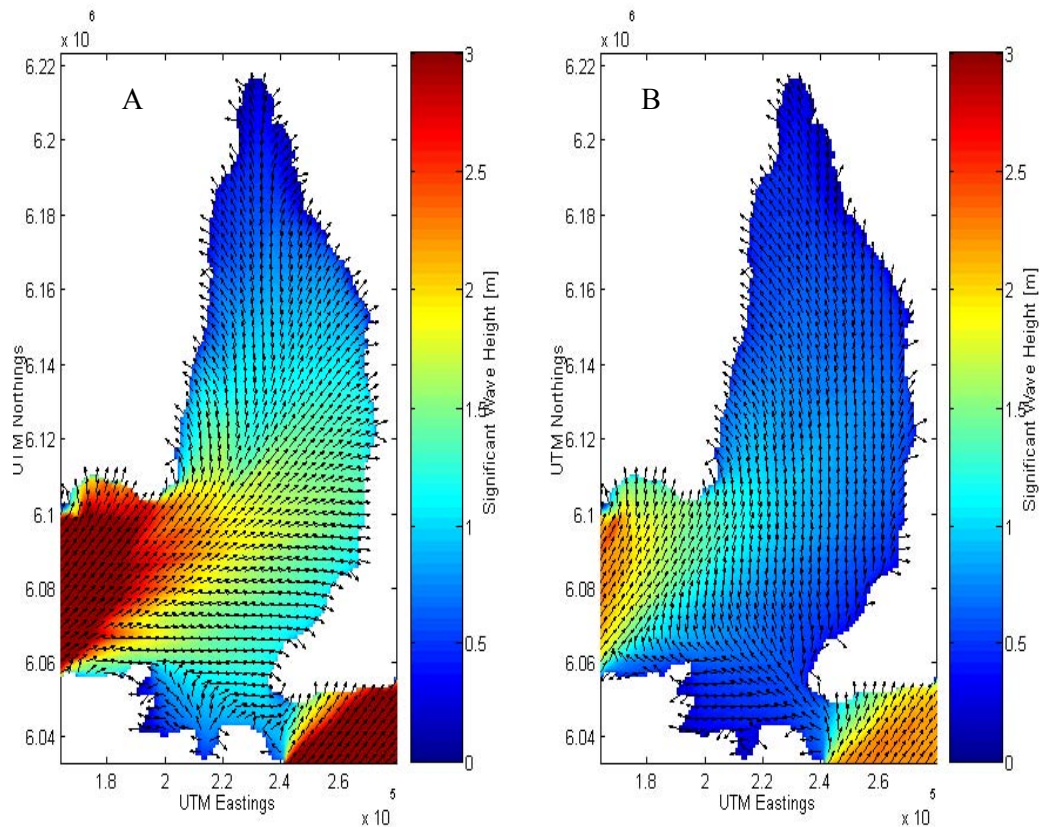
Figure 2.5: Mean wave conditions for the Gulf of St Vincent for September (A) and March (B) calculated using SWAN.

Winds

The Adelaide metropolitan coastline is influenced by a full spectrum of wind directions throughout the year, which are represented in Figure 2.9. This figure also displays the relative distribution of the incident wind bearings and velocities, thus demonstrating the prevalence of southwesterly conditions (between 180° and 270°), which make up over 40% of the total readings over four years. Due to the Adelaide coastline's westerly facing aspect along a north-south axis, winds with a component of westerly direction have the greatest impact on coastal processes through the generation of waves that are incident upon the shoreline. In particular, the angle of incidence upon the shoreline of waves generated through the prevailing southwesterly conditions correlates with the optimal conditions for the promotion of a longshore current system, which in turn stimulates northward sediment transport. The likely influence of these conditions was further demonstrated through analysis of the high wind occurrences, which revealed that 74.3% of wind speeds greater than 10.8 m/s were recorded between the westerly and southerly bearings.

Seasonal variation was also significant with northeasterly conditions prevailing during the winter months of June through to August compared to the dominant south-southwesterly winds throughout the majority of the year. In contrast to the prevailing conditions throughout the rest of the year, almost 40% of recordings obtained during the winter months were between northerly and easterly bearings (Figure 2.10). Northerly and easterly winds have little impact on the Adelaide metropolitan coastline, as they blow cross shore and offshore, respectively, and hence do not create waves that are incident upon the beaches on the Gulf of St Vincent's eastern shore. During summer, the wind regime is dominated by

southwesterly to southeasterly winds. These conditions are a result of the interactions between local and continental scale meteorological conditions, which will be explained below.
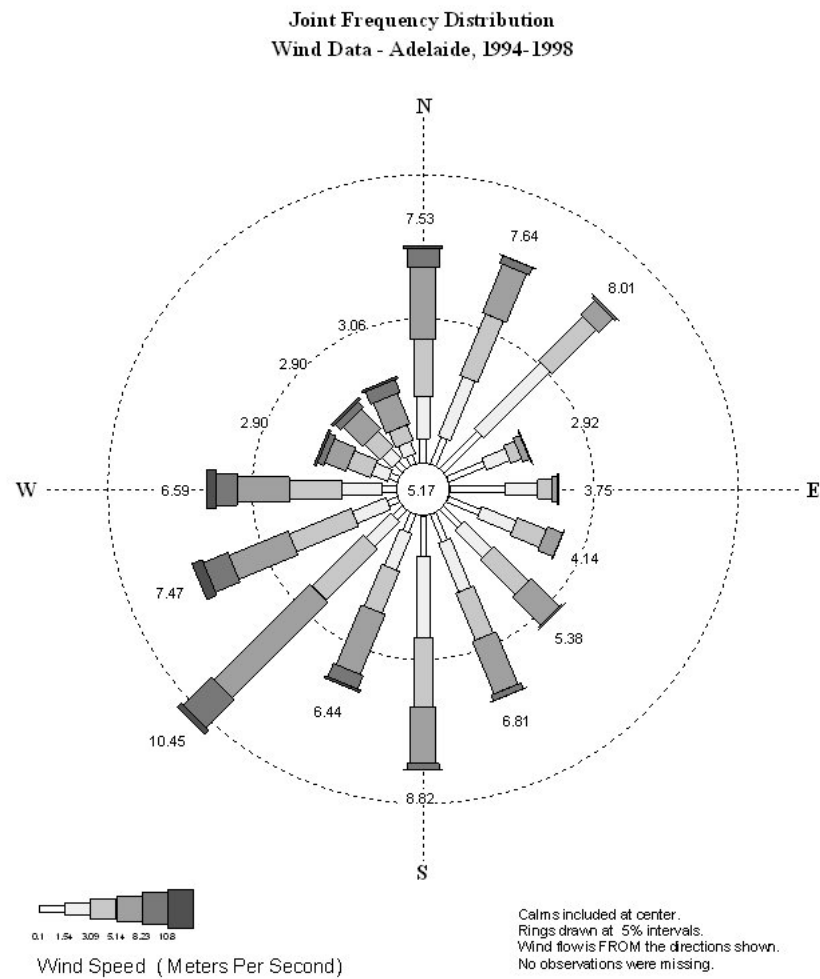
Figure 2.6: Wind rose of half-hourly measurements from Adelaide airport showing prevailing southwesterly conditions over the period 1994 to 1998 (Data courtesy of the Bureau of Meteorology).
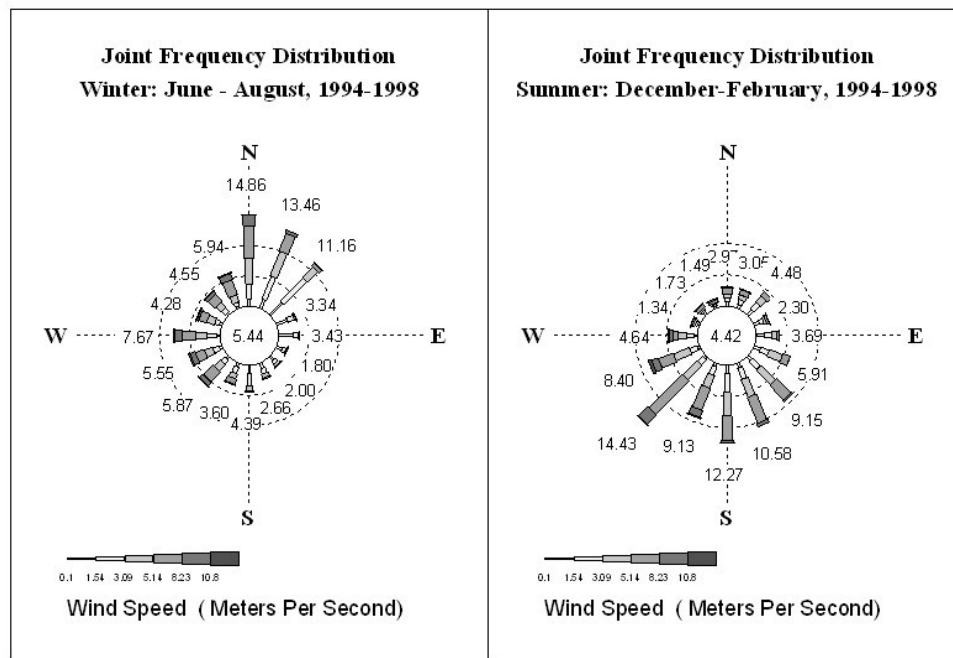
Figure 2.7: Comparative wind roses of summer and winter conditions 1994 to 1998 (Data courtesy of the Bureau of Meteorology).

The Sea Breeze

The sea breeze is a meso-scale meteorological feature that recurs on a relatively constant diurnal cycle along approximately two-thirds of the world's coastlines, particularly in tropical and sub-tropical areas (Pattiaratchi et al., 1997). Sea breeze activity is characterised by an onshore directed wind that typically gains in strength throughout the day, reaching a maximum in the late afternoon, and subsequently dissipates or even reverses direction, creating a 'land breeze' overnight (Abbs and Physick, 1992; cited in Pattiaratchi et al., 1997). The sea breeze arises because of the differences in the thermal conductivity of the land and the sea, respectively (Masselink and Pattiaratchi, 1997). Land has a relatively low thermal conductivity and heats and cools more rapidly than the ocean. As such, during the day, the land heats more rapidly then the neighbouring sea. The heat being radiated from the land heats the air above the ground, causing it to expand leading to a reduction in pressure. As the ocean does not heat at the same rate as the land, the same effect does not occur over the ocean, leading to a pressure differential over a relatively minor distance. This induces a flow from the relatively high pressure zone over the ocean to the lower pressure zone over the land (Masselink and Pattiaratchi, 1997). The sea breeze strength is directly proportional to the size of the pressure differential; typically, this leads the sea breeze's enhancement during the summer months when the highest temperatures occur on the land (Masselink and Pattiaratchi, 1997). During the night, the land cools more rapidly, resulting in the pressure over the land increasing relative to the ocean, inducing an offshore directed 'land' breeze (Abbs and Physick, 1992; cited in Pattiaratchi et al., 1997).

The recordings of afternoon (13:30–16:30) wind speeds and directions during the summer and winter months, respectively, are presented in Figure 2.11. This figure clearly demonstrates the dominance of the southwesterly sea-breeze conditions during the summer afternoons, with 38% of total recordings occurring from a direct south westerly bearing and 77.92% of all measurements recorded between bearings of 180°'s and 270°'s. During winter, the same sea breeze pattern was no longer observed. The winter wind pattern was induced through the northward migration of a sub-tropical ridge of high pressure during the

winter months (Petrusevics, 2004). This ridge of high pressure produced northerly winds in southern Australia (Petrusevics, 2004), which are evident in Figure 2.10.

While these results indicated the presence of an active sea breeze system during the summer months, they also indicated the presence of other factors influencing the breeze direction. This was because a 'typical' sea breeze will blow perpendicular to the coastline directly across the local pressure gradient (Pattiaratchi et al., 1997). In the case of Adelaide, the sea breeze originates from the southwest. This is due to the Coriolis force effects, which act to the left in the southern hemisphere, deflecting westerly winds towards the north, thereby creating southwesterly conditions (Pattiaratchi et al., 1997).

The impact of the sea breeze on coastal processes within the Gulf of St Vincent has not been studied to the authors' knowledge. However, it has been noted by Pattiaratchi et al. (1997) and Masselink and Pattiaratchi (1997) that in coastal regions, sheltered from the direct impact of swell and storm activity, locally generated wind waves play a dominant role in controlling nearshore and foreshore processes. The investigations conducted by Pattiaratchi et al. (1997) referred specifically to the sheltered coastline of southwest Western Australia, where sea breeze conditions are accepted to be among the strongest in the world, with maximum values known to exceed 20 m/s. Pattiaratchi et al. (1997) demonstrated that the sea breeze intensifying led to a rapid response within the nearshore hydrodynamic environment with significant increases observed in the incident wave energy, the longshore current velocity and cross-shore undertow. Mixing and dispersive processes were not addressed.

Although the Adelaide metropolitan coastline is not regularly exposed to the same sea breeze intensity as Western Australia, the breeze magnitude was still significant, with an average velocity of 11.47 m/s recorded between 13:30 and 16:30 in the summer months of November through to March (1994–1998). The nature of the Gulf of St Vincent enables shelter from major storm and swell activity and ensures that locally generated wind waves are a key source of energy in driving coastal hydrodynamic processes. In these respects, the sheltered coastlines of southwest Western Australia and the Gulf of St Vincent are quite similar. Consequently, it is not unreasonable to suggest the sea breeze impacts observed by Pattiaratchi et al. (1997) would be equally applicable to the sheltered South Australian coastline.

Joint Frequency Distribution
Summer 13:30-16:30

Wind flow is FROM the directions shown.
No observations were missing.

Joint Frequency Distribution
Winter 13:30-16:30

Wind flow is FROM the directions shown.
No observations were missing.
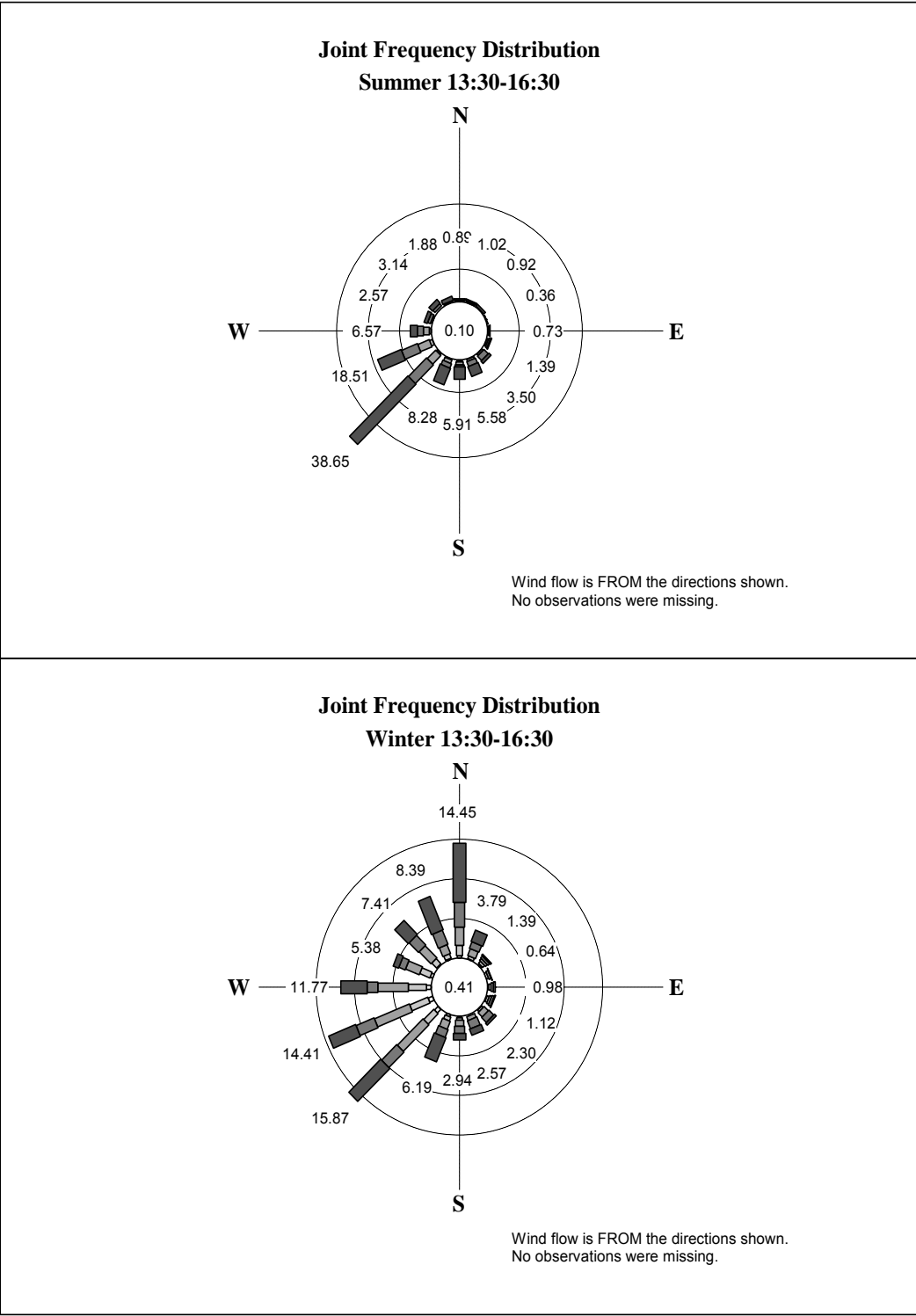
Figure 2.8: Wind roses depicting the mean afternoon wind conditions between 13:30 and 16:30 in summer and winter, respectively. The dominant southwesterly conditions during the summer months illustrate the presence of a sea breeze system. The winter wind rose does not display the same sea breeze pattern. This is interpreted as being due to the northward transgression of the sub-tropical high pressure system during the cooler months, resulting in an increase in southwesterly through north westerly conditions.

2.2   Mixing and Dispersion

Mixing and dispersion are key processes within the surf zone and coastal waters. They are critical parameters to consider when investigating the ability of coastal waters to receive and dilute discharged material (List et al., 1990). In the case of the Adelaide coastal waters, the level of mixing and dispersion determines the transport and dilution of contaminants entering the nearshore zone from outlets such as the Patawalonga and Torrens rivers.

The energy required for driving mixing and dispersive processes in the nearshore region is derived primarily from wave action incident on the shore as well as wind and coastal currents (Inman et al., 1971). Within the surf zone, waves interact with currents and other waves, resulting in two well-defined mechanisms that drive mixing. The first of these is the breaking wave turbulence which drives rapid mixing along the wave bore's path in an onshore direction. Secondly, wave-current interactions drive advective transport in both the alongshore and cross-shore directions, forming circulative cells; these interactions are complex and are known to involve the current field's low frequency fluctuations (Oltman-Shay et al., 1989) and circulation through the vertical plane, driving horizontal momentum mixing (Svendsen and Putrev, 1996; cited in Takewaka et al., 2003). Circulative cells (Figure 2.16) consist of longshore currents and seaward flowing rips and are responsible for a continuous interchange of water between the nearshore and offshore regions. As such, they are key dispersal mechanisms for material injected into the surf zone. The incident wave climate's intensity, frequency, and direction, as well as the nearshore circulatory cells' dimensions have been found to be key variables impacting on the nearshore mixing processes (Inman et al., 1971).

2.2.1   Key Definitions and Concepts

The terminology used to describe mixing and dispersion can be somewhat convoluted and in many cases in the literature the same term is used to describe quite different phenomena. For consistency and clarification, the key terms used in this document pertaining to mixing and dispersive processes within the surf zone are defined according to Fischer et al. (1979):

  ➢ *Mixing*: Any process that leads to one parcel of water becoming intermingled with, or diluted by, another, referring specifically to the action of dispersion and diffusion.
  ➢ *Dispersion*: The process of scattering particles or a cloud of contaminants through the combined effects of shear and transverse diffusion.
  ➢ *Diffusion (Turbulent)*: The random spreading of particles through turbulent motion. Turbulent diffusion is considered to be somewhat analogous to molecular diffusion; however, the scales of motion described by 'eddy' diffusion coefficients are significantly larger.
  ➢ *Diffusion (Molecular)*: Refers to the scattering of particles through random molecular motion. This is described by Fick's Law of diffusion (Equation 3), where q represents the solute mass flux, C is the mass concentration of a diffusing solute, and D is the coefficient of proportionality otherwise known as the molecular diffusivity.

$$q = -D \frac{\delta C}{\delta x} \tag{3}$$

These definitions should be complemented (for the purpose of consistency within this document) with the following definitions of transport mechanisms.
  ➢ *Advection:* Transport due to an imposed current system, including quasi-steady and variable currents in the nearshore region.

> ➢ *Shear:* The advection of fluid at varying velocities at different positions. Shear occurs in changes in current velocity and direction with depth in complex estuarine and coastal flow regimes.

2.2.2   Richardson's Law and the Dispersion Coefficient

Richardson (1926) established the concept of turbulent relative dispersion in his analysis of the observed increase in turbulent diffusivity between molecular scales of motion and general circulation. In his analysis, Richardson (1926) considered the separation statistics of a cluster of a large number of marked molecules and argued that the mean square separation attained a limit as the averaging time was increased. He reasoned this was because only eddies comparable in size with the separation of the particles would be effective in increasing their separation (cited in Sawford, 2001). Richardson (1926) used a range of diffusion data obtained from molecular to global scales to derive the following equation describing the regime of relative turbulent diffusion through the relationship of horizontal variance and eddy diffusivity:

$$\sigma^2 = c_1 \varepsilon t^3$$
(4)

where σ^2 represents the marked particles' horizontal variance, c_1 is a numerical constant, t is the time, and ε is the rate of kinetic energy dissipation. When Equation 4 is used, it is possible to derive the relationship between the apparent diffusivity (K_a) and the scale of diffusion (Fischer et al., 1979):

$$K_a = c_2 \varepsilon^{1/3} l^{4/3}$$
(5)

K_a is the apparent diffusion coefficient derived from the variance and is defined by:

$$K_a(t) = \left(\frac{1}{2}\right)\left(\frac{\partial \sigma^2(t)}{\partial t}\right) = \alpha\left(\sigma^2\right)^{(2/3)}$$
(6)

These relationships are derived on the basis that the eddies responsible for the horizontal spread of a cluster of particles are locally isotropic and homogenous; thus, suggesting the eddy properties are dependent only on the rate of energy dissipation. However, in the surf zone's turbulent flow, it is clear neither homogeneity nor isotropy is maintained.

While Richardson's 4/3 power law was initially developed in the description of turbulent diffusivity in the atmosphere, it also formed the basis of turbulent relative dispersion theories in the ocean. Witting (1933) was the first to demonstrate that the effective diffusivity increased with the scale of diffusion in the ocean, and Richardson and Stommel (1948) applied the atmospheric eddy diffusion laws to the sea surface (cited in Sawford, 2001). Richardson's (1926) developments influenced the work of Kolmogorov (1941) who derived a similar theory for small-scale processes. This formed the basis of Okubo's (1974) analysis of observed oceanic diffusion diagrams. Okubo developed two types of diffusion diagrams: the first representing horizontal variance σ^2 with time, and the other plotting the apparent diffusivity K_a against a length scale of diffusion, nominally σ, as shown in Figure 2.9. Okubo concluded that the apparent diffusivity increased with the scale of diffusion at a rate fitting the 4/3 law, remaining accurate over a wide range of scales ranging from 10 m to 1000 km.
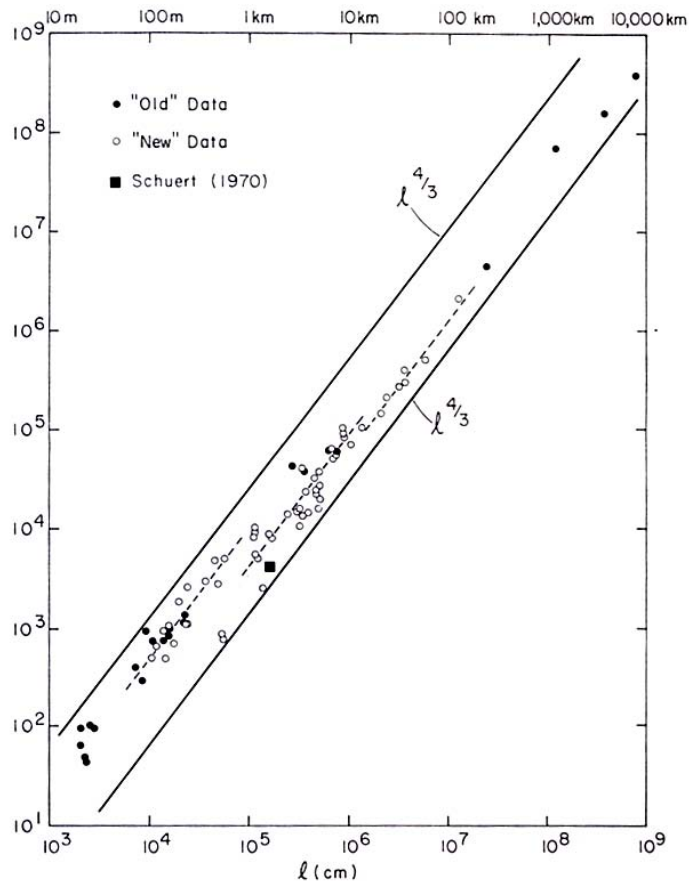
Figure 2.9: Float dispersion compared to diffusion coefficient (Okubo, 1974). The vertical axis is the apparent diffusivity K_a (cm^2s^{-1}).

This scale variation was significantly larger than that predicted by Batchelor (1952) and Kolmogorov (1941), and significantly, none of the conditions cited in the derivation of this coefficient were valid within the surf zone. Namely, within the surf zone, conditions are neither homogeneous nor stationary and a clear boundary exists. However, various other diffusion studies collated by Okubo (1974) not reliant on such strict conditions gave rise to the same diffusion law (cited in Johnson et al., 2004). Thus, processes other than those described by the classical analysis of Batchelor (1952) might lead to the 4/3 law (Fischer et al., 1979). Scale dependence was observed in the results of Johnson (2004) when compared with those of Rodriguez (1995). At smaller scales, the derived values of K compared favourably; however, at larger scales, the values of K varied by orders of magnitude. This suggests caution is required when comparing dispersion values in the nearshore (Johnson, 2004).

The dispersion estimate obtained from the analysis of drifter positions using Equation 24 also included the effects of shear flow and turbulent diffusion. By removing shear-induced spreading, rotation, and divergence from the apparent dispersion (K), it is possible to estimate the true horizontal turbulent diffusivity (Tseng, 2001).

2.3   Studies of Mixing and Dispersion in the Surf Zone

The measurement of spatially variable currents within the nearshore zone is an area of research that has been relatively neglected in the literature with relatively few studies having been conducted in this area. The majority of field investigations have used Eulerian

measurement techniques involving the deployment of an array of stationary sensors that measure the current properties from a fixed frame of reference at a specific location. While the use of Eulerian arrays has been the pre-eminent field investigation approach, the number of sensors required to define spatial scales of motion accurately has restricted their potential application in the analysis of mixing and dispersion.

Conversely, a minority of field studies have used Lagrangian measurement techniques, relying on a moving frame of reference through which the fluid flow behaviour and properties can be tracked with time. Lagrangian experimental approaches provide reliable data pertaining to the spatial structure of current formations from a small number of instruments (in the case of drifters). As a result, Lagrangian methodologies are generally less expensive to deploy, as fewer instruments, and consequently less manpower, are required to obtain the same data as a Eulerian array. Significantly, for determining the fate of contaminants in the nearshore zone, Lagrangian techniques allow the calculation of diffusion coefficients with a greater level of accuracy than fixed current meters (Pal et al., 1998). Johnson (2004) comprehensively addressed several studies using Lagrangian measurement techniques. These studies focused primarily on the description and quantification of topographic rip currents and used a variety of tracking techniques.

Table 2.4: Lagrangian methods employed in tracking currents in the nearshore zone (adapted from Johnson, 2004).

Lagrangian Field Measurement Techniques	Reference
Surface floats and drogued drifters fixed using a compass from shore or boat	Shepard *et al.* (1941); Shepard & Inman, (1950); Sonu, (1972)
Live floats, swimmers tracked by theodolite	Short and Hogan, (1994); Brander and Short (2000)
Floats and balloons tracked by successive aerial photographs	Sasaki & Horikawa, (1975, 1978)
Dye releases tracked by sequential aerial photography and observations	Bowen & Inman (1974), Rodriguez et al (1995); Takewaka *et al.* (2003)
Surface drifters tracked by noon-differential GPS technology	Johnson, (2004); Olson (2004)

The dye diffusion experiments, specifically those conducted by Inman et al. (1971), Bowen and Inman (1974), Rodriguez et al. (1995), and Takewaka et al. (2003), used the original measurement technique of dispersion in real surf zones. However, following the concurrent development of surf zone drifters utilising satellite GPS technology by Johnson et al. (2003) and Schmidt et al. (2003), Johnson (2004) and Olsson (2004) conducted further studies into surf zone mixing and dispersion.

GPS tracked drifters have also been used in larger-scale oceanographic deployments. List et al. (1990) performed investigations into diffusion and dispersion in coastal waters offshore from California using large sea going drogues and Tseng (2004) deployed drifters in the eddy formations formed in the wake of small islands. These studies formed much of the theoretical and analytical foundations for later dispersion-based work undertaken in the nearshore region.

2.3.1   Dye Diffusion Experiments

Dye diffusion experiments have been used since the late 1950s to study mixing processes in the open sea (Bowles et al., 1958; cited in Riddle and Lewis, 2000); however, to the authors' knowledge Inman et al. (1971) performed the first field studies into mixing and dispersion

within the surf zone. These investigations were undertaken at three natural beaches across southern California and northern Mexico with incident wave climates ranging between 0.3 m and 1 m at sites in the sheltered Gulf of California and between 1 m and 2 m at sites exposed to the Pacific Ocean. Rhodamine B dye, a conservative tracer, was injected into the surf zone, and water samples were collected at various temporal and spatial intervals. The analysis of the water samples' fluorescence, with respect to calibrated standards of known concentration, allowed the effective dilution calculation. Further measurements were taken to obtain information pertaining to the direction and flux of wave energy entering the surf zone, the current system's large-scale circulation, and the beach morphology. Through this, Inman et al. (1971) were able to identify and quantify two key mixing mechanisms within the surf zone, each having distinctive length and time scales determined by the incident wave climate and surf zone dimensions. Rapid turbulent mixing in the onshore direction associated with wave breaking and the wave bore motion, was described by Equation 27, where ε_x is the onshore-offshore diffusivity coefficient, H_{rms} is the root mean square (rms) breaker height, X_b is the surf zone width, and T is the period of the wave energy spectra's peak (Inman et al., 1971). Equation 27 directly relates the incident wave regime to the level of mixing in the onshore-offshore direction (the y axis is denoted as lying parallel to the beach).

$$\varepsilon_x \cong \frac{\left(H_{rms}\right)_b X_b}{T}$$ (6)

Along the ocean beaches Inman et al. (1971) investigated, the diffusivity coefficient value was found to be in the order of 2–5.9 m^2s^{-1} in the cross-shore direction, and ranging between 0.13–0.17 m^2s^{-1} in the longshore direction. In the more sheltered beaches of El Moreno, Mexico, the cross-shore diffusivity was found to be significantly lower, ranging between 0.08–0.3 m^2s^{-1} in the cross-shore, and between 0.03 and 0.08 m^2s^{-1} in the longshore direction.

Inman et al. (1971) were also able to describe advective mixing within the surf zone associated with longshore and rip current systems. Their description is shown in Equation 28, where N is the concentration of dye in the nth cell down current from the point of injection and is a function of the initial tracer concentration N_0, the longshore discharge of water *between* adjacent cells Q_l, and the maximum longshore current discharge Q_m (Inman et al., 1971):

$$N_n = N_0 \left(\frac{Q_l}{Q_m}\right)^n$$ (7)

Inman et al.'s (197l) analysis also showed diffusion patterns could be described approximately by one and two-dimensional Fickian diffusion parameters, depending on the injected patch size and the surf zone width. In its simplest form, the eddy diffusivity ε is assumed to be constant in any direction; hence, diffusion follows Fick's Law. However, in large-scale oceanic diffusion, Fickian parameters are not effective descriptors, as the flux of a diffusing quantity is dependent primarily on length and time scales of eddies. Inman et al. (1971) found the diffusive processes within the surf zone were highly organised with length and time scales related to the incident wave climate, Equation 7, and hence could be described by Fickian processes. When the patch size was small compared with the surf zone width, the diffusion patterns could be described using the two-dimensional Fickian diffusion relationship:

$$N'(x,y,t) = \left(\frac{A_0}{4\pi t \left(\varepsilon_x \varepsilon_y \right)^{1/2}} \cdot \exp\left\{ -\left(\frac{x^2}{4\varepsilon_x t} \right) - \left(\frac{y^2}{4\varepsilon_y t} \right) \right\} \right) \times \left[\left(\left(\frac{1}{(2\pi)^{1/2}} \right) \times \int_{-a}^{a} \exp\left\{ -\left(\frac{x^2}{4\varepsilon_x t} \right) - \left(\frac{y^2}{4\varepsilon_y t} \right) \right\} \right)^{-1} \right]$$

(8)

Here, the patch was effectively unbounded; as such, diffusion was able to occur in the longshore and on-offshore planes (y and x, respectively). However, when the patch dimensions were of a similar magnitude to the surf zone width, the diffusive behaviour was effectively bounded in the on-offshore direction along the x plane. In this situation, only longshore diffusion was possible and was described by Inman et al. (1971):

$$N(y,t) = \left(\frac{A_0}{(4\pi \varepsilon t)^{1/2}} \right) \times \exp\left\{ -\frac{y^2}{4\varepsilon_y t} \right\}$$

(9)

which is normalised for boundaries at the waterline and the surf zone edge through which minimal transport takes place (except via defined rip currents). Eventually, the spread of dye throughout the surf zone means that patches that were originally two-dimensional reach the boundaries and are able to be described by the one-dimensional Equation 9. Equations 8 and 9 describe the concentration of an injected tracer at a point with time; A_0 represents the total volume of tracer injected, and ε_x and ε_y are the diffusivity coefficients in their respective planes. Note that the one-dimensional equation, Equation 9, acts only on the y-plane in the direction of longshore transport.

Following from the significant advances of others including Longuet-Higgins (1970 and 1972) and Inman et al. (1971), Bowen and Inman (1974) were able to assign quantitative values to the nearshore mixing due to waves within and offshore of the surf zone as well as through longshore currents. However, rather than deriving the eddy diffusivity coefficient (as shown in Equation 6 and used in Equations 8 and 9), Bowen and Inman (1974) used the nomenclature A_H to describe the horizontal kinematic eddy viscosity—a value equivalent to ε_x. Offshore of the surf zone, Bowen and Inman (1974) cited the work of Masch (1963) and Thornton (1973) in developing two equations for the kinematic eddy viscosity. The derivation of eddy viscosity by Masch (1963) takes two forms, depending on the presence of wind:

$$A_H \approx \frac{ak\left(U u_m^2 + u_m^3 \right)}{g}$$

(10)

$$A_H \approx \frac{ak.u_m^3 (1 + ak)}{g}$$

(11)

The derivation is based on the linear Airy theory and relates the eddy viscosity to the wave amplitude a, the wave number k, the maximum orbital velocity u_m, the wind speed U, and gravity. The wave steepness (ak/π) range, under which these equations Masch (1963) evaluated, is limited, ranging between 0.08 and 0.12. Consequently, Equations 10 and 11 are not directly applicable to realistic coastal situations under which the wave steepness may vary by orders of magnitude.

Thornton (1970) approached the derivation of A_H, outside of the surf zone from a different perspective from Masch (1963), finding the eddy viscosity to be dependent on the orbital velocity u and the particle displacement τ:

$$A_H = |u\tau| = \frac{a^2 \sigma}{\pi}$$

(12)

The values of A_H derived from Thornton's (1970) equation were significantly higher than those Masch (1963) derived owing to the fact that Equation 12 was applicable for higher wave steepness such as was encountered close to the surf zone edge where more vigorous mixing was expected. From this comparison it is evident that deep water results and assumptions are not directly applicable to shallower areas.

Bowen and Inman (1974) also addressed the quantification of mixing rates in longshore currents and within the surf zone, obtaining the same outcomes as described in Inman et al. (1971). Bowen and Inman (1974) suggested that in the longshore direction, mixing was described by Equation 28, while in the surf zone, mixing was dominated by the incident wave field properties, as described in Equation 27. Also noteworthy is the work of Longuet-Higgins (1970a and b), who suggested the eddy viscosity in the surf zone was a function of the distance from shore and a characteristic velocity given by the celerity ($\sqrt{gh}$):

.

$$A_H = 0.4 N_{x_b} \sqrt{(gh_b)}$$ (13)

The primary drawback of this approach is that the eddy viscosity is overestimated beyond the wave breaking depth, where eddies induced by the wave turbulence motion decrease rapidly.

Following the dye diffusion experiments of the early 1970s, little field work addressing mixing and dispersion in the nearshore zone was undertaken until 1995 when Rodriguez et al. (1995) used a combination of numerical models and field dye diffusion experiments to investigate pollutant dispersal on beaches along the Spanish Mediterranean coastline. The dispersion coefficient value obtained from the numerical model of K_h = 0.018 m²s^{-1} correlated well with the experimental results of K_h = 0.03±0.01 m²s^{-1}, which was obtained by relating the dispersion coefficient to a numerical constant β, the water depth, and the shear velocity u_*. In this work, Rodriguez et al. (1995) noted the complexity of non-linear turbulence-wave-current interactions and commented that this complexity was why 'after 20 years of studies, there are no universally accepted "complete" formulations either for dispersion or for eddy viscosity'.

Takewaka et al. (2003) conducted dye dispersion experiments in a longshore current driven by an obliquely incident wave field of significant height 0.56 m and period 6.5 s. The experimental design consisted of a dye discharging apparatus mounted on a pier and an ensemble of photographic and video recording equipment suspended from helium-filled balloons at a height of approximately 200 m above the sea. This equipment was used to obtain imagery of the spatial and temporal variation in the injected dye patch. Through the imagery analysis, Takewaka et al. (2003) were able to describe qualitatively the dye behaviour as resembling dispersion in a shear flow field, as described by Fischer et al. (1979) and Svendsen and Putrevu (1996). The patch was advected alongshore with the dominant longshore current; spreading along this axis was due to variations in the longshore current velocity field as well as turbulent diffusion. Spreading observed in the cross-shore direction was due to turbulent diffusion in the surf zone and cross-shore transport. Digital processing techniques were applied to the imagery, which allowed the patch size to be calculated by setting thresholds for the colouration of individual pixels. Through this process, the patch's standard deviation could be determined in the x and y directions:

$$\sigma_x(t) = \sqrt{\left(\frac{1}{N}\sum\left((x - X_c(t))^2\right)g(x,y,t)\right)}$$ (14)

$$\sigma_y(t) = \sqrt{\left(\frac{1}{N}\sum\left((y - Y_c(t))^2\right)g(x,y,t)\right)}$$

Here, the values of $X_c(t)$ and $Y_c(t)$ are values representative of the patch's average size, calculated through assigning values of 1 or 0 to each pixel, depending on whether it met assigned threshold values and averaging across the entire image.

The standard deviations derived in Equation 14 were used to verify quantitatively the physical observations. This allowed the identification of three distinct stages in the dye patch evolution. The stage initially following injection was characterised by a consistent, steady increase in σ_x and σ_y, as the patch deformed from its original circular shape into a stretched, somewhat elliptical form. Following this stage, the patch underwent rapid deformation in the longshore direction because of the prevailing longshore current shear effects, resulting in an increase in σ_y. Physical observations verified the increase in σ_y was due to shear dispersion in the longshore current, as breaking waves across the patch path did not induce turbulence. The final stage of patch evolution was characterised by the increasing contribution of diffusion in the cross-shore direction and an increase in the rate of change of σ_x. The calculated values of σ_x and σ_y were plotted against time and Takewaka et al., (2003) used them to determine the dispersion coefficient K_x. Takewaka et al. (2003) determined the value of K_x by assuming a Gaussian diffusion process and neglecting the effects of cross-shore flow:

$$\sigma_{xa}(t) = \left\{ \frac{1}{3}\left(-4K_x t \log\left(\frac{C}{C_0}\sqrt{4\pi K_x t} \right) \right) \right\} \tag{15}$$

It is also possible to assume the vertical flow was absent, as no waves were observed breaking across the flow path; as such, the effects of wave motion and return could be neglected. By assuming concentration ratios C/C_0 of 0.1%, 0.5%, and 1.0% Takewaka et al. (2003) were able to determine K_x values 0.01, 0.017, and 0.025, respectively, by varying the value of K_x to make Equation 36 fit the plot of observed σ_x values with time (Figure 2.10).
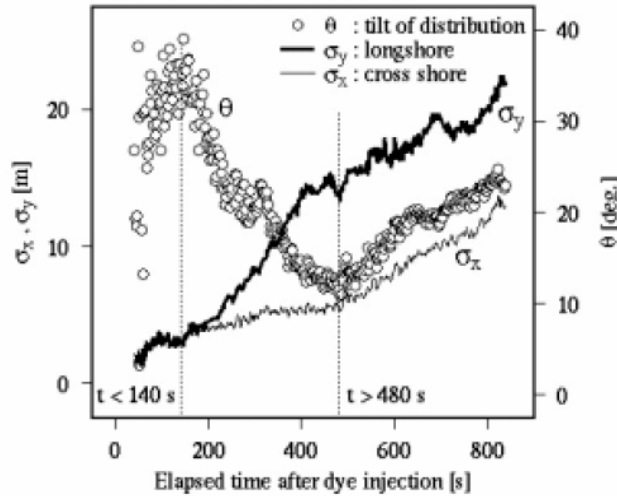
Figure 2.10: Time series of std deviation in x and y, with time, for the calculation of K (Takewaka et al., 2003).

Takewaka et al.'s (2003) calculated dispersion coefficient values correlated relatively consistently with those determined by Riddle and Lewis (2000), who reviewed dispersion data from 25 nearshore and estuarine sites predominantly around the United Kingdom. They found lateral dispersion coefficients ranging between 0.003 m²s⁻¹ and 0.42 m²s⁻¹ with a mean

of 0.05 m²s⁻¹, compared these values to experimental data from the southeast U.S.A. and Ireland, and found all data sets to be relatively similar. The experimental results Riddle and Lewis (2000) addressed were not obtained from the surf zone.

2.3.2   Drifter Experiments

The use of Lagrangian drifters in measuring mixing and dispersion processes has traditionally been restricted to large-scale offshore and oceanic applications. In particular, List et al. (1990) and Tseng (2001) provided valuable examples of applying drifter technology to the measurement of dispersion phenomena. List et al. (1990) deployed several drogues in coastal waters offshore of southern California and used their movements to calculate transport and dispersing properties over diurnal periods, concurrently pioneering many of the analysis techniques used in this study. The analytical approach List et al. (1990) employed involved analysing the individual drifter coordinates at each point in time to determine the average x and y coordinates. These coordinates comprised the mean location of all the drifters or the 'centroid', which was subsequently used to determine the cluster variance. By plotting the variance with time it is possible to determine a dispersion estimate, as described by Equation 6. Tseng (2001) made similar measurements through the deployment of drifters near estuary openings and in the wake of small eddies offshore from southwestern Taiwan. However, Tseng (2001) applied a slightly different analytical approach, utilising the relationship:

$$K = \frac{1}{4}\frac{\partial \sigma_x \sigma_y}{\partial t}$$

(16)

This relationship differs slightly from the classical relationship (Equation 6) Richardson (1926) developed and List et al. (1990) used; however, this difference is mainly superficial, as Equation 16 was still derived according to the same principles of turbulent dispersion. Rather, the variation is due to a different approach to the derivation of σ² used by Tseng (2001), and is inconsequential in terms of the effect on derived values of K. This is highlighted by the fact that Tseng (2001) derived K values in the order of 12–15 m²s⁻¹ in tidally forced estuarine zones, during periods of strong tidal flow. Tseng (2001) used an alternative relationship for the derivation of K. The formula is not fundamentally different from the classical relationship derived by Richardson (1926), but does differ 'cosmetically' in the utilisation of σ_x and σ_y, rather than a combined σ² derived from the variation average in the x and y directions, respectively.

The lack of drifter deployments within the nearshore zone has largely been due to the absence of appropriate technology, dictating that drifters were cumbersome, expensive, and somewhat inaccurate over scales of less than 100 m. The removal of selective availability from the international global positioning system (GPS) in May of 2000 greatly enhanced the GPS system's accuracy and cleared the way for the development of small, relatively inexpensive drifters suitable for use in the shallow nearshore region (Johnson et al., 2003). Schmidt et al. (2003) and Johnson et al. (2003) concurrently and independently developed the drifters suitable for use in the nearshore; as such, only a limited number of experiments have been conducted utilising this technology.

As part of their drifter validation tests, Schmidt et al. (2003) conducted synchronized dye and drifter release experiments and were able to display qualitatively that the behaviour of dye patches and drifters within the surf zone were analogous. This was significant, as it suggested that the dispersion coefficients obtained from dye diffusion experiments were comparable to coefficients obtained from drifter experiments (Schmidt et al., 2003). Schmidt et al. (2003) validated the velocities obtained from their drifters by comparing the velocities measured by simultaneously deployed fixed position current meters. These results confirmed a high degree of correlation between the Lagrangian and Eulerian measurements

in the longshore direction, obtaining a high correlation of 0.95. However, they also demonstrated a very poor correlation in the cross-shore domain. This was attributed to the fact that the drifters measured the current structure at the top of the water column, while the fixed current meters obtained data from the seabed. As such, the Eulerian measurements were likely to have been affected by surf zone phenomena, such as undertow, which was enhanced with proximity to the bed. The validation processes adopted by Johnson et al. (2003) were similar to those of Schmidt et al. (2003). Johnson et al. (2003) performed drifter experiments with concurrent Acoustic Doppler Current Profiler (ADCP) deployments within the surf zone. Comparisons were made by collating the data obtained by ADCP and the drifters during periods when their separation was less than 10 m. This velocity data were averaged over two peak wave periods, centering on the period of smallest instrument separation. The data obtained through this approach showed a slight, but consistent, underestimate of the depth averaged velocity by the drifters in the longshore and cross-shore direction. This was the same effect Schmidt et al. (2003) noted. Johnson et al. (2003) justified this variation, suggesting it was to be expected owing to the knowledge that surf zone wave averaged velocities measured by the drifters were greater near the surface and hence could be expected to exceed the depth averaged flow.

Johnson (2004) has undertaken the most extensive deployments of surf zone drifters to date. Johnson deployed drifters within longshore and rip-current formations along high-energy beaches in Perth, Western Australia. In the analysis of transient rip currents, Johnson (2004) addressed several factors ranging from a qualitative description of the rip motion and behaviour through to the analysis of dispersion at the rip head. Cluster dispersion analyses were performed following the methods of List et al. (1990) for a total of four rip events. The total dispersion coefficient was found to range substantially between 1.29 and 3.88 m^2s^{-1}, which was of similar magnitude to the diffusion rates determined for the surf zone, as determined by Inman et al. (1971). Qualitatively, Johnson (2004) noted the apparent local suppression of horizontal dispersion within the 'rip neck'—the region of rapid, offshore directed flow through the surf zone. Subsequent rapid expansion at the rates noted was then observed in the 'rip head'—an area of enhanced local dispersion. Johnson (2004) performed further dispersion analyses that involved the plotting of dispersion coefficients against the lengths scale σ, following from the analysis of Okubo (1974). Through this, Johnson (2004) derived the power laws describing the relationship between the scale of drifter separation and relative dispersion rates. These power laws were found to have exponents ranging between 1.3 and 1.5 within the surf zone and between 1.47 and 1.85 in the rip head outside of the surf zone. These results, particularly within the surf zone, demonstrated the relatively high data correlation with Richardson's (1926) proposed 4/3rds law. They also further highlighted the enhancement of dispersion in the rip head region.

In the analysis of longshore currents, Johnson (2004) used simultaneous deployments of an ADCP (to record current magnitudes and directions) and an InterOcean S4 wave recorder. The Eulerian recording devices' presence allowed the consideration of the incident wave climate and current field, thus providing a reference for the drifter data. Johnson (2004) performed extensive cluster and drifter trajectory analysis allowing the calculation of dispersion coefficients K_x and K_y of 0.2 m^2s^{-1} and 0.3m^2s^{-1}, respectively, for 10 m average drifter separation. These results are not directly comparable to those obtained by Takewaka (2003)—the only other known longshore dispersion results—because Takewaka (2003) assumed a Fickian diffusion process. However, the values of K_x obtained for a cloud size of 5 m, or a 5 m drifter separation of 0.025 m^2s^{-1} and 0.039 m^2s^{-1}, respectively, were consistent. These results were significantly less than the values Johnson (2004) determined in the rip head. Johnson (2004) also noted the apparent scale dependence of dispersion in the longshore flow field. As with the rip current analysis, Johnson (2004) derived the exponents of the power laws describing the lines of best fit for the relationship between the dispersion coefficients and a length scale of separation. The power law exponents were found to range significantly, with the total longshore value found to be 1.92, and the cross-shore component calculated as 2.41. The relationships used to derive these values are plotted in Figure 2.11.
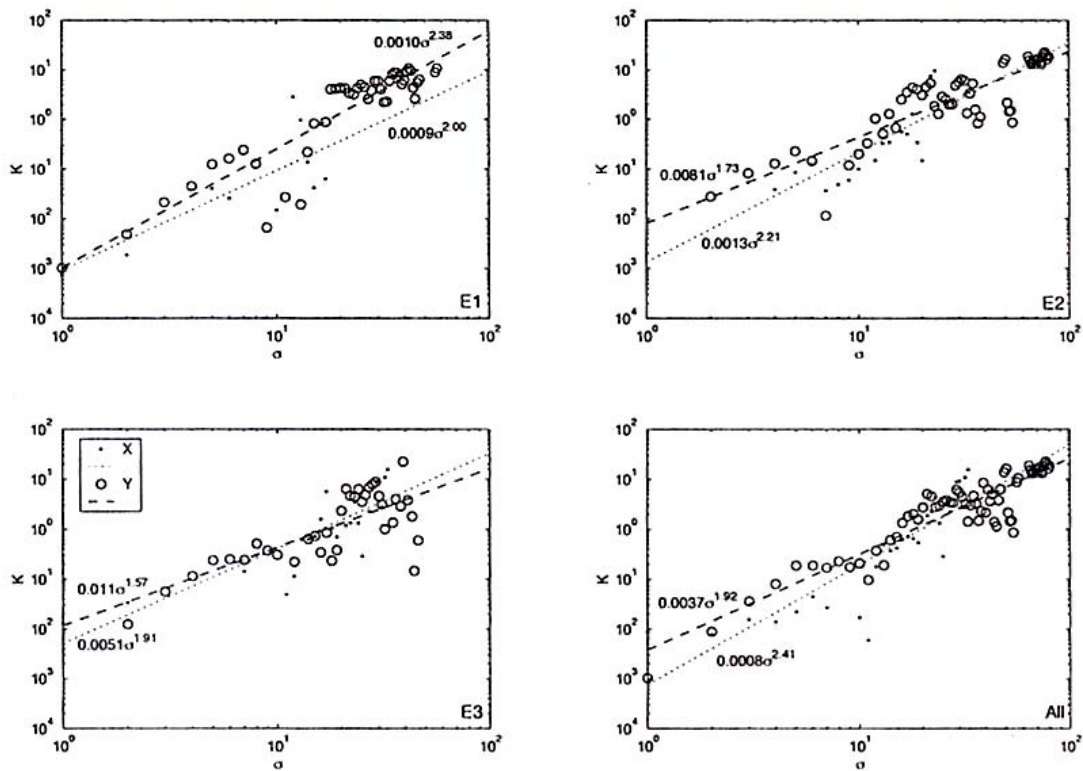
Figure 2.11: Cross-shore (●) and longshore (○) dispersion coefficients averaged in 1 m bins of standard deviation of cross-shore and longshore separation. The lines shown are the least squares fit for the cross-shore (···) and longshore direction (---), and the equation of each line is shown (from Johnson, (2004).

Olsson (2004) deployed Lagrangian surf zone drifters while analysing eddies formed in the lee of coastal structures, primarily groynes, along the metropolitan coastline of Perth, Western Australia. The primary focus of Olsson's (2004) work was the qualitative analysis of the currents' spatial structure in the eddy field through tracking the drifter paths and their respective velocities. This also included calculating the dispersion coefficient at the seaward extremity of the offshore eddy flow located near the groyne structure's tip. The dispersion coefficient was calculated on a limited number of occasions and ranged markedly between 0.6 m²s⁻¹ and 4.1 m²s⁻¹. Olsson (2004) noted that owing to the small number of sample points, it was not possible to estimate reasonably the dispersion coefficient representative of the underlying system.

3   Methodology

3.1   Lagrangian GPS Drifters

Lagrangian measurements are obtained by utilising a moving reference frame through which the behaviour and properties of individual fluid particles can be tracked with time (Munson et al., 2002). This is in contrast to Eulerian approaches, which employ fixed frames of reference to analyse the behaviour of fluid particles and the variation in their properties with time. Lagrangian approaches are far more practical in the analysis of mixing and dispersion across significant spatial scales; this is because Eulerian experimental formats require multiple reference points to resolve the spatial scales of motion and hence the rate of dispersion (Tseng, 2001; Winant, 1983). In the case of Brander (2001), it was necessary to deploy a total of five pressure sensors and nine current meters to resolve the flow kinematics of a small relatively stable low-energy rip. In larger, transient, or more spatially variable formations, the use of Eulerian arrays rapidly becomes impractical because of the numerous sensors' high cost as well as the manpower required to set up, maintain, and operate extensive instrument arrays.

Conversely, Lagrangian drifters are able to provide reliable data pertaining to the structure of current formations by tracking the paths of a relatively small number of floating drifters (Johnson, 2004; Tseng, 2001; List et al., 1990) or by measuring the growth of dye patches (Takewaka, 2003; Rodriguez et al., 1995; Inman et al., 1971). The data obtained is particularly valuable in observing the spatial structure of flow fields and their dynamics and, significantly, determining the fate of pollutants in ecological investigations allows diffusion coefficients to be determined more accurately than with the use of fixed current meters (Pal et al., 1998; cited in Johnson et al., 2003). Traditionally, the use of drifters has been restricted to large-scale oceanographic applications (Tseng, 2001; List et al., 1990); however, Johnson et al. (2003) developed drifters suitable for use in the nearshore zone. These drifters provide the benefits attributable to Lagrangian measurement techniques— namely, the ability to determine reliable diffusion coefficients and define spatial variability of current systems over a significant scale; yet, they are more compact and less expensive than previous ocean going drogues, allowing their deployment by individuals or small groups directly into the nearshore zone.

3.1.1   Design

The GPS surf zone drifters Johnson et al. (2003) developed have the primary advantages of being inexpensive, simple to construct, and reliable in applications where larger, more sophisticated drifters may not be required, such as the nearshore zone, lakes, estuaries, and rivers. The drifter units consist of four primary components (represented in Figure 3.1).
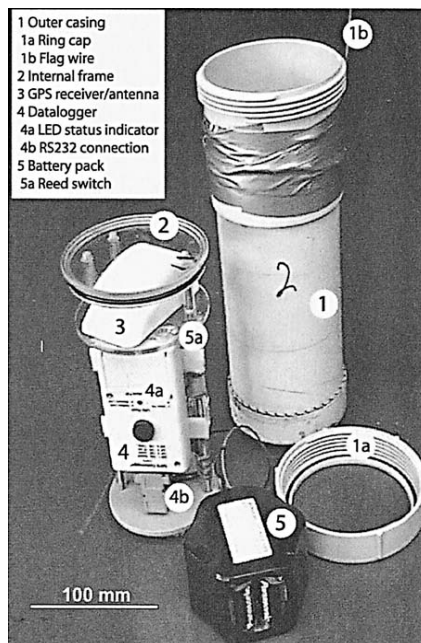
Figure 3.1: Components of the surf zone drifters developed by Johnson et al. (2003) and utilised in field studies of mixing and dispersion in the nearshore zone.

The drifter's main casing is constructed of 100 mm diameter polyvinyl chloride (PVC) pipe of 320 mm total length, and is able to withstand pressure testing up to the equivalent of at least 40 m of seawater (Johnson et al., 2003). The casing is fitted with a standard screw on ring seal fitting (1a) and a clear Perspex lid with a further o-ring mounted on the internal frame, which both act to prevent leakage into the casing. The internal frame acts to secure the GPS, the data logger, and the battery pack, with the GPS located immediately below the clear Perspex cover and the heavy battery pack, consisting of seven standard alkaline D-cell batteries, located at the drifter's base to act as ballast. This ensures the drifters maintain upright stability with almost neutral buoyancy. By maintaining almost neutral buoyancy, it is possible to minimise inertial effects and wind forces on the drifter, as only 2 cm of the drifter is exposed above the water's surface in calm conditions (Johnson, 2004). The GPS and data logger are powered by the battery pack and are configured such that once the power is connected, initialisation and satellite acquisition occurs automatically, and recordings of location, time, and date are stored in the data logger at a frequency of 1 Hz.

The drifters can be modified through the addition of various drogue configurations for use in both larger-scale oceanographic applications (Verspecht, 2002) or in the surf zone (Johnson, 2004; Olsson, 2004) and at varying water depths (Johnson et al., 2003). The modification for use in the surf zone involves the attachment of parachute drogues to the base of the drifter's main casing. These parachutes act to prevent the drifter from 'surfing' along the wave bore when it is caught in breaking waves. The parachutes are almost neutrally buoyant, so a small lead weight is attached to their base to orientate them in the water column, ensuring they hang vertically below the main casing and receiver unit. Under calm conditions, or in non-breaking waves, the parachutes are closed and present only their cross-sectional area; thus, they do not significantly influence the drifter trajectory (Johnson et al., 2003). However, under rapid vertical motion such as that experienced when the drifter is lifted and projected towards the shore by the motion of a breaking wave or wave bore, the parachute opens. This dramatically increases the drag on the drogue and has the effect of anchoring the drifter to the orbital velocities below the breaking region (Johnson, 2004). The drogue is also effective in damping vertical and horizontal oscillatory motion in the receiver unit, as experienced by non-drogued drifters.

The drogue attachments' length varies significantly depending on the number of parachutes used; however, given the surf zone's relatively shallow nature, it is not unusual for the drogue apparatus to come into contact with the bottom. Johnson (2004) addressed this issue through drag tests in a tow tank and found the effect of the drogue dragging along the bottom was small, however some measurement error was inevitable. As such, the minimum viable depth of operation is the length of the main casing itself—320 mm. Additionally, the initial depth at which contact occurs can be significantly reduced by utilising one parachute arrangement rather than the two Johnson et al. (2003) originally developed. Johnson (2004) investigated the effect of having fewer parachutes and found it was negligible in the measurement of wave averaged velocities as long as at least one parachute was attached.

3.1.2   Accuracy

While the removal of selective availability (SA) has greatly enhanced the accuracy and reliability of non-differential GPS systems, there are still several factors that can cause positioning errors. These include limitations in the precision of GPS receivers, satellite clock errors, variation between the known satellite position and actual location, atmospheric effects influencing the speed of light, and the reflection of signals off large structures (Hofmann-Wellenhof et al., 1997; cited in Johnson et al., 2003). Some of these effects create errors in the form of 'noise'—random positioning errors following no particular trends and apparent only for individual readings. Other factors, however, have the effect of creating position errors, which oscillate with a preferred frequency (Johnson et al., 2003). The key factor when assessing satellite positioning errors for the purpose of surf zone drifter analysis is whether the errors are absolute or relative. Absolute errors have little practical impact, as while they do record erroneous locations, the relative difference between these positions is correct and hence does not affect the drifter's recorded path. Relative errors, which are changes in the position of a stationary receiver relative to an arbitrary datum point, have the potential to disrupt seriously any position, velocity, or acceleration calculations performed on the data.

Johnson (2004) addressed the level of relative error affecting the GPS surf zone drifters by conducting a series of stationary tests. GPS units and data loggers were left in open spaces for periods of 45 minutes to obtain data, which was then analysed to obtain the standard deviation of the easting and northing coordinates. Eastings were found to have a smaller variation in recorded positions, with a standard deviation among the data of 1.3 compared with 1.6 m for northings (Johnson et al., 2003). Maximum displacements from the datum point were significantly larger with readings of 4.2 m and 5.2 m for easting and northing, respectively (Johnson et al., 2003). Errors due to the data loggers' precision were noted with the recording of coordinate significant figures only sufficient to ensure accuracy of 0.16 m easting and 0.19 m northing at a latitude of 32°S. Johnson (2004) showed that non-differential GPS systems were sufficiently accurate to measure movements with frequencies of less than 0.05 Hz, a period of 20 s. However, it was also noted this could be improved upon by using differential GPS systems, which allow movements with frequencies as high as 1 Hz to be measured (Schmidt et al., 2003; cited in Johnson, 2004).

3.2   Eulerian Measurements

Eulerian descriptions of fluid motion are obtained by making the necessary recordings such as velocity, direction, pressure, and density as functions of time and space. This is in contrast with Lagrangian techniques under which fluid properties are a function of time only (Munson et al., 2002). The relative advantages and drawbacks of Eulerian and Lagrangian approaches have been discussed previously, where it was demonstrated that within the nearshore zone, Lagrangian drifters provide the most effective tool to investigate the spatial structure of currents and associated mixing and dispersion. However, Eulerian measurements provide the advantage of spatially constant measurements of current properties.

Consequently, Eulerian measurements were obtained to determine the dominant direction and magnitude of current flow profiles as well as data pertaining to water level variability and as such, the prevailing wave climate at the selected deployment site. The fact that the spatial domain remained constant during the sampling period allowed the analysis of changes in the current regime with time and hence the possible factors leading to these variations.

Previous drifter-based studies into nearshore currents have also utilised Eulerian measurements, including Olsson (2004) who deployed an ADCP in the wave shadow of Cottesloe groyne to determine comparative flow magnitude profiles, and Johnson (2004), who used concurrent drifter and ADCP deployments in the analysis of rip current formations.

3.2.1   Acoustic Doppler Current Profiler

The 'Aquadopp' ADCP was used to collect current and pressure data during the March 2005 deployments. The ADCP was programmed to record current direction and velocity across 10 cm cells at a frequency of 1 Hz. The cell size refers to the interval over which individual measurements are made, allowing the derivation of complete current profiles through the water column from the seafloor to the water surface. In the case of a 2 m deployment depth, the water column is divided into twenty 10cm cells, each of which is sampled individually. The flow characteristics in each of the cells are measured in terms of the three-dimensional components. The easterly, northerly, and vertical current magnitudes in metres per second (ms^{-1}) are then stored as separate output files, which can be analysed individually.

The ADCP was used to measure pressure, also at a frequency of 1 Hz. The relationship between pressure and water depth consequently allowed the direct derivation of the water level from the pressure data. The relatively high frequency of measurements allowed for the recording of shorter period water level variations in the form of locally generated wind waves (3–5 s) as well as longer period swell waves (10–14 s) and tidal oscillations. The tidal period length (~12 hrs) compared with the period of deployment (~6 hrs) prevented completely measuring the tidal cycle during a single deployment.

3.3   Field Deployment

The experiments were conducted in the nearshore zone along West Beach on the Adelaide metropolitan coastline. This site was selected because of the presence of the artificial waterway 'Breakout Creek', which is the Torrens River outflow point into the sea. Hence, it is a key location when investigating contaminant inflows and subsequent dilution through mixing and dispersion in the coastal zone. Two approaches were adopted within the experimental process; specifically the deployment of surf zone drifters, which rely on a Lagrangian moving frame of reference to calculate the dispersion coefficient as well as the eulerian fixed frame of reference ADCP, which is able to provide data on the current direction and velocity throughout the water column in addition to pressure, depth, and variations, which indicate the motion of waves and longer period phenomena including tides.

The first step in the drifters' deployment was to survey the shoreline in the experimental area. A single drifter was carried around the shoreline, while the remaining drifters were left stationary at a central location. This allowed the relatively simple derivation of the shoreline profile, which provided a valuable reference in data analysis. Drifters were then carried by hand offshore from the surf zone to water depths ranging between ~1.2 m and 2 m and released simultaneously as clusters. The drifters were allowed to float independently until they washed ashore, or reached depths of less than 32 cm on sandbars, at which point the main casing started dragging on the seafloor, significantly impeding motion.

In some cases, drifters moved offshore and had to be retrieved; this was particularly influenced by the wind speed and direction. Once drifters were recovered either onshore or offshore, they were removed from circulation by placing them on the beach until the next cluster could be initiated. Drifter deployments were performed in two tranches: over three consecutive days from 1 to 3 September 2004 and between 20 and 23 March 2005. These dates were able to provide a comparison between the level of mixing and dispersion under seasonally variable conditions in winter and summer as well as providing a comparison between times of peak and residual contaminant inflows.

Many individual drifter experiments were performed and it is not practical to describe each individual drift; however, the basic procedures described were used consistently through each deployment. The wind, wave, and tidal conditions encountered during each of the deployment periods are discussed in the following section.

The ADCP was deployed on three occasions: 20, 21, and 22 March 2005. On each occasion, the ADCP was deployed in water of approximately 2 m depth, within a channel, on the shoreward side of a major sandbar over which the water depth was reduced to as little as 50 cm. The instrument was fastened to a cross-beam structure, facing upwards, to maintain stability and orientation. A buoy, which floated freely at the surface, was attached to this frame structure by rope to provide easy identification of the ADCP location and subsequent equipment retrieval. Generally, the sensors' deployment position was relatively calm with little wave or current activity observed. However, it was noted that during periods of greater wave activity, breaking was induced over the shallow sandbar; the bores of these waves were observed to pass over the ADCP, inducing shoreward currents in the water column upper levels.
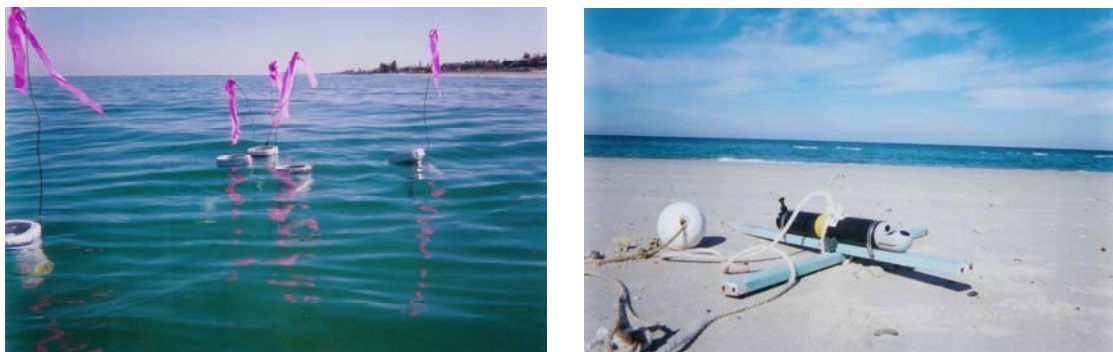
Figure 3.2: Photographs of the drifter and the ADCP deployment configurations, respectively.

3.3.1   September 2004

Owing to the necessity of traveling from Perth to Adelaide in order to perform field work, it was not possible to select specific conditions in which to deploy the drifters. Factors such as winds and waves could not be predicted for significant periods in advance; thus, drifters had to be deployed under the prevailing conditions during the pre-determined sampling dates. The average wind conditions recorded during September and the preceding winter months are presented in Table 3.1. The data in this table suggests conditions became windier in the mornings and afternoons in late winter and early spring. However, the variation between the morning and afternoon conditions actually decreased over the same period, representing a decrease in the sea breeze activity.

Table 3.1: Mean wind speeds collected at Adelaide Airport for the period 1955–2004 (courtesy of the Bureau of Meteorology, 2005).

JUN	JUL	AUG	SEP
Mean 9am Wind Speed (km/hr)			
12.6	13.8	16.1	17.6
Mean 3pm Wind Speed (km/hr)			
17.1	18.9	20.6	21

Tidal oscillations during the sampling period could be accurately predicted, and form the basis (in the absence of 'random' phenomena such as storm surge) of water level oscillations. The water level recordings during the sampling period from the nearby tidal gauge at Outer Harbour are represented in Figure 3.3. This shows the high water level variation due to the spring tides during the sampling period. While the sampling was conducted opportunistically, as noted previously, it was fortunate that drifter deployments were conducted across a representative cross-section of tidal conditions. As represented in Figure 3.3, deployments were conducted during periods of rising and falling water levels, thus allowing the comparison of dispersion rates at different periods of the tidal cycle.

The typically gentle slope of Henley beach exacerbated the motion in the mean water level position, from a horizontal perspective, through the tidal cycle. On several occasions during the drifter deployments, the shoreline retreat or advance was observed to be in the order of tens of metres. On these occasions, shoreline profile surveys were conducted prior to and post-drifter deployment to quantify the shoreline transgression/regression during the experimental period.
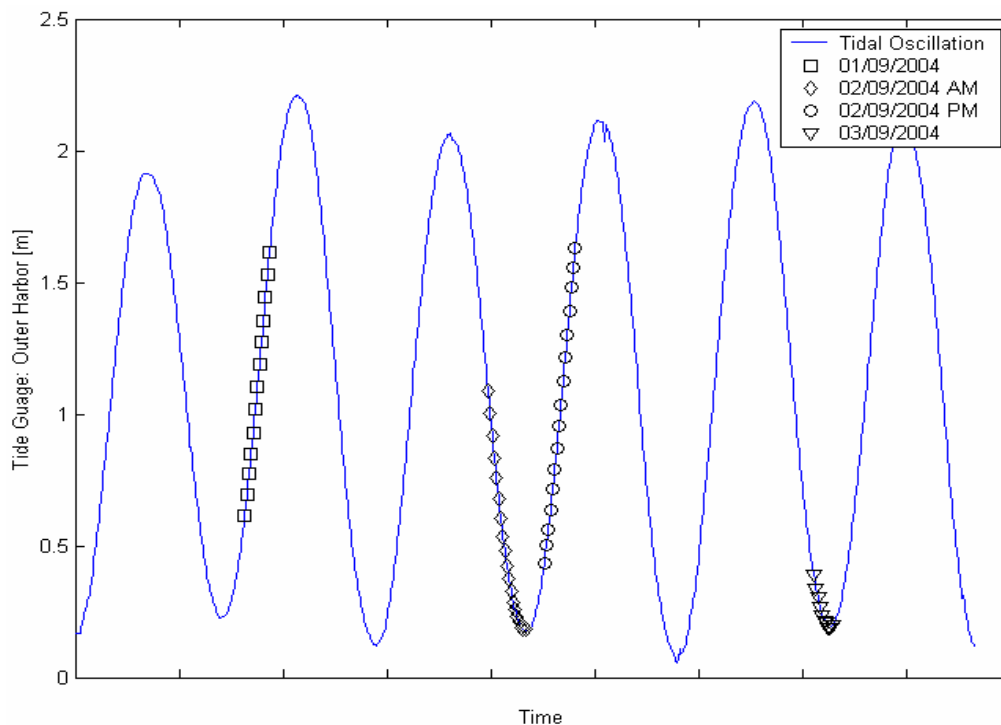
Figure 3.3: Water level variations recorded at the Outer Harbour tidal gauge during the first tranche of sampling in September 2004. The data shows the high 'spring' tidal range of ~2 m as well as the periods of drifter deployment. It should be noted that deployments were performed on both rising and falling tides as well as at the extremes of the tidal range. (Data supplied by Greg Pearce of HydroSurvey Australia, Flinders Ports Pty Ltd.)

1st September 2004

Sampling was conducted on 1 September 2004 between approximately 13:30 and 15:30. The wind direction was predominantly from the south west and ranged between velocities of 3.6ms^{-1} and 5.7ms^{-1}, as shown in Table 3.2, which lists the meteorological recordings of wind speed and direction at the nearby Adelaide airport. Wave conditions were choppy, driven by the relatively strong sea breeze, and although accurate measurements of wave characteristics including amplitude and period were not available, observations suggested significant wave heights in the order of 0.4 m and a significant wave period of 4–6 s. Drifters were deployed in several clusters close to shore and rapidly washed into shallow water, resulting in generally short drift times. The longshore current direction was northerly. This resulted in successive deployments being positioned in a northerly progression along the coast before retrieval and redeployment at the original point. The conditions under which the clusters were released are noted in Table 3.2; this also includes brief comments pertaining to the clusters' behaviour and other significant points of interest.

Table 3.2: Summary of drifter deployments on the 1st of September 2004 including wind data (courtesy of the Bureau of Meteorology, 2005) and tide data from the nearby gauge at Outer Harbor (Hydrosurvey Australia and Flinders Port Authority, 2005).

Date: 1/09/2004				Wind			
Cluster	Time	Drifters	Shortest Duration [s]	Velocity [m/s]	Direction [°]	Tide [m]	Comments
1	13:30	2,3,4	296	4.61	230	0.62	Deployed ~35m offshore, drifters follow generally NW bearing, except drifter 4 which moves offshore and had to be recovered by hand.
2	14:00	2,3,4,5	47	3.61	240	0.82	Deployed ~25m offshore, to the north of cluster 1. Short drift terminated by drifters running aground. Drifted ~10m directly north.
3	14:30	all	49	5.69	220	1.1	Deployed near Cluster 2 start, ~25m offshore. Drifters moved north and onshore up to 50m. Drifter 5 ran aground at an early stage after moving directly onshore after release.
4	15:00	all	381	4.11	230	1.36	Deployed ~40m offshore and moved north ~55m before retrieval, drifter 3 moved offshore initially before moving back onshore, without interference
5	15:30	2,3,4,5	166	4.61	220	1.62	Deployed ~30m offshore. Drifters moved north and slightly onshore. Some, particularly drifter 4, followed highly variable, meandering paths.

The deployment period was characterised by a rising tide (Figure 3.3), which resulted in the waterline's shoreward retreat, as represented in Figure 3.4. During the sampling period, the shoreline location was observed to regress by between approximately 6 and 12 m, depending on bathymetric features, which affect the beach face profile slope.
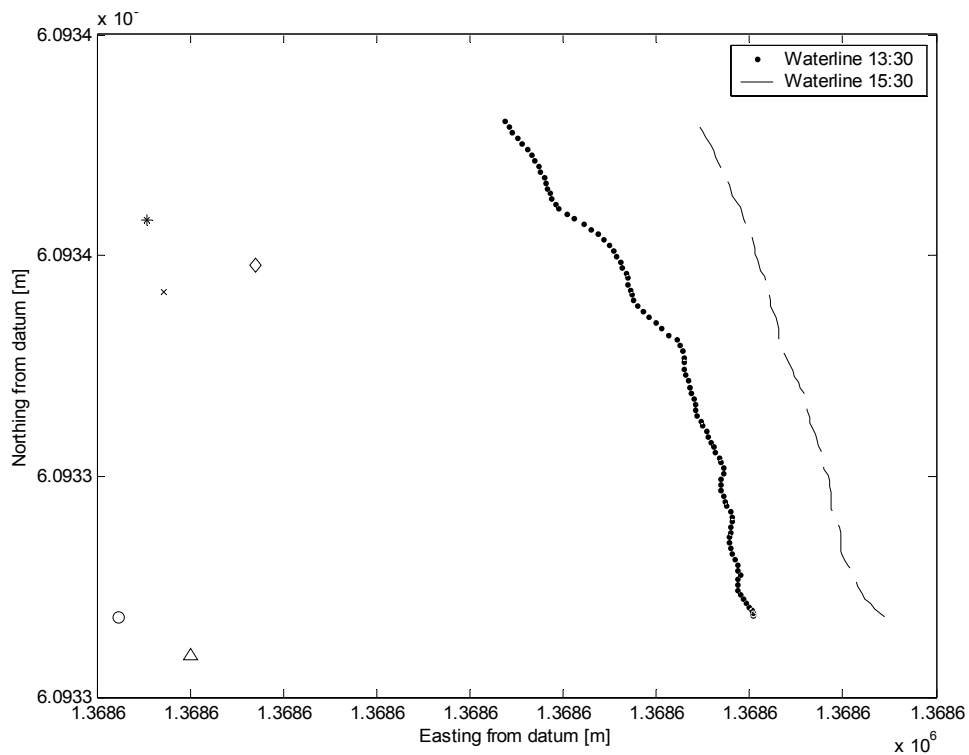
Figure 3.4: Schematic representation of the variance in the shoreline location during the sampling period of two hours. This figure also shows the deployment positions of the individual clusters: Cluster 1 (o), Cluster 2 (x), Cluster 3 (*), Cluster 4 (Δ), and Cluster 5 (◊).

2nd September 2004

The drifters were used in two separate deployments: the first between 9:00 and 12:00 and the second between 13:30 and 16:00. The conditions during the morning deployment were calm with little wind and virtually no waves present (Figure 3.5). Owing to the lack of wind and wave forcing, the drifters' motion was particularly sluggish and clusters took a long time to disperse relatively short distances.

Figure 3.5: Photograph of Henley Beach on the morning of September 2nd 2004 noting the calm wind and wave conditions.

Initially, clusters were released immediately offshore from the mouth of Breakout Creek and tended to meander southwards. Subsequent clusters were released progressively farther north from the rivermouth—a process that was enhanced by the increasing west-southwesterly winds. These winds consequently instigated a steady increase in the northerly longshore drift. A summary of the individual cluster releases completed during the sampling period is included in Table 3.3.

Table 3.3: Summary of drifter deployments on the 2nd of September 2004 (morning) including wind data (courtesy of the Bureau of Meteorology, 2005) and tide data from the nearby gauge at Outer Harbor (Hydrosurvey Australia and Flinders Port Authority, 2005).

Date: 2/09/2004 Morning				Wind			
Cluster	Time	Drifters	Shortest Duration [s]	Velocity [m/s]	Direction [°]	Tide [m]	Comments
1	9:20	all	742	1.5	360	0.916	Cluster moved slowly south and onshore after deployment ~80m offshore from the Breakout Creek outflow. Drifters moved into shallower water and had to be retrieved as the casing was dragging, thus impeding motion.
2	9:45	all	2212	1	30	0.716	Drifters deployed slightly north of Cluster 1, still ~80m offshore. All drifters moved almost directly south ~30 before reversing direction and moving in a NNE direction.
3	10:40	all	713	0.5	330	0.377	Deployed ~65m offshore, ~20m north of previous deployment, drifters moved in a NE direction, before running aground on the shallow sandbar. Drifter 3 didn't move onshore as rapidly and thus was transported ~30 further north then the other drifters.
4	11:35	all	954	4.61	250	0.198	Similar drift pattern as cluster 3 moving onshore and northerly. Drifters 5 and 6 remained further offshore and were recovered when the others ran aground.

The afternoon drifter deployments were associated with vastly different conditions from the morning. The wind was predominantly southwesterly at velocities ranging between 2.6 ms^{-1} and 4. 6 ms^{-1} .The wave conditions were choppy with significant wave heights observed to be in the order of 0.4 m with an associated period around 3–5 s.

Clusters were deployed up to 100 m offshore in water depths approaching 2 m—well beyond the surf zone. They were observed traveling significant distances northwards before being washed ashore. It was also observed that the drifters' velocity increased as they moved closer to the shore. A description of each individual drift is summarised in Table 3.4, which also includes specific wind and tidal measurements at the time of the cluster release.

Table 3.4: Summary of drifter deployments on the 2nd of September 2004 (afternoon) including wind data (courtesy of the Bureau of Meteorology, 2005) and tide data from the nearby gauge at Outer Harbor (Hydrosurvey Australia and Flinders Port Authority, 2005).

Date: 2/09/2004				Wind			
Cluster	Time	Drifters	Shortest Duration [s]	Velocity [m/s]	Direction [°]	Tide [m]	Comments
1	13:30	2,3,4	1025	3.61	260	0.435	Deployed ~60m offshore, cluster drifted north before drifter 3 moved offshore and needed to be recovered
2	14:10	2,3,4	829	3.61	230	0.717	Deployed ~100m offshore, drifters moved in an almost linear fashion to the north east.
3	15:00	2,3,4	569	2.61	220	1.125	Deployed ~30m offshore, drifters moved in an onshore-northerly direction. Drifter 4 changed direction and moved directly offshore, before it was recovered by hand.
4	15:30	2,3,4	512	4.11	250	1.39	Deployed ~35m offshore,drifter 3 moved offshore before, meandering in seemingly random directions, moving slowly shorewards.

Tidal conditions varied significantly between the morning and afternoon deployments. The morning drifter deployments were performed under falling tidal conditions, with the low tide level at Outer Harbor of 0.179 m recorded at 12:15 shortly after sampling finished (HydroSurvey Australia, 2005). Conversely, the afternoon period was characterised by a rapidly rising tide, which had reached a level of 1.63 m by the end of the drifter deployment at 16:00. This was short of the maximum tidal level of 2.116 m recorded at 17:50 (HydroSurvey Australia, 2005). The variation in the shoreline positions during the deployment periods are represented schematically in Figure 3.6, which clearly illustrates the interrelationship between the tidal oscillations and shoreline transgression/regression.

Figure 3.6 shows the beach profile changed dramatically though the tidal cycle. An overall perspective of the beach profiles measured throughout the day is shown in A; B shows a direct comparison of the shoreward transgression over a 70 m section of beach. Between 09:00 and 13:30, the tide fell and the mean water level mark moved offshore; subsequently, between 13:30 and 16:00, the shoreline was observed to advance onshore more than 50 m. During periods of low or falling tides (09:00 and 13:30), the shoreline was located up to 70 m farther offshore than during higher tides. Of particular note is the river outflow clearly shown in A in the 09:00 profile; it is also possible to see the relic discharge channels farther to the north in the 09:00 and 13:30 profiles.
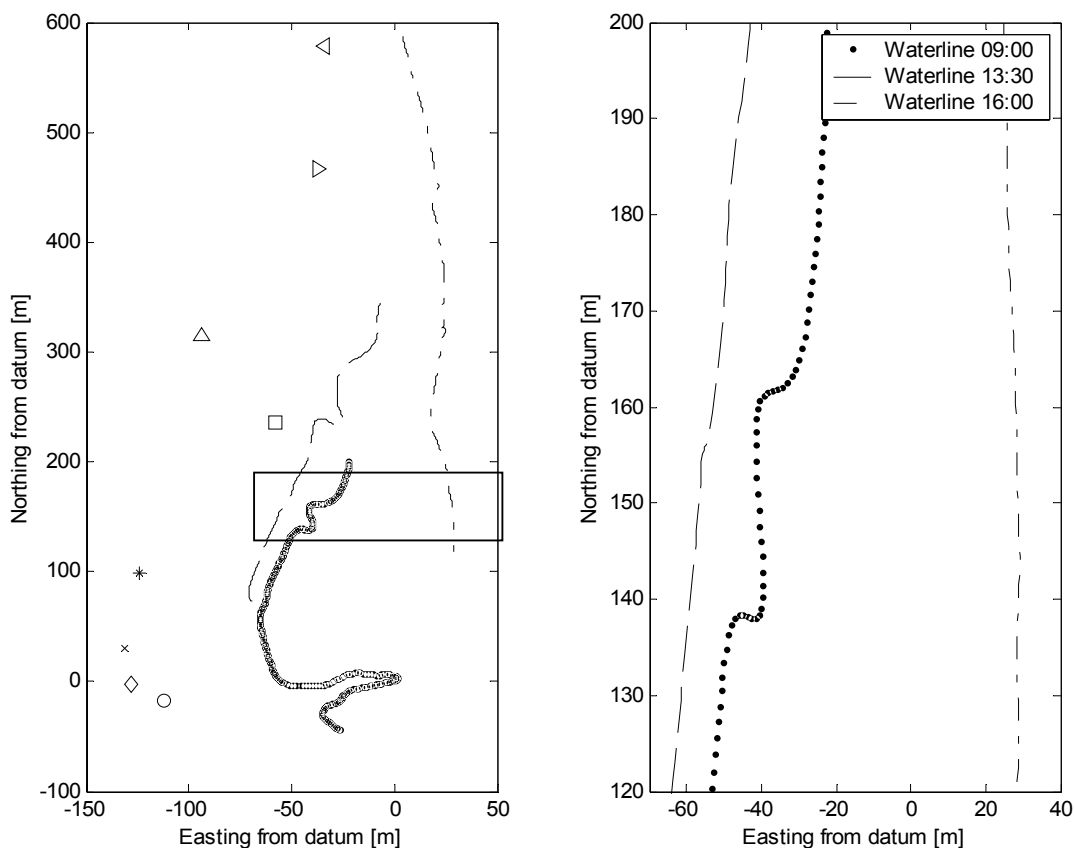
Figure 3.6: Schematic representation of the variation in the shoreline profile through the tidal cycle. The deployment positions of each of the clusters released during the experimental period are noted as follows: from the morning deployments—Cluster 1 (o), Cluster 2 (x), Cluster 3 (*), Cluster 4 (Δ); in the afternoon—Cluster 1 (◊), Cluster 2 (|), Cluster 3 (>), and Cluster 4 (<).

September 3rd 2004

On 3 September, the drifters were deployed in two clusters between 11:00 and 12:00 with drift durations of approximately 20 and 30 minutes, respectively. The winds were relatively calm (not exceeding 3.1 ms^{-1}) and were predominantly from the west-northwest.

Prior to commencing the drifter experiments on the morning of the 3rd, an InterOcean S4 Vector Averaging Current Meter was deployed at a location approximately 2 km offshore from the study site. Consequently, it was recorded that at 11:00 the incident wave regime was approaching from a bearing of 212° (south-southwesterly) with a significant wave height of 0.64 m and a period of 10.6 s.

Table 3.5: Summary of drifter deployments on the 3rd of September 2004 including wind data (courtesy of the Bureau of Meteorology, 2005) and tide data from the nearby gauge at Outer Harbor (Courtesy of Hydrosurvey Australia and Flinders Port Authority, 2005).

Date: 3/09/2004				Wind			
Cluster	Time	Drifters	Shortest Duration [s]	Velocity [m/s]	Direction [°]	Tide [m]	Comments
1	11:20	all	539	1.5	280	0.325	Deployed ~100m from shore, in relatively calm conditions, drifters moved north ~100m before changing direction and moving onshore
2	12:05	all	701	2.61	300	0.212	Deployed ~80m from shore, drifters moved shoreward following an erratic, meandering path, at low velocity. Drifters recovered from shallow water when casing began dragging.

A mixing zone was evident from shore with a clearly defined boundary apparent between the murky brown nearshore waters containing the river discharge and the clearer offshore waters. The drifters were deployed at this boundary layer approximately 100 m from the shore and in water depths close to 2 m. Table 3.5 contains descriptions of the two cluster deployments, the first of which was released at the of the mixing boundary edge while the second was deployed slightly inside of the boundary.
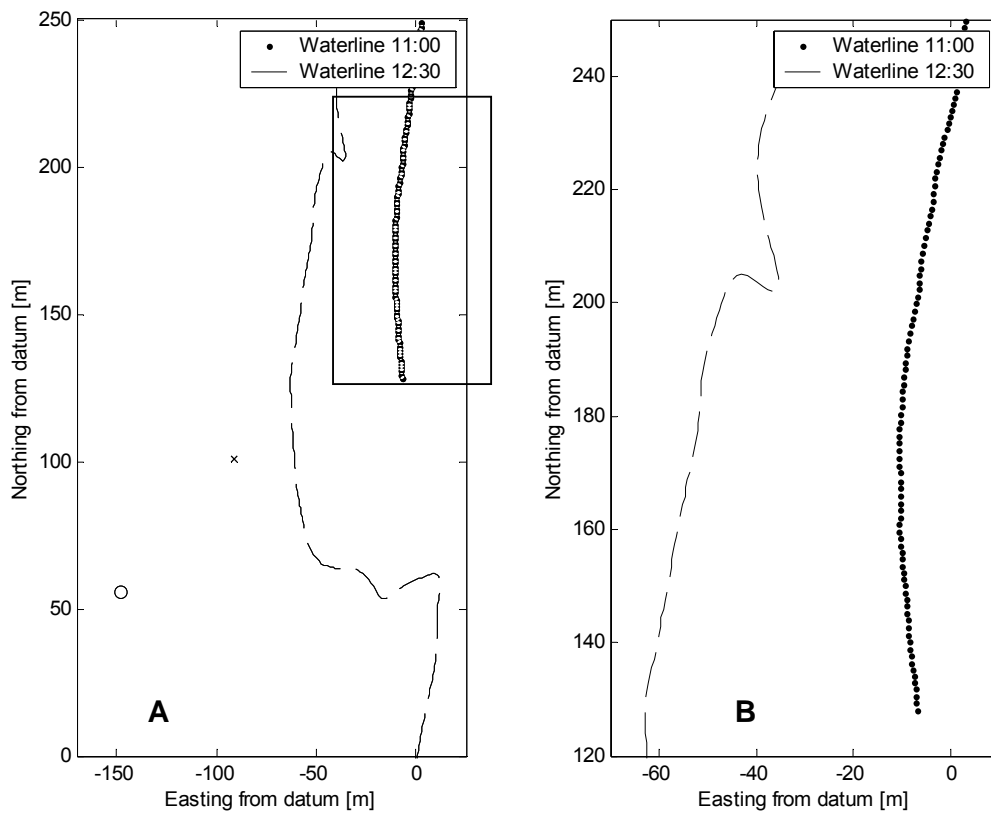
Figure 3.7: Graphical representation of the shoreline profiles observed on the 3rd September 2004. The large (>50 m) and rapid (1.5 hours) transgression in the position of the shoreline is evident between A and B. The points o and x represent the release points of drifts 1 and 2, respectively.

The drifters were deployed during a period of decreasing tides, which fell from 0.427 m at 11:00 to 0.196 m at 12:30 (HydroSurvey Australia, 2005). This decrease was associated with a shoreline transgression of up to 50 m in the areas of shallow sand flat described previously around the river mouth (shown in Figure 3.7).

3.3.2   March 2005

As noted previously, the necessity of traveling interstate to conduct field work prevented the selection of specific conditions for drifter deployments; as such, the 'summer' deployments were performed in early autumn; however, through analysis of the long-term weather records it was evident that the wind conditions, which have the greatest effect on dispersion rates in a sheltered water body such as the Gulf of St Vincent, in March were very similar to those experienced in December, January, and February. Average morning and afternoon wind velocities are compiled in Table 3.6.

Table 3.6: Mean wind speeds collected at Adelaide Airport for the period 1955–2004 (Bureau of Meteorology, 2005).

DEC	JAN	FEB	MAR
Mean 9am Wind Speed (km/hr)			
15.4	13.5	11.5	12.1
Mean 3pm Wind Speed (km/hr)			
23	22.9	21.6	20.5

Table 3.6 shows that while the afternoon wind speed was lower than that experienced in the summer months, it was still substantially greater than the morning readings, and can be interpreted as indicating the presence of an active sea breeze system. The general similarity of the wind regimes across the four months also verified the suitability of using dispersion measurements obtained in March as a proxy for the other months in the wind dominated Gulf environment.

The March 2005 deployments were performed during a period of 'dodge' tides (described in Section 2.1.3.1) and characterised by minimal tidal oscillations. This was due to the effect of the M_2 and S_2, primary semi-diurnal solar and lunar tidal constituents, acting in opposition and effectively cancelling each other out. At equinoxes (including the vernal equinox, which usually occurs around 21 March), the luni-solar diurnal component K_1 and the principal lunar diurnal component O_1 also act in opposition, leading to a period of up to several days during which almost no tidal oscillations are observed (Grzechnik, 2000).

The water level variation observed during the sampling period at the nearby Outer Harbor monitoring station is presented in Figure 3.8. This highlights the low level of tidal variation during the sampling period with the tidal range observed to be in the order of 1 m compared with a maximum of ~2 m observed during September. It is evident that the tides' mode was diurnal during the deployment period, with two high tides and two low tides observed during the tidal cycle. The drifters were deployed daily on a rising tide, allowing the collection of dispersion data across a wide spectrum of tidal levels. The reduced tidal range during the March deployments resulted in minimal shoreline transgression/regression during the tidal cycle when compared with the September deployments.
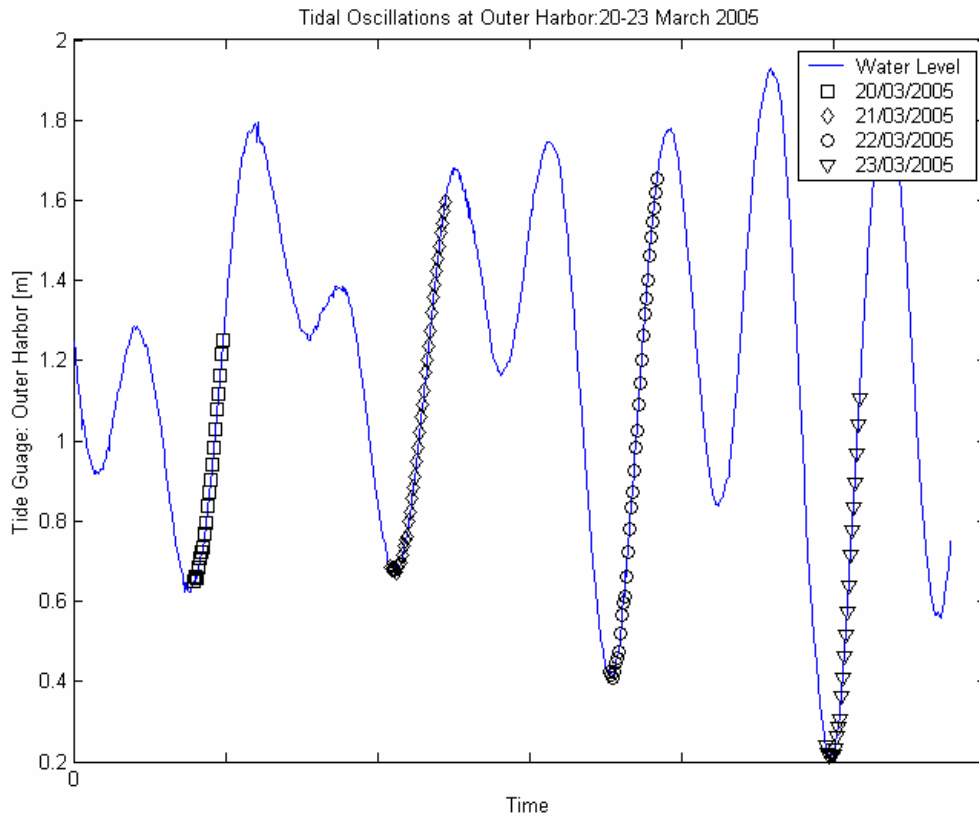
Figure 3.8: Diurnal tidal regime at Outer Harbor, between the 20th and 23rd of March 2005, noting the small range of the 'dodge' tides focusing around the 19th and 20th.

The drifters' deployment was conducted in a manner similar to that previously described during the September experiments; the primary exception being that rather than deploying the drifters in sequence along the beach, resulting in a net northerly progression of drifter deployment sites, drifters were retrieved and redeployed close to the original site. This allowed the comparison of drifter behaviour at a relatively constant location with changing wind, wave, and tidal conditions. While the deployment sites' longshore position was kept relatively constant (northings), the presence of a substantial sandbar parallel to the shoreline provided cross-shore topographic control. Drifters were deployed within the channel and offshore from the sandbar to determine whether the presence of such a feature had any control over dispersion rates.

March 20th 2005

The drifters were deployed in conjunction with the ADCP on 20 March 2005 between 12:45 and 16:25. The ADCP was positioned at 1368505, 6092962 in the UTM zone 53, which correlated to approximately 25 m offshore from West Beach—approximately 200 m north of the Breakout Creek Weir. It was deployed in approximately 2 m water depth in the channel formed in the lee of a substantial sandbar structure running parallel to the shoreline in a N-S direction. The sandbar was primarily located between 30 and 60 m offshore, and at its shallowest point reduced the water depth to approximately 0.5 m. The ADCP's location was used as a reference point, and drifter clusters were released repeatedly within its general vicinity, varying primarily in the cross-shore direction with deployments inside and outside of the sandbar structure (shown in Figure 3.9).
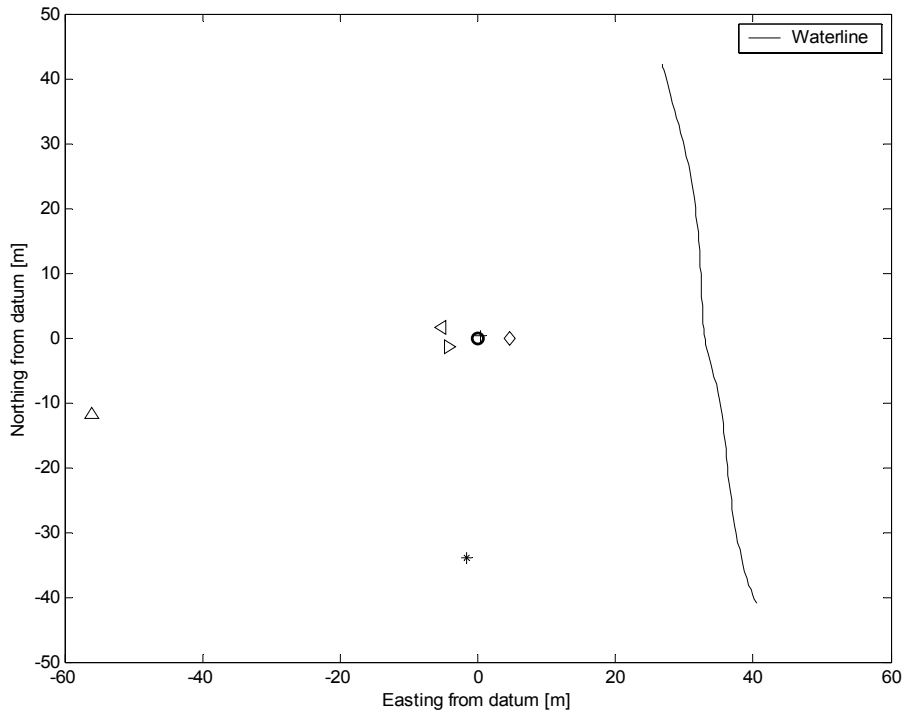
Figure 3.9: Graphical representation of the ADCP (o) location compared to the shoreline and each of the cluster release positions. Cluster 1 (+), Cluster 2 (*), Cluster 3 (Δ), Cluster 4 (◊), Cluster 5 (<), and Cluster 6 (>).

The individual drifters behaved differently after each release owing to the random nature of transport and the dispersive process within the nearshore zone. However, in each deployment, the drifter group tended to follow the same general patterns, specifically, moving in a northwesterly direction, within the channel and offshore from the sandbar, until reaching waters sufficiently shallow that the parachutes, and eventually casing, ran aground and prevented further motion. As soon as drifters were observed to be dragging, they were removed from circulation; in the case of Drifter 6 in Cluster 3, the data obtained from the drifter were removed from analysis completely. A summary of the completed drifts is compiled in Table 3.7.

Table 3.7: Summary of drifter deployments on the 20th March 2005 including wind data (courtesy of the Bureau of Meteorology, 2005) and tide data from the nearby gauge at Outer Harbor (Hydrosurvey Australia and Flinders Port Authority, 2005).

Date: 20/03/2006				Wind			
Cluster	Time	Drifters	Shortest Duration (s)	Velocity (m/s)	Direction (°)	Tide (m)	Comments
1	12:45	5	1151	4.11	250	0.624	Cluster deployed ~40m offshore, directly above the ADCP. Drifters moved NW between 40 and 100m, before D3 ran aground and drift was terminated.
2	13:20	5	989	4.37	245	0.661	Deployed near the ADCP and followed generally NW path. Drifter 4 followed particularly erratic path, moving rapidly on/offshore. Drift terminated when D6 ran around.
3	13:40	4	3271	4.62	240	0.686	Drifters deployed offshore from sandbar ~100m offshore, drifters moved northwards up to 350m. D6 caught on sandbar and removed from data analysis.
4	15:00	5	779	5.14	230	0.902	Deployed near the ADCP and moved northwards ad eventually onshore. D2 and D3, were still offshore when D5 ran aground and had to be retrieved by hand.
5	15:20	3	979	5.14	230	0.985	Deployed at ADCP and followed northerly path up to 160m. D4 and D5 data removed from analysis due to unexplained data irregularities that could not be removed through smoothing.
6	15:40	4	906	5.65	220	1.079	Deployed slightly offshore from ADCP. Followed longshore northerly path, D5 data removed from analysis.

The wind conditions during the deployment were relatively constant between 12:30 and 14:00; however, after this point they increased markedly, reaching 7.2 m/s by 16:30 (Bureau of Meteorology, 2005) and resulting in an increase in activity in the nearshore zone with whitecapping observed from 14:40 onwards. The wind direction was relatively consistent, originally blowing from the west-southwest, but switching to a more direct southwesterly bearing by the time maximum wind speeds were observed.

March 21st 2005

The ADCP was deployed inside the sandbar in a water depth approximately 1.8 m at 10:15 on 21 March, coinciding with the low tide. Deployment conditions changed markedly during the deployment period. The initial morning conditions were dominated by gentle breezes with highly variable directions, predominantly northerly and easterly. No wind-generated waves or white capping was noted. These conditions persisted until around midday, when the wind direction switched to a dominant south-southwest bearing and steadily increased in magnitude to a peak velocity of 8.2 m/s at 18:30 (courtesy of the Bureau of Meteorology, 2005). This behaviour in the dominant wind regime is representative of typical sea breeze activity. Coinciding with the change in the dominant wind regime, the wave climate altered significantly throughout the day from inactive conditions in the morning, under which no wave activity was observed, to an active white capping and 'wind wave' regime typified by short period (2–3 s) locally generated waves (.3 m–0.5 m) breaking near the shoreline as well as on the shallow offshore sand bar. Clusters were released at various locations, including two deployments on the sandbar's seaward side, up to 100 m offshore. These deployment sites are displayed in Figure 3.10. The sandbar's approximate location is marked, and it should be noted that the beach transect profile changed dramatically over this feature; at the ADCP location inside the channel, the water depth was ~2 m, before decreasing to ~0.3 m over the sandbar and increasing to ~ 2 m at the deployment site of Drifter 2.
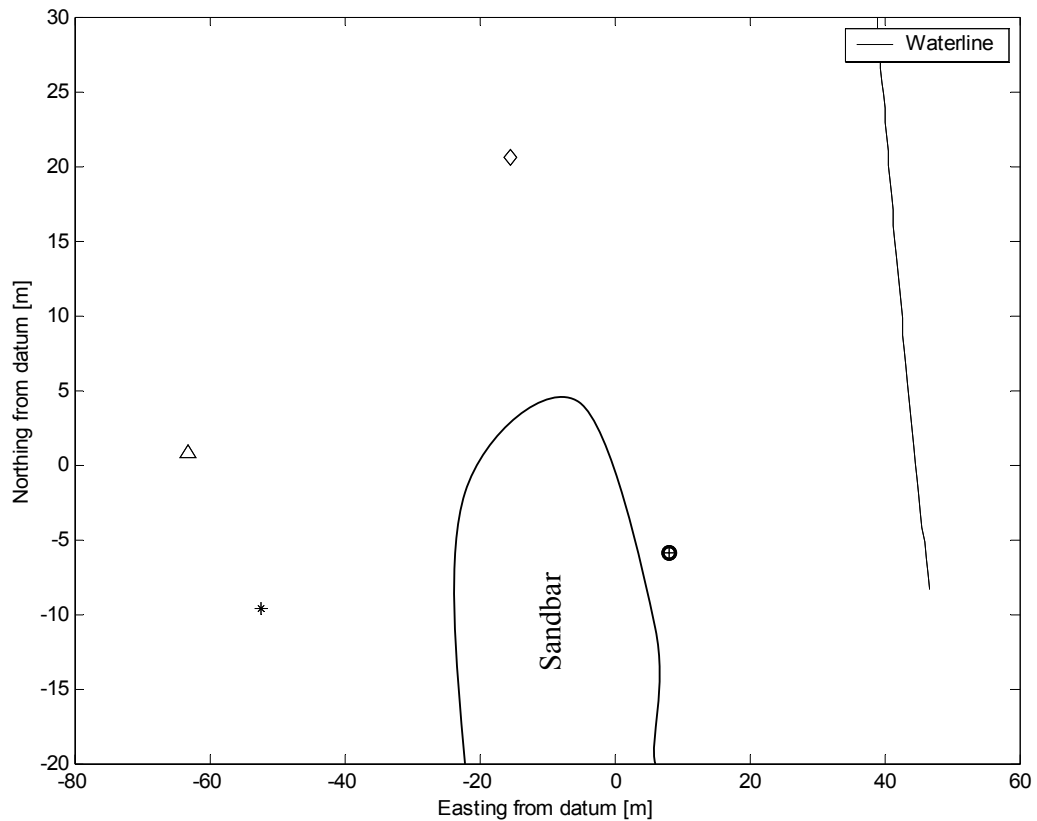
Figure 3.10: Graphical representation of the ADCP (o) location compared to the shoreline and each of the cluster release positions, particularly noting the sandbar's presence, which imposes topographic control on the spatial distribution of local currents. Cluster 1 (+), Cluster 2 (*), Cluster 3 (Δ), Cluster 4 (◊).

The drifters' behaviour (summarised in Table 3.8) was heavily influenced by the dominant wind conditions at the time of deployment; as such, the morning drifter deployments tended to follow southerly paths, while the drifter deployments coinciding with the increase in the sea breeze followed northerly paths.

Table 3.8: Summary of drifter deployments on the 21st March 2005 including wind data (courtesy of the Bureau of Meteorology, 2005) and tide data from the nearby gauge at Outer Harbor (Hydrosurvey Australia and Flinders Port Authority, 2005).

Date: 21/03/2006				Wind			
Cluster	Time	Drifters	Shortest Duration (s)	Velocity (m/s)	Direction (°)	Tide (m)	Comments
1	10:15	5	1113	1.51	30	0.718	Drifters deployed at the ADCP in calm conditions with only a slight north-westerly breeze. Drifters moved in a southerly direction onshore
2	11:26	5	2994	2.05	320	0.674	Drifters deployed offshore from the ADCP in calm. Drifters moved in a southerly direction onshore, skirting around the sandbar before moving more directly onshore.
3	13:15	5	3349	3.59	280	0.899	Deployed ~80m offshore, drifters moved back onshore and southwards (D6) before running aground. Higher tidal levels allowed the drifters to pass areas (the sandbar) previously too shallow for motion.
4	15:40	5	1569	7.2	240	1.422	Drifters deployed offshore from the ADCP. A strong sea-breeze (WSW) was blowing, resulting in a direct NW drift pattern for the drifter cluster, before being they were affected by the wave action, which directed the drifter motion more directly onshore through the localised 'surf' zone

March 22nd 2005

Drifters were deployed on 22 March from 10:00; however, because of technical problems associated with downloading the data, satisfactory results were obtained only from the second drift of the day (initiated at 11:35) onwards. The drifters were deployed at several locations including the ADCP offshore of the sandbar, and to the north of the ADCP inside the channel. These deployment positions are indicated in Figure 3.11, which shows their positions relative to the ADCP and the shoreline.

The wind regime was somewhat atypical to the conditions observed on each of the other days during the sampling period. The conditions were characterised by consistent and relatively strong southeasterly winds, which were maintained and actually intensified throughout the day. These winds resulted in a noticeable level of white capping and generated wind waves that appeared to be moving away from the shore. These conditions instigated a noticeable longshore drift, which could be observed in the longshore motion of detrital matter, primarily seagrass, in a northerly direction.
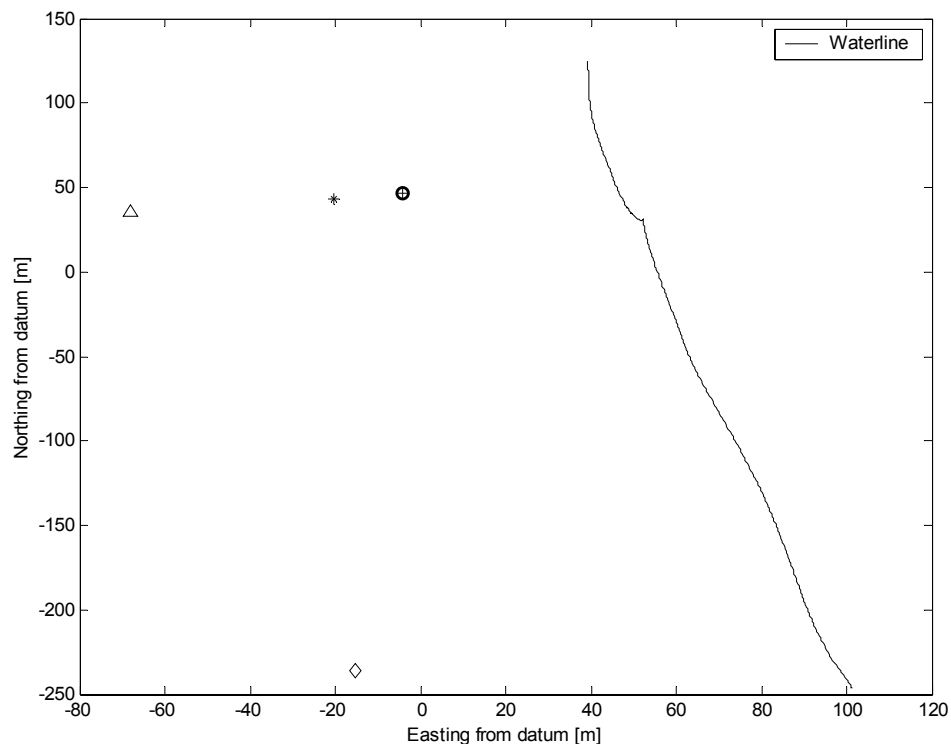
Figure 3.11: Graphical representation of the cluster release positions and the ADCP relative to the shoreline. Cluster 1(Δ), Cluster 2 (*), Cluster 3 (+), Cluster 4 (◊). Note the release position of Cluster 4, which was directly offshore from the Torrens River outflow point.

Significantly, the wind's easterly component influenced the drifters' motion, as rather than promoting an onshore flux in the water column's surface layer, a significant offshore drift was generated. This resulted in the drifters being transported in a northeasterly direction and necessitated the author swimming significant distances offshore to retrieve them. A brief summary of each of the cluster deployments is included in Table 3.9.

Table 3.9: Summary of drifter deployments on the 22nd March 2005 including wind data (courtesy of the Bureau of Meteorology, 2005) and tide data from the nearby gauge at Outer Harbor (Hydrosurvey Australia and Flinders Port Authority, 2005).

| Date: 22/03/2006 | | | | Wind | | | |
Cluster	Time	Drifters	Shortest Duration (s)	Velocity (m/s)	Direction (°)	Tide (m)	Comments
1	11:35	5	2028	5.14	140	0.475	Drifters deployed offshore from sandbar and travelled ~400m north and 60m further offshore before retrieval ~160m from shore. Drifters did not run aground and were retrieved due to their substantial offshore motion.
2	12:20	5	1443	6.68	150	0.612	Drifters were deployed ~ 20m offshore from the ADCP on the same northing. The drift pattern was similar to cluster 2 with the drifters moving northwards and offshore before retireval from deep water.
3	2:20	5	1301	7.2	150	1.262	Drifters deployed at the ADCP, retrieved after being transported northwards and offshore up to 270m and 80m respectively
4	2:45	5	2976	7.2	150	1.39	Deployed at the outflow point of Breakout Creek ~250m south of previous deployments. Drifters followed path largely parallel to the shore before moving offshore around the same position as the previous clusters.

March 23rd 2005

The ADCP was not used on 23 March, as it was unavailable for deployment. Rather, the experimentation's focus was to obtain multiple samples of dispersion and flow field characteristics over the same section of beach to be able to derive the experimental area's average flow field, as conducted by Mariani (2005) and Johnson (2004). This involved repeatedly deploying the drifters at close to the same location, under relatively constant conditions, to determine the mean flow characteristics over that area. This also served the purpose of obtaining multiple measures of dispersion rates over the same area, allowing the analysis of the inherent variability in the co-efficient. The cluster deployment positions and the shoreline's profile are represented in Figure 3.12.
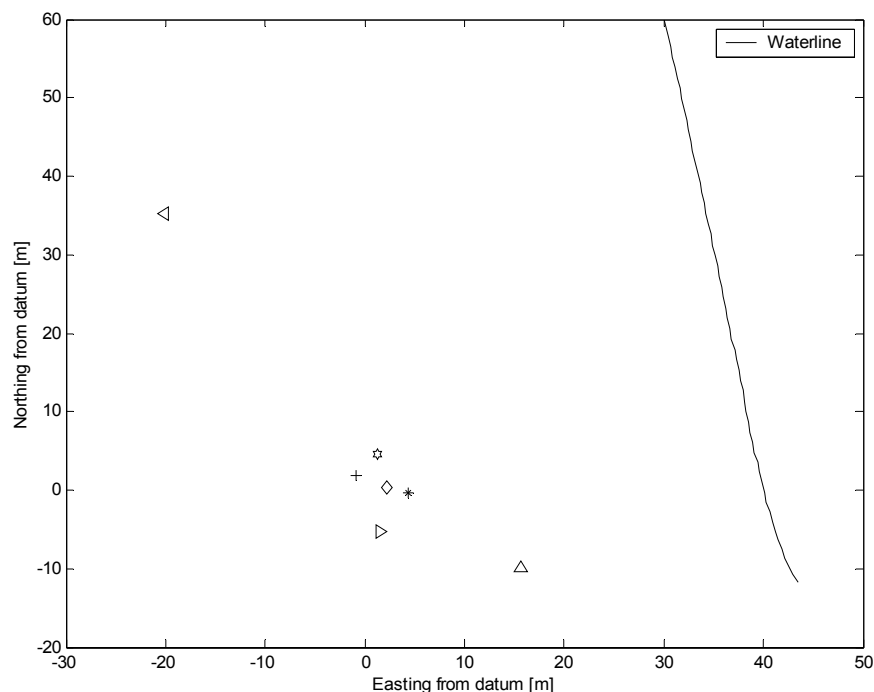
Figure 3.12: Release positions of the drifter clusters on the 23rd of March noting the high number of drifts repeated around the coordinates (0,0).

The drifters' behaviour during the various deployments was very similar. This was not unexpected given the similarity of their deployment locations. This similarity was enhanced by the consistency of the wind conditions during the experimental period. Only a relatively minor intensification in the wind magnitude was experienced from 2.57 m/s to 5.17 m/s along with a mild deviation in the mean wind direction from an easterly (bearing 110°) at the beginning of the deployments to a south-southeasterly (bearing 160°) at the time the last cluster was released. These wind conditions drove drifter motion contiguous with that experienced previously on the 22nd, specifically, northwards longshore drift. Offshore directed drift was also noted; however, the drifters' path was largely confined by the sandbar. Upon reaching the northern extent of this feature, it was ensured they were recovered before being transported any significant distance offshore. A summary of drifter deployments and their behaviour subsequent to release is included in Table 3.10.

Table 3.10: Summary of drifter deployments on the 23rd March 2005 including wind data (courtesy of the Bureau of Meteorology, 2005) and tide data from the nearby gauge at Outer Harbor (Hydrosurvey Australia and Flinders Port Authority, 2005).

Date: 23/03/2006				Wind			
Cluster	Time	Drifters	Shortest Duration (s)	Velocity (m/s)	Direction (°)	Tide (m)	Comments
1	9:55	5	1510	2.57	110	0.311	Deployed in calm condition inside the sand bar at a depth of ~1.5m. Cluster centoid moved north, parallel to the shoreline until D2 ran aground.
2	10:57	5	1117	4.11	100	0.22	Deployed close to shore inside the channel. Northerly motion was observed to be quite rapid through the channel with little cross-shore dispersion.
3	11:30	5	642	4.11	130	0.262	Drifters again deployed inside the sandbar. Transported north, parallel to the coast. Retrieved before they were taken to far offshore.
4	11:55	5	792	4.11	140	0.323	Drifters again deployed inside the sandbar. Transported north, parallel to the coast. Retrieved before they were taken to far offshore.
5	12:20	5	776	4.62	130	0.461	Deployed on sandbar, transported, onshore over edge of sand bar and north parallel to the coast.
6	12:47	4	881	4.62	180	0.607	Drifters again deployed inside the sandbar. Transported north, parallel to the coast. Retrieved before they were taken to far offshore.
7	1:15	5	918	5.14	160	0.801	Drifters again deployed inside the sandbar. Transported north, parallel to the coast. Retrieved before they were taken to far offshore.

3.4   Data Analysis

A range of analysis techniques was required to convert the raw data from the ADCP and the drifters into the desired information. The majority of this processing used MATLAB and was concerned predominantly with determining dispersion characteristics from the drifter data and mean current profiles from the ADCP. The methodology involved with this processing is described in Sections 3.4.1 and 3.4.2, which focus on the drifter and ADCP data, respectively.

3.4.1   Lagrangian Drifters

A substantial amount of data processing and analysis had to be undertaken to obtain meaningful results from the drifter experiments. The raw data were downloaded from the individual drifters subsequent to each deployment or series of deployments. These data were then processed into a useable format and analysed by hand to determine cluster points from which subsequent analysis derived dispersion values.

Initial Processing

The drifters store data according to the National Marine Electronics Association (NMEA) default format, which includes the location, time, and date at a frequency of 1 Hz, as seen in Table 3.10. The location is recorded in latitude and longitude positions with an accuracy of 0°0.0001", or approximately 0.16 m of easting and 0.19 m of northing at a latitude of 32° south (Johnson, 2004). Johnson's (2004) analysis of measurement errors also determined the displacement standard deviations were 1.24 m and 1.98 m for easting and northing, respectively, and over 95% of location fixes fell within circles of radii 2.2 m and 3.6 m, respectively. Johnson (2004) also demonstrated that the non-differential GPS fixing system was sufficient to measure accurately motions with frequencies below 0.05 Hz. This was not as high as the differential GPS system Schmidt et al. (2003) utilised, which was accurate for frequencies as high as 1 Hz, but was suitable for use in the measurement of longer period motion in the surf zone.

Table 3.11: Example of the raw data downloaded from the data loggers.

Raw Drifter Data

Status	Northing	Label	Easting	Label	Time (s)	Date
V	3501.96	S	13834.505	E	24838	10904

The raw recordings from the drifters were downloaded to computer using the software package 'Data Download Version 5.5.6'. These data were then converted to the Universal Transverse Mercator (UTM) coordinate system for all further analysis using a MATLAB script developed by Johnson (2004). UTM coordinates project latitude and longitude coordinates onto a concentric cylinder to minimise distortion experienced in distances at high latitudes, thus allowing the representation of latitude and longitude coordinates on a 'flat' map. The UTM system divides the earth into 60 zones, each six degrees of longitude wide. These zones define the reference point for UTM grid coordinates within the zone and extend from a latitude of 80° S to 84° N. UTM grid coordinates within each of the zones are expressed as a distance in metres to the east and north. Adelaide is located in Zone 53, and an example of the UTM coordinates converted from the raw data is presented in Table 3.12.

Table 3.12: Example of data converted from latitude/longitude coordinates to the UTM co-ordinate system.

Converted UTM co-ordinates

Easting	Northing	Time	Date (Julian)
1374218.40	6083107.00	16977	1706

The raw data recorded by the drifters contained a level of scatter due to limitations in the technology's capacity (as outlined in Section 3.1.2) as well as high frequency oscillations induced by the passage of waves. The drifter parachute largely neutralized the wave-induced oscillations; however, on some occasions, the drifter was rapidly transported onshore with the wave bore in what is termed a 'surfing' event. These effects acted to introduce short duration scatter into the dataset, which was not indicative of the underlying current properties; as such, it was necessary to remove the distortion caused by these effects through a smoothing process. Smoothing was applied to the converted UTM coordinates using a MATLAB script developed by Johnson (2004). The script required the data's input to be smoothed and a specification of the pass-band filter to be applied. The smoothing program had the effect of removing oscillations in the data set with frequencies

higher than the prescribed pass band, which, in most cases, was set at 0.1 Hz. At a pass-band filter of 0.1 Hz, the effects of waves with periods of the order of 5–10 seconds (frequencies of 0.2–0.1 Hz) were effectively removed from consideration, as were momentary measurement errors derived from the GPS.

In order to perform dispersion calculations, the smoothed datasets had to be analysed by hand to determine the location of clusters—points where all the drifters were at the same location at the same time. This was one of the most time consuming elements of the data analysis. The smoothed data sets for each of the drifters were plotted on the same graph in Microsoft Excel to determine the cluster points' location. Once these points had been identified, the subsequent drift patterns were analysed to determine the drift's end point. The end point was usually characterised by a rapid change in velocity and/or direction, indicating the drifter had been retrieved by hand, and in some cases the drift plot was compared with the shoreline to determine when the drifter ran aground. Once the drift's beginning and end points had been located within the full dataset, the data specifically representing the drift period were copied into separate files. The data for each drifter for each cluster were separated in this manner, resulting in a total of 63 individual files for the September deployments alone. The data in these files were in UTM coordinates; as such, each point was referenced according to UTM Zone 53. While this was accurate, the coordinates' values were very high; thus, for simplicity, all the 'broken up' drifter files were re-referenced back to the individual cluster origin (Table 3.13). Essentially, this represented the creation of a new datum point at the point of release for each cluster. These files formed the basis of all further analysis.

Table 3.13: An example of the process involved in the re-referencing of the coordinates datum point to the cluster origin. No accuracy is lost in this process.

Original co-ordinates - Cluster origin: 1368444, 6092903

Easting (m)	Northing (m)	Time (s)	Date (days)
1368443.6	6092902.5	19001	1708

Re-referenced Co-ordinates

Easting (m)	Northing (m)	Time (s)	Date (days)
-0.4	-0.5	19001	1708

The Dispersion Coefficient

The calculation of the dispersion coefficient was based on List et al.'s (1990) work analysing drifter dispersion in waters offshore from southern California, which Johnson (2004) and Olsson (2004) later used in the surf zone. The first step of the analysis is the determination of the drifter paths' centroid. The centroid's location at a given time is the instantaneous average of each of the drifter's easting and northing coordinates. This is determined individually for the x and y coordinates using:

$$\overline{x}_i = \frac{\sum_j x_{ij}}{N} \qquad \overline{y}_i = \frac{\sum_j y_{ij}}{N} \tag{17}$$

where N is the number of drifters and (x,y) are the co-ordinates of a drifter j at time i. The variance of the drifters is subsequently determined as the squared sum of differences between the centroid and the location of each drifter as described by (List et al., 1990):

$$\sigma^2_{x_i} = \frac{\sum_j (x_{ij} - \bar{x}_i)^2}{(N-1)} \quad \sigma^2_{y_i} = \frac{\sum_j (y_{ij} - \bar{y}_i)^2}{(N-1)} \tag{18}$$

This result provides the variance in the x and y coordinates; however, the drogue distribution dispersion, as defined by Okubo (1974) and cited by List et al. (1990), is determined as a mean of both of these results:

$$\sigma^2_i = \frac{(\sigma^2_{x_i} + \sigma^2_{y_i})}{2} \tag{19}$$

When σ^2 is used, it is possible to calculate the relative dispersion coefficient K (Johnson, 2004; Okubo, 1974) using the relationship (see also Equation 6):

$$K(t) = \frac{1}{2} \frac{\partial \sigma^2_i}{\partial t} \approx \frac{1}{2} \frac{\Delta \sigma^2_i}{\Delta t} \tag{1}$$

The preceding calculations were all performed using a specifically developed MATLAB script, which requires only the input files' names in order to run. The script determines the centroid location, which is then used in the variance calculation σ^2, σ_x^2, σ_y^2. These variances are then plotted with time, as shown in Figure 3.13. The gradient of the least squares regression line of best fit is equivalent to the dispersion coefficient K, as described above in Equation 20 and in Section 2.3.3.2, Equation 6.
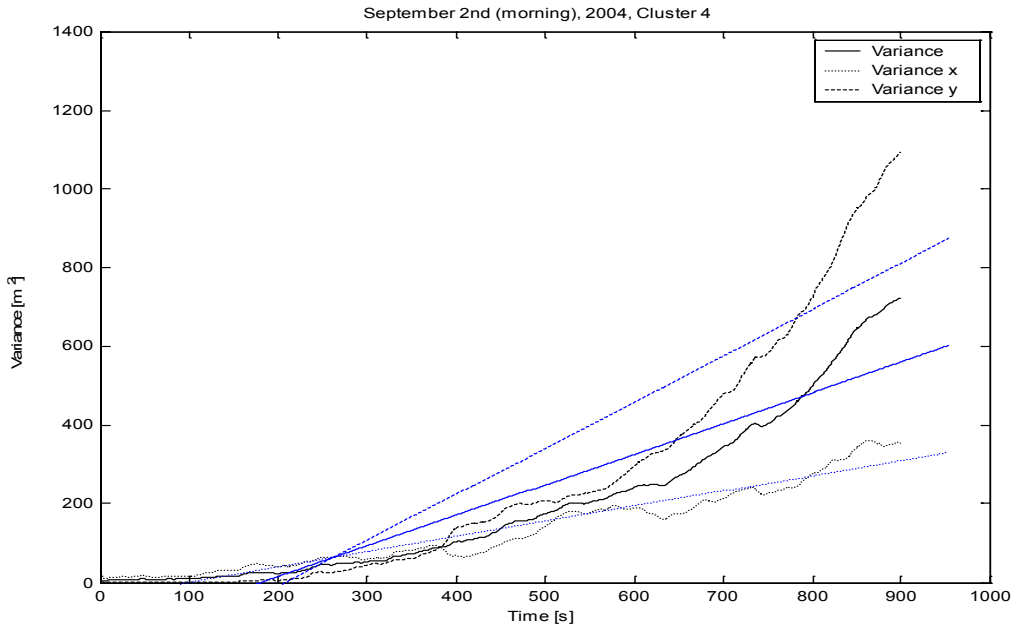
Figure 3.13: Calculation of the values of K as the gradient of the least squares line of best fit for the plot of σ2 with time.

K was determined using the data from the entire duration of the cluster, as opposed to during periods of rapid dispersion such as Johnson (2004) conducted in the analysis of rip head dispersion. The coefficient of determination r^2 was also determined for the least squares line of best fit to quantify the accuracy of the relationship between the regression line and the raw data. Values of K, K_x, and K_y with associated r^2 values less than 0.5 were deemed insufficiently representative of the data and were excluded from further analysis.

Dispersion coefficient values that were not removed from consideration in this manner were compared with the average values were excluded if they differed by a factor of 10 or more. This occurred in only two cases, and in both situations, the data appeared to have been unduly biased by a short period of rapid dispersion combined with a relatively short period of deployment. The remaining values were analysed to determine the value of the mean, and subsequently, the 95% confidence intervals.

As noted by List et al. (1990), the relationship between K and σ^2 is valid only for a large number of drifters and under the assumption that any one cluster is fully representative of an ensemble. Johnson (2004) also noted that a similar approach could be used to determine the directionally dependent values K_x and K_y from σ_x and σ_y, respectively, representing the cross-shore and longshore components of dispersion, respectively.

Values of K, K_x, and K_y were determined for each of 37 clusters by plotting σ^2, σ^2_x, and σ^2_y against time, and finding the gradient of the linear least squares regression line.

Scale Dependence

The dispersion coefficients K, K_x, and K_y were calculated for 1 m bins of standard deviation σ to represent the relationship between the rate of dispersion and the cluster size. This employed a MATLAB script, which initially determined σ the standard deviation of the drifter clusters. Dispersion coefficient K values were then calculated for each 1 m increase in σ, resulting in independent dispersion coefficient values for each 1 m increase in the drifter deviation. K was calculated by determining the amount of time the value of σ remained in the specified 1m range (Δt) and comparing this with the change in σ^2 during the period ($\Delta\sigma^2$).

> From t1 to t2, the cluster increases by $\sigma2 - \sigma1$ thus representing Δt and $\Delta\sigma^2$ respectively. These values are related by:

$$K(t) = \frac{1}{2}\frac{\partial \sigma_i^2}{\partial t} \approx \frac{1}{2}\frac{\Delta\sigma_i^2}{\Delta t}$$

> As such, it is possible to calculate K1 over the interval, $\sigma1$ to $\sigma2$.
> Subsequent, iterations for increasing σ values allows the calculation of K1-Kn where n is the maximum average deviation of the drifters from the cluster mean
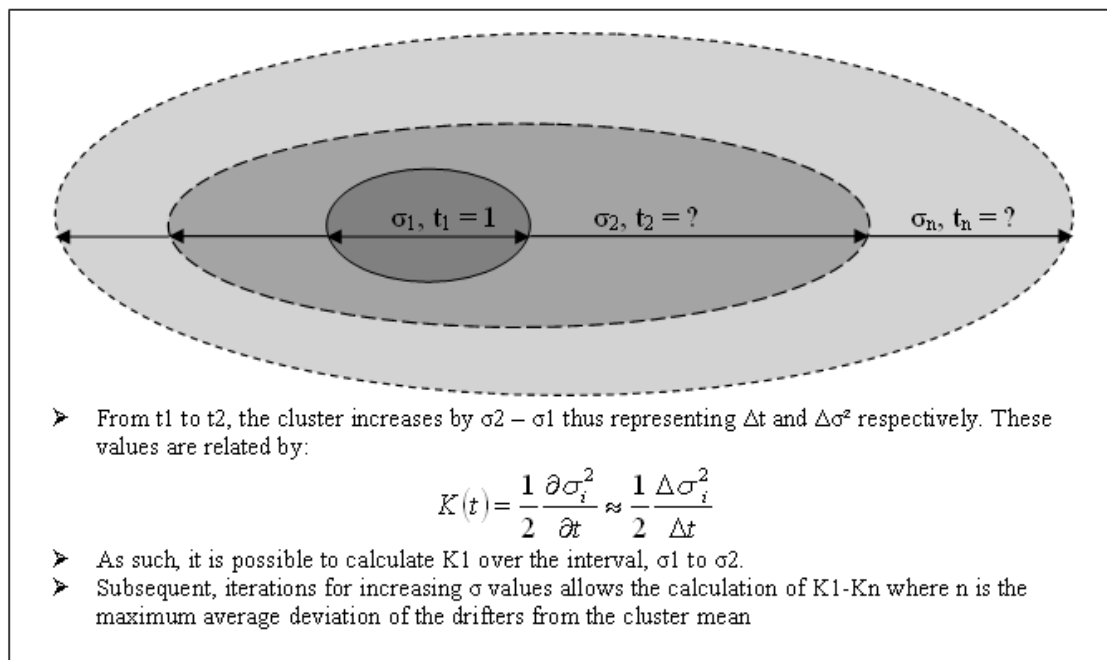
Figure 3.14: Schematic representation of the methodology involved in calculating K for increasing cluster deviation.

These values were then used to calculate K through the relationship described by Equation 20. This process is represented schematically in Figure 3.14. Identical procedures were also used in the cross-shore and longshore directions in determining the relationships between K_x, K_y and σ_x, σ_y, respectively. Following the determination of the dispersion coefficients K, K_x, and K_y for the 1 m increments of σ, σ_x, and σ_y, log-log scale graphs were plotted for each of the clusters. The dispersion coefficients were plotted on the vertical axis against the standard deviation (shown in Figure 3.15).
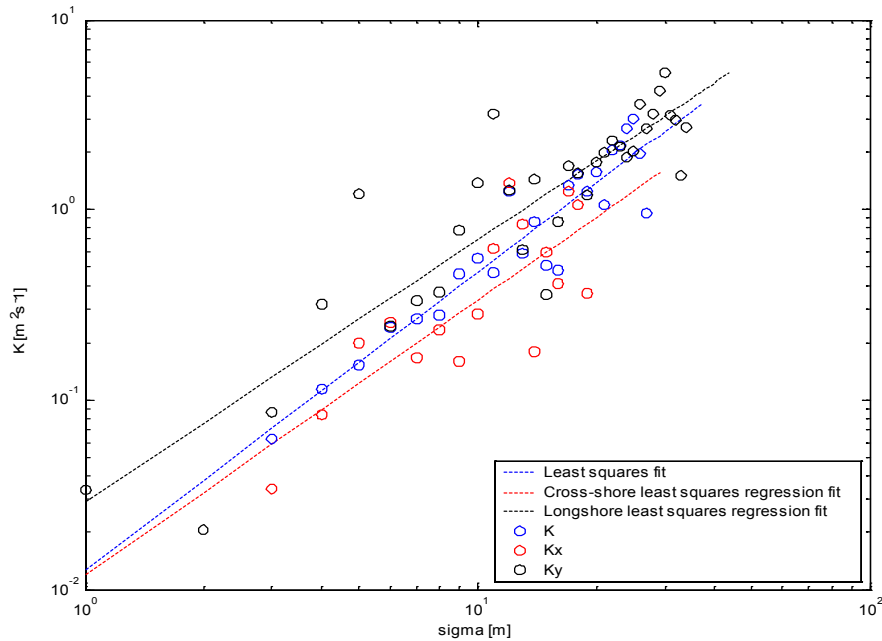
Figure 3.15: Example of the graph derived when the dispersion coefficients K, K_x, and K_y were plotted against 1 m increments of σ, σ_x, and σ_y.

A linear least square regression line of best fit was determined for the log-log plots; however, as the raw data described a non-linear function, it was transformed into a linear function using the parameters outlined in Table 3.14. These transformed the raw data, which is described by a non-linear relationship, $y = c_1 x^{c_2}$, to a format where it could be described by a linear relationship, $v = \alpha u + \beta$. The line of best fit coefficients were determined for the transformed data, and then transformed back to the original format. The lines of best fit coefficients represented the relationship between the drifters' average deviation in the cluster and the rate of dispersion.

Table 3.14: The data transformation used in the fitting of the least squares line of best fit (adapted from Recktenwald, 2000).

Non-linear Function of C_1 and C_2	Transformation to: $v = \alpha u + \beta$
$y = C_1 x^{c_2}$	$v = \ln(y)$ $u = \ln(x)$ $\beta = \ln(C_1)$ $\alpha = C_2$

After determining the variables in the line of best fit, the values were compiled and analysed. As with the method used in the analysis of dispersion coefficients, line of best fit coefficients with associated r^2 values less than 0.5 were deemed insufficiently representative of the data and were excluded from further analysis. Coefficient values that were not removed from consideration in this manner were compared with the average values and were excluded if they differed by a factor of 10 or more. The remaining values were analysed to determine the value of the mean, and subsequently, the 95% confidence intervals.

3.4.2 Eulerian ADCP Measurements

The ADCP was deployed on only three days, from which only a single full day's measurements were obtained. Current velocity recordings were derived at a frequency of 1 Hz in three dimensions for individual cells positioned at 10 cm intervals from the sensor head to the water surface. The velocities recorded in each of the three dimensions (vertical, longshore, and cross-shore) were stored in individual data files, thereby allowing individual analysis. Pressure data were also recorded at a frequency of 1 Hz, allowing for the calculation of wave and tide-based water level oscillations.

Analysis of current profiles was conducted using MATLAB. The data files were loaded into the program prior to the initiation of a script developed by the author. The script was then used to conduct some relatively simple procedures. Specifically, the mean velocity values in each cell were determined, thus allowing them to be plotted relative to the seafloor. Such plots were determined in the cross-shore and longshore domains in conjunction with the derivation of the mean water depth and the depth averaged current velocity. By selecting the relevant data points, it was possible to determine velocity profiles for given periods of time, thus allowing the comparison of morning and afternoon conditions.

The ADCP ran out of memory on 22 March, as the storage facility had not been erased prior to deployment. This resulted in an incomplete dataset being recorded from 10:00 until 12:54 despite the ADCP having been deployed from 10:00 until ~16:30.

3.4.3 Nearshore Directional Wave Measurements

Two directional wave recorders were deployed in the Adelaide nearshore waters between 3 September 2004 and 25 October 2004 (Figure 3.16). The southern location, offshore Brighton Beach, consisted of an InterOcean S4DW electromagnetic current meter, while the northern location, offshore Henley Pier, consisted of an RD Instruments' 600 KHz Acoustic Doppler Current Profiler with the directional wave option. Although the instrument collected reliable data in terms of currents, either a malfunction in the pressure sensor or the movement of the mooring (its mean depth changed from 6 m to 2 m during the deployment period) resulted in unreliable data for waves. Hence, only data collected from the S4DW instrument for the period 3 September 2004 to 16 October 2004 will be presented here.
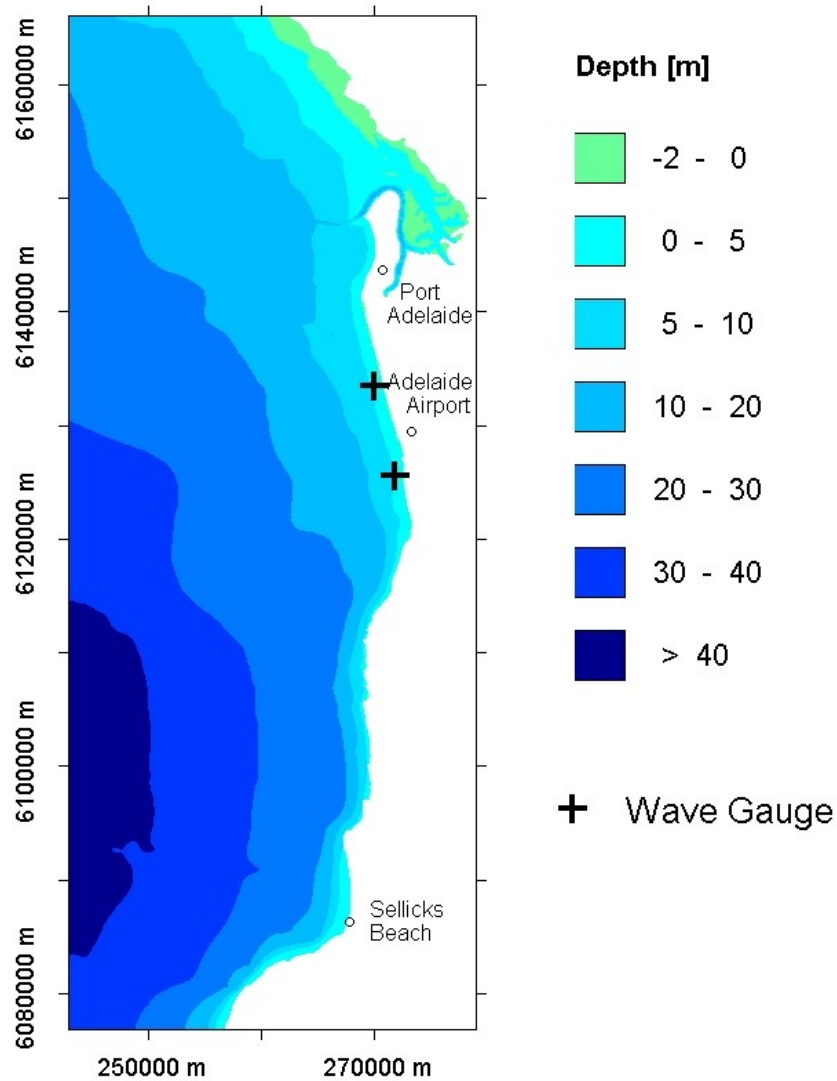
Figure 3.16: Location of the directional wave gages along the Adelaide Metropolitan region.

The S4DW current meter comprises a pressure to measure the water surface vertical excursion and electromagnetic velocity sensors to measure the horizontal currents. Velocities are measured using the principles of Faraday's Law of electromagnetic induction. Here, as the water flows through an electromagnetic field generated by the current meter, it produces a voltage proportional to the water flow velocity past the sensor. Two orthogonal pairs of electrodes located symmetrically on the sensor sense this induced voltage, and an internal flux-gate compass measures current direction. The sensor was programmed to burst sample at a sampling rate of 2 Hz (i.e., once every 0.5 s) for 20 minutes every 2 hours yielding 2400 data points per burst.

The data analysis was undertaken using DIWASP (DIrectional WAve Spectra) Toolbox (Version 1.1) for MATLAB, which was developed at the Centre for Water Research (Johnson, 2004). DIWASP is a toolbox of MATLAB functions for the estimation of directional wave spectra with five estimation methods available: Direct Fourier Transform Method (DFTM), Extended Maximum Likelihood Method (EMLM), Iterated Maximum Likelihood Method (IMLM), Extended Maximum Entropy Method (EMEP), and Bayesian Direct Method (BDM). The EMEP was chosen for use in this study, as this method provided the best overall results. The speed and direction data recorded by the current meter were resolved into east-west and north-south components for use with the DIWASP toolbox.

4. Results and Discussion: Nearshore Waves and Currents

4.1 Directional Wave Data

Time series of wave height, period, and direction together with wind vectors are presented in Figure 4.1. The wave height series shows a diurnal variation (maximum of 0.5 m) due to tide-induced changes in water depth. The mean and maximum wave heights on 8 September were 0.5 m and 1.7 m, respectively, and the wave period ranged from 3 to 12 seconds. Here, the lower periods coincided with storm events, while the longer periods were associated with 'calm' periods when swell was dominant. The wave direction ranged between 20° and 40° indicated waves (wave direction is presented as positive anti-clockwise relative to east) incident from the southwest (between 230° and 250°).
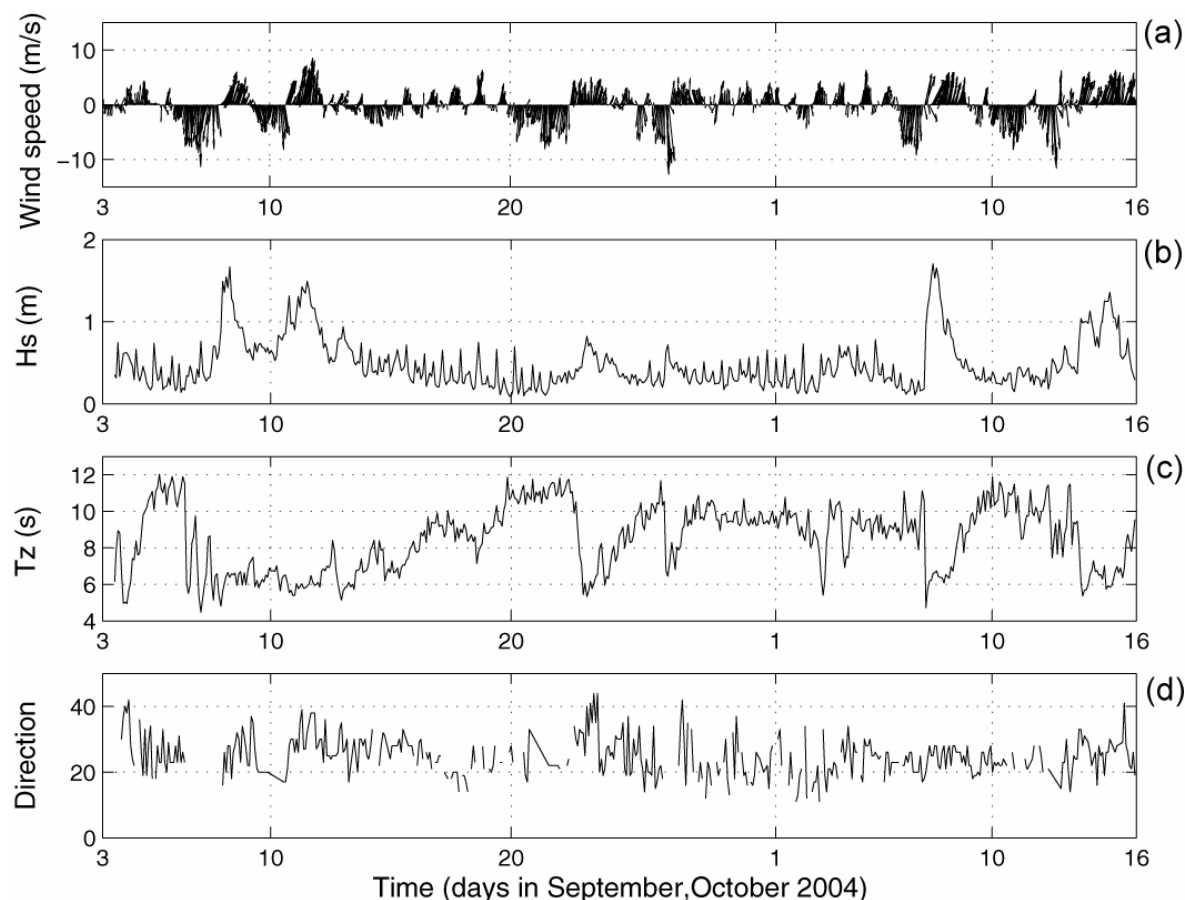
Figure 4.1: Time series of (a) wind vectors; (b) significant wave height (Hs); (c) zero up-crossing period (Tz); and, (d) the mean wave direction obtained offshore Brighton Beach. Note: wave direction is presented as positive anti-clockwise relative to east.

The wave heights over the whole measurement period indicated the occurrence of four storm events: (1) 8 September; (2) 10–11 September; (3) 7–8 October; (4) 14–15 October. Interestingly, these storm events coincided with the southwesterly winds although stronger winds from the north and northwesterly directions were recorded during the measurement period (Figure 4.1a). This indicated that only winds from the southwest quadrant were capable of generating higher waves in the region. In the absence of locally generated waves, the decrease in wave heights were associated with an increase in the wave periods (e.g., between 12 and 21 September), showing the transition from a locally generated sea to swell dominated system. This is highlighted in the wave spectra (Figure 4.2), which indicate a range of frequencies (periods ranging from three to ten seconds) present during the four southwesterly storms, and an absence of wave energy from any direction other than the southwesterly quadrant.
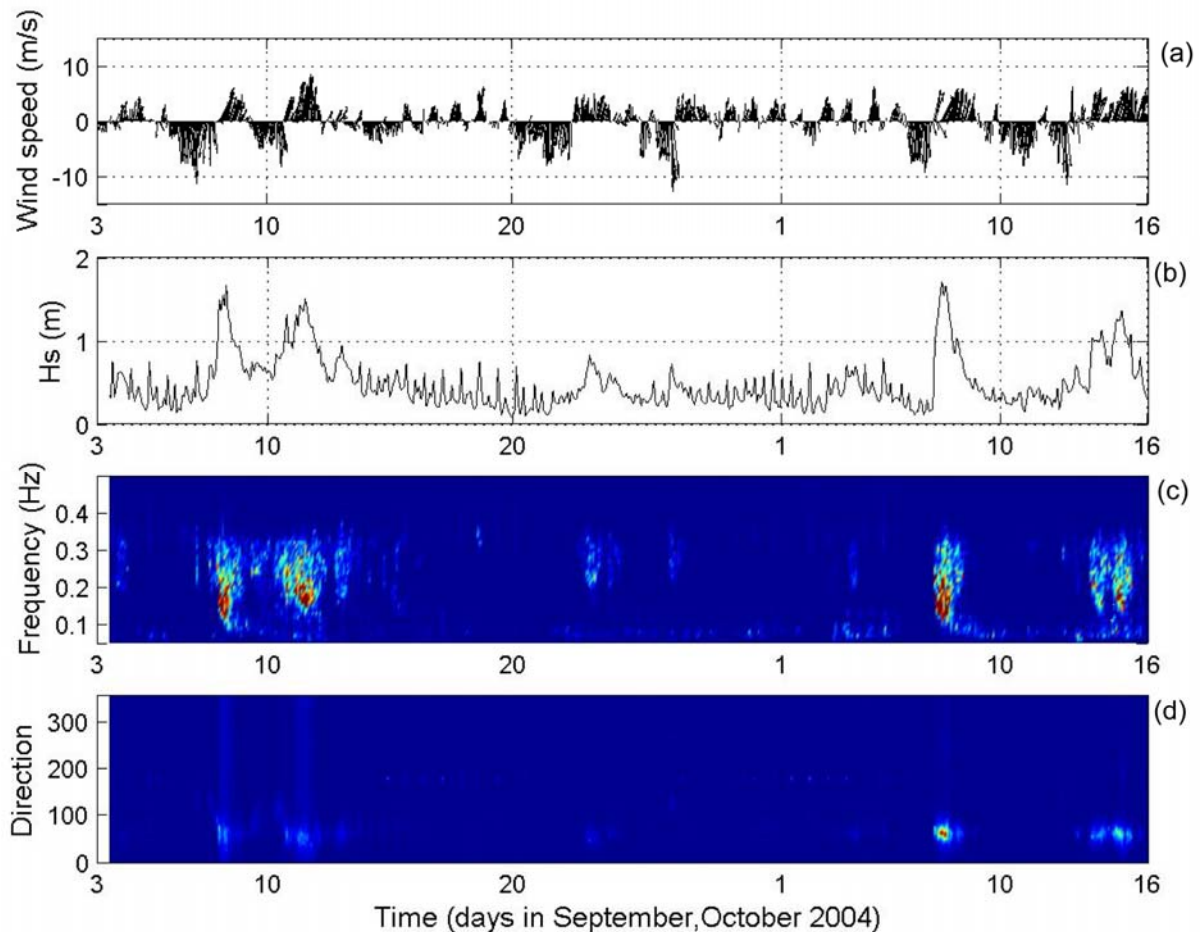
Figure 4.2: Time series of (a) wind vectors; (b) significant wave height (Hs); (c) the amplitude spectrum; and, (d) wave direction spectrum obtained offshore Brighton Beach. Note: wave direction is presented as positive, anti-clockwise relative to east.

Examples of individual wave spectra (Figure 4.3) show three different wave climates experienced in the Adelaide coastal waters over three days before, during, and after a storm: (1) a swell dominated period with a significant wave height of 0.2 m, peak period 11 s incident from the southwest; (2) with a significant wave height of 1.0 m, peak period 4 s incident from the southwest; and, (3) a bi-modal spectra where waves of 10 s and 5 s are present with both wave periods incident from the southwest.
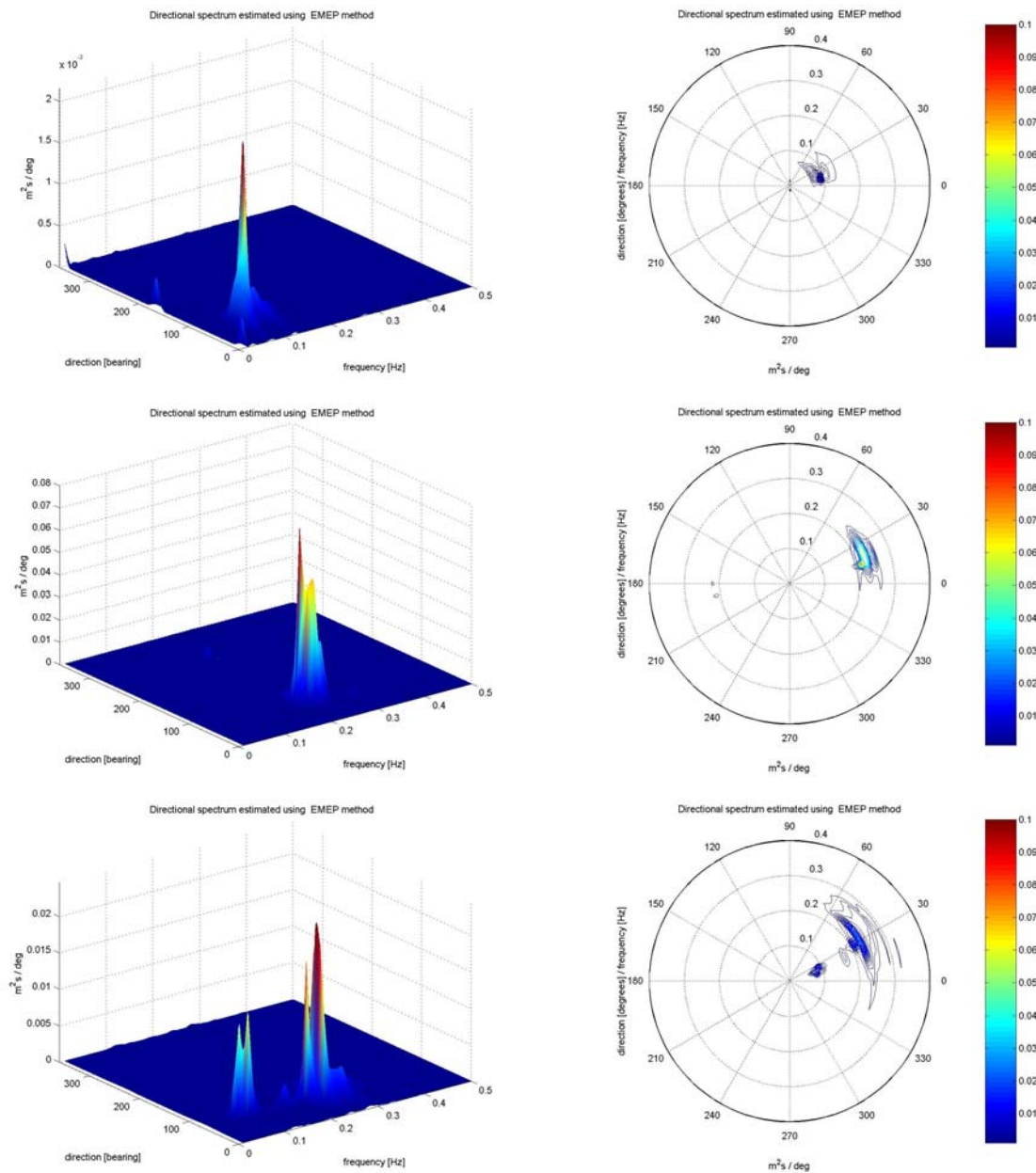
Figure 4.3: Examples of directional wave spectra obtained from the Adelaide coastal waters: (a) a swell dominated spectra on 6 October prior to storm; (b) a wind wave dominated spectra on 7 October during the storm; and, (c) a bi-modal spectra showing both swell and wind waves on 8 October at the end of the storm.

The above results indicated that for the Adelaide coastal waters, the predominant wave direction, both swell and locally generated waves, was from the southwest between 230° and 250°. It also appeared that only southwesterly wind had an influence in generating storm waves.

5   Results and Discussion: Dispersion

5.1   Cluster Dispersion

The dispersion coefficient K value as well as the cross-shore and longshore components K_x and K_y, respectively, were determined for each of the 37 drifter clusters released during the September 2004 and March 2005 deployments. The results for each of the deployment periods are presented in Tables 5.1 and 5.2, respectively, allowing the clear representation of seasonal variation in the dispersion characteristics. These tables include the determination of the dispersion coefficients, with K = 0.11 m²s^{-1} within a 95% confidence interval of 0.08, K_x = 0.10±0.09 m²s^{-1}, and K_y = 0.15±0.14 m²s^{-1} for the September deployments compared with K = 0.12±0.07 m²s^{-1}, K_x = 0.05±0.02 m²s^{-1}, and K_y=0.19±0.09 m²s^{-1} for the March deployments. These values showed the inherent variability associated with turbulent dispersion in the nearshore zone as well as the relatively low number of samples.

The dispersion coefficient values determined for the nearshore zone at Henley Beach were much smaller than the values reported in oceanic diffusion experiments such as those Tseng (2001) and Proehl et al. (2005) conducted. Tseng (2001) recorded dispersion coefficient values as high as 45 m²s^{-1} in enhanced flow regimes in the wake formations off islands near the coast of Taiwan, and Proehl et al. (2005) determined total dispersion values of up to 131 m²s^{-1} around the north flank of Georges Bank. These values demonstrate the potential for high dispersion rates within open ocean enhanced flow regions; however, they have little relevance to the nearshore zone where the conditions and factors driving dispersion are markedly different. The calculated dispersion coefficients were also significantly lower than the values Johnson (2004) found in the rip-neck, where total dispersion, K, ranged between 1.29 and 3.88 m²s^{-1}. This indicated the Adelaide study site's less energetic nature as well as the enhancement of dispersion encountered at the rip head, outside of the surf zone, as noted by Johnson (2004), Olsson (2004) and Inman (1971). However, the obtained results did show a greater level of correlation with Johnson's findings *inside* the surf zone. Johnson (2004) investigated longshore currents inside the surf zone and found dispersion coefficient values of K_x = 0.2 m²s^{-1} and K_y = 0.3 m²s^{-1} for a 10 m separation. This correlation was somewhat surprising, given the difference in the two study sites' energy levels, and suggested similar processes dominated dispersion within the surf zone at each site.

Table 5.1: Dispersion coefficients calculated for each of the drifter clusters released between the 1st and 3rd of September 2004. Data omitted from the calculation of the mean and the confidence intervals are shown.

Date	Cluster	Number of Drifters	Shortest Time (s)	Kx	R^2	Ky	R^2	K	R^2
1/09/2004	Cluster 1	3	296	-0.01	0.04	0.07	0.56	0.03	0.30
	Cluster 2	4	47	0.17	0.92	0.10	0.95	0.14	0.95
	Cluster 3	5	49	0.10	0.93	0.08	0.98	0.09	0.96
	Cluster 4	5	381	1.24	0.95	0.09	0.80	0.00	0.96
	Cluster 5	4	166	0.07	0.44	0.01	0.02	0.04	0.41
2/09/2004 (AM)	Cluster 1	5	742	0.00	0.64	0.01	0.67	0.01	0.77
	Cluster 2	5	2212	0.01	0.80	0.00	0.00	0.00	0.28
	Cluster 3	5	713	0.04	0.80	0.02	0.41	0.03	0.78
	Cluster 4	5	954	0.19	0.93	0.59	0.84	0.39	0.87
2/09/2004 (PM)	Cluster 1	3	1025	0.05	0.31	0.03	0.36	0.04	0.38
	Cluster 2	3	829	0.02	0.39	0.11	0.55	0.07	0.60
	Cluster 3	3	569	0.24	0.88	0.02	0.05	0.13	0.90
	Cluster 4	3	512	0.37	0.11	0.00	0.00	0.19	0.10
3/09/2004	Cluster 1	5	539	0.02	0.41	0.05	0.27	0.04	0.33
	Cluster 2	5	701	0.05	0.71	0.02	0.31	0.04	0.71
			Mean	0.10	0.84	0.15	0.76	0.11	0.82
			Std Dev	0.09	0.11	0.20	0.17	0.12	0.13
			95% CI	0.07	0.08	0.14	0.13	0.08	0.09

Data excluded due to high deviation from mean
Data excluded due to low r^2

Table 5.2: Dispersion coefficients calculated for each of the drifter clusters released between the 20th and 23rd of March 2005. Data omitted from the calculation of the mean and the confidence intervals are highlighted.

Date	Cluster	Number of Drifters	Shortest Time (s)	Kx	R^2	Ky	R^2	K	R^2
20/03/2005	1	5	1151	0.04	0.93	0.10	0.66	0.07	0.78
	2	5	989	0.01	0.40	0.04	0.67	0.03	0.73
	3	4	3271	0.00	0.19	0.05	0.71	0.03	0.67
	4	5	779	0.01	0.39	0.15	0.60	0.08	0.67
	5	3	979	0.08	0.77	0.11	0.55	0.10	0.68
	6	4	906	0.05	0.87	0.02	0.21	0.04	0.66
21/03/2005	1	5	1113	0.04	0.98	0.02	0.85	0.03	0.98
	2	5	2994	0.02	0.82	0.18	0.93	0.10	0.94
	3	5	3349	0.12	0.98	0.36	0.89	0.24	0.94
	4	5	1569	0.01	0.75	0.00	0.72	0.00	0.76
22/03/2005	1	5	2028	0.02	0.82	0.32	0.75	0.17	0.76
	2	5	1443	0.11	0.87	0.83	0.59	0.10	0.87
	3	5	1301	0.03	0.67	0.02	0.19	0.02	0.56
	4	5	2976	0.08	0.83	0.06	0.71	0.71	0.80
23/03/2005	1	5	1510	0.06	0.91	0.17	0.86	0.12	0.89
	2	5	1117	0.01	0.23	0.34	0.67	0.17	0.67
	3	5	642	0.04	0.92	0.21	0.76	0.13	0.83
	4	5	792	0.01	0.41	0.32	0.86	0.17	0.87
	5	5	776	-0.02	0.52	0.03	0.58	0.01	0.17
	6	4	881	0.01	0.26	0.06	0.67	0.03	0.70
	7	5	918	0.03	0.49	0.02	0.28	0.03	0.44
			Mean	0.05	0.81	0.19	0.72	0.12	0.78
			Std Dev	0.04	0.15	0.20	0.12	0.16	0.12
			95% C.I.	0.02	0.41	0.09	0.05	0.07	0.05

Data excluded due to high deviation from mean
Data excluded due to low r^2

Mariani (2005) measured dispersion coefficients inside the surf zone under relatively high-energy conditions at Floreat Beach, along the exposed Perth coastline, a location similar to that of Johnson (2004). Mariani (2005) determined dispersion co-efficient K values ranging between 0.2m²s⁻¹ and 1.78 m²s⁻¹ with an associated mean value of 0.77±0.33 m²s⁻¹ within a 95% confidence interval. In addition, the cross-shore and longshore dispersion coefficients were determined; K_x ranged between 0.27 and 2.1 m²s⁻¹ in the cross-shore plane while K_y varied between 0.35 and 3.34 m²s⁻¹ in the longshore direction. Mariani (2005) noted the variation in the dispersion coefficient magnitude between the cross-shore and longshore planes. This was attributed to the presence of boundaries in the cross-shore plane, in the form of the breaker line and shoreline, compared with the almost complete lack of boundaries in the longshore direction. These conditions were enhanced by the prevailing experimental conditions Mariani (2005) favoured, which were strong sea breezes. This introduced a level of bias in the data, as the presence of strong sea breezes has the effect of restricting the surf zone width and maintaining a clear boundary at the breaker line, preventing the cross-shore spread of wave-induced turbulence. This was noted by Inman et al. (1971) and Bowen and Inman (1974) who observed that in dye release experiments, the dispersion appeared to be contained within the surf zone, because of the absence of turbulence seaward of the break point and the advection of offshore water through the breaker line. Turbulent diffusion is the key dispersive mechanism in the nearshore zone, and the restriction of its cross-shore distribution, due to the bounding effect of the surf zone, thus acts to restrict the extent of nearshore dispersion (Bowen and Inman, 1974).

Significantly, the relative enhancement of dispersion in the longshore direction was noted in Adelaide only in the results from the March deployments, where sea breeze conditions, similar to those Mariani (2005) used, prevailed. The values Mariani (2005) obtained were significantly larger than those observed in Adelaide. This could be attributed to the more energetic nature of Mariani's (2005) study site, where sampling was conducted under sea breeze strengths as high as 18 ms⁻¹, and was often associated with highly energetic wave conditions, leading to increased turbulence within the surf zone.

A better correlation was observed in the results of the dye dispersion experiment and concurrent numerical modeling Rodriguez et al. (1995) conducted, which revealed dispersion coefficients in the surf zone to be 0.03 m²s⁻¹ ± 0.01 m²s⁻¹. While this result was smaller than that recorded at Henley Beach, it was significant because it was recorded on a geometrically simple linear beach on the sheltered Spanish Mediterranean coast—a location similar to that of the Adelaide metropolitan coastline. Numerical modeling confirmed the experimental results of Rodriguez et al. (1995), predicting a horizontal eddy diffusivity of K_h = 0.018 m²s⁻¹, again, correlating to some extent with the measured dispersion coefficients.

To the authors' knowledge, Takewaka et al. (2003) undertook the only other direct measurements of dispersion in the surf zone. Takewaka et al. (2003) conducted dye diffusion experiments in the surf zone under significant wave height conditions of 0.56 m associated with a peak period of 6.5 s and a longshore current of 0.3 ms⁻¹. This allowed the calculation of cross-shore dispersion values of 0.01, 0.017, and 0.025 m²s⁻¹. These values could not be directly compared to the calculated dispersion values, as Takewaka et al. (2003) assumed a Fickian diffusion process; however, it could be seen that at scales of 5 m, Takewaka et al.'s (1995) results were consistent with those of Johnson (2004) who did not assume Fickian diffusion.

Riddle and Lewis (2000) reviewed data from 25 dye dispersion experiments from estuarine and coastal locations, and found the lateral dispersion coefficient to range between 0.003 and 0.42 m²s⁻¹ with a median value of 0.05 m²s⁻¹. Riddle and Lewis (2000) compared their data to similar experiments conducted off the coasts of Ireland and Cape Kennedy in the United States, which returned median dispersion coefficients of 0.18 m²s⁻¹ and 1.0 m²s⁻¹. The dispersion values calculated in this experiment could thus be seen to fit within the range of dispersion coefficients encountered within the literature, albeit the bulk of recorded values were calculated from sites offshore from the surf zone.

The comparison of the recorded experimental results with values from the literature thus demonstrated the low rate of dispersion present in Adelaide nearshore waters. It has been established that the experimental results were lower than those obtained in more active, energetic surf zone areas addressed by Mariani (2005) and Johnson (2004), and were also significantly lower than the rates of dispersion Tseng (2001) and Proehl et al. (2005) quoted for the open ocean. The values were also an order of magnitude lower than dispersion coefficient values of 1–5 m²/s, which were considered representative of the semi-enclosed water body of Port Philip Bay, as quoted by Pattiaratchi et al. (1995). In contrast, the values obtained correlated to a reasonable extent with the results reported from other low-energy environments, specifically, the sheltered Mediterranean coastline that Rodriguez (1995) investigated, and to a lesser extent, the values Riddle and Lewis (2000) presented when they addressed locations across a variety of geographical settings and thus reported a wide range of dispersion values. A summary of the dispersion coefficient values reported in the literature and their relationship to the values presented in this paper is presented in Table 5. 3.

Table 5.3: Summary of the various dispersion coefficient values quoted in the literature and a comparison to the values obtained in Adelaide's coastal waters.

Paper	Location	Comment	Method	K (m²/s) Minimum	Maximum	Median	Kx(m²/s)	Ky(m²/s)	Comparison to Adelaide
Johnson (2004)	Surf Zone	Rip neck	Drifters	1.29	3.88				*higher*
Johnson (2004)	Surf Zone	Longshore current 10m separation (using power law relationship)	Drifters				0.2	0.3	*close*
Mariani (2005)	Surf Zone	Longshore current	Drifters	0.2	1.78	0.76	0.93	0.96	*higher*
Rodriguez (1995)	Surf Zone	Low energy mediterranean beach	Dye diffusion			0.03			*lower*
	Surf Zone	Low energy mediterranean beach	Modelling	0.018					*lower*
Takewaka *et al*. (2003)	Surf Zone	Fickian assumption (5m separation)	Dye diffusion	0.01	0.025				*lower*
Riddle & Lewis (2000)	Nearshore	Estuaries, bays, offshore, UK	Dye diffusion	0.003	0.42	0.05			*close*
	Nearshore	Ireland	Dye diffusion			0.18			*close*
	Nearshore	Cape Kennedy	Dye diffusion			1			*higher*
Tseng	Oceanic	Island wakes	Drifters		45				*higher*
Proehl	Oceanic	Georges bank	Modelling		131				*higher*
THIS PAPER	Surf Zone	September	drifters			0.11	0.23	0.15	
		March	drifters			0.12	0.05	0.19	

5.1.1 Seasonal and Daily Variations

A significant level of variation in the derived dispersion coefficients is observable in the results presented in Tables 5.1 and 5.2. The timescale over which these variations occurred was significant, with clear trends visible in the seasonal comparisons as well as shorter period discrepancies observed during single days, or over a period of days, in the same sampling period. The derived dispersion coefficients' variability across the different timescales as well as the reasons for these disparities will be addressed in this section.

Seasonal Variation

A summarised version of the dispersion coefficients obtained during the September and March deployments, respectively, is presented in Table 5.4. This represents the total dispersion coefficient K's relative consistency; a large deviation is noted in the cross-shore results and a smaller, yet significant, variation is noted in the longshore direction.

Table 5.4: Summary of dispersion coefficients determined in each season.

	K	C.I.	Kx	C.I.	Ky	C.I
September	0.11	0.08	0.23	0.07	0.15	0.14
March	0.12	0.07	0.05	0.02	0.19	0.09

The factors influencing these deviations included: changes in the dominant wind regime (which indirectly controls the wave conditions), tides, and topographic controls.

Changes in the dominant wind regime are likely to have the greatest effect, as the nature of the relatively sheltered study site dictated that the dominant factor influencing turbulence in the nearshore zone, and hence dispersion, was wind-generated waves. Waves influence the rate of mixing in the surf zone through a variety of mechanisms including a combination of mixing generated by the production of turbulence due to breaking wave activity, mixing generated by the oscillatory flow over the bed, and shear dispersion (Pearson et al., 2002). As noted in the Literature Review in Section 2.1.3.4, the Adelaide metropolitan coastline is subjected to an active sea breeze system during the summer months. This system causes strong southwesterly winds to blow during the afternoon, driving the generation of short period, relatively high-energy wind waves. The breaking of these waves in the nearshore zone creates turbulence, which is the dominant force driving dispersion. However, the sea breeze's influence does not extend to the same extent through winter, providing a major differentiating factor between the experimental periods' wind regimes

During the sea breeze, several changes in the surf zone are typically induced including: an increase in the height of incident waves, a decrease in the wave period (or zero-upcrossing period), and an increase in the longshore current velocity (Masselink and Pattiaratchi, 1997). These factors combined to produce an increase in the wave energy incident on the generally calm Adelaide coastline, leading to an increase in turbulence in the nearshore zone. Logically, this should lead to an increase in the observed dispersion coefficients, and this was true for the longshore direction; however, this was not the case in the cross-shore direction, where the dispersion coefficient was greatly reduced compared with the September deployments. This reduction might be attributed to a combination of factors.

The sea breeze system's onshore direction has the effect of increasing the onshore advective flux, particularly in the water column surface layers (Inman et al., 1971). Essentially, water is pushed shoreward through wind forcing and its associated wave regime. This has the effect of constraining the surf zone width. As Bowen and Inman (1974) noted, turbulent dispersion is effectively contained within the surf zone owing to the barrier created by the breaker line restraining the drifters' motion to within these boundaries. As the sea breeze has the effect of narrowing the surf zone while simultaneously increasing turbulence and the longshore current, it is a reasonable outcome that:

1   Dispersion in the longshore direction, which is effectively unbounded and enhanced through the higher generation of turbulence and the stronger longshore current, increases;

2   Dispersion in the cross-shore direction is restrained by the decrease in the surf zone width.

Another factor potentially impacting hydrodynamic processes, and hence dispersion rates, in the nearshore zone is the presence of topographic features. While no beach profiles were obtained, simple observations confirmed the presence of a large shore parallel sandbar approximately 40 m offshore from the beach during the summer deployments. This influenced the experimental area's hydrodynamic regime by instigating wave breaking at a point farther offshore than would be expected if it were not present. This reduced the amount of wave energy reaching the shoreline, which in turn might have influenced the magnitude of wave-induced longshore transport and turbulence close to the shore. However, given the observed result that longshore dispersion inside the sandbar was greater when the sandbar was present, this scenario was unlikely to be a dominant process.

Rather, the primary influence of the sandbar was likely to be as a barrier to cross-shore dispersion in the offshore direction, similar to the breaker boundary line described previously. In fact, the sandbar's presence would complement the breaker line effect, as during sea breeze conditions, their locations coincided as a result of wind-induced waves breaking at the shallow sandbar. The onshore advective flux associated with wave breaking dominates the water column (Bowen and Inman, 1974), with the sandbar's shallow depth effectively preventing offshore directed undertow. As such, the sea breeze and the sandbar act in conjunction with each other to create a boundary through which offshore movement is heavily retarded or completely prevented.

While the sea breeze is a daily phenomenon that has a maximum duration in the order of several hours, the formation and duration of sandbars in a relatively low-energy environment, such as Adelaide, is in the order of several weeks or months (Komar, 1976). Thus, while the sea breeze's effect on dispersion is limited in duration to periods where favourable winds prevail, the sandbar forms a semi-permanent feature that has the combined effects of forming a boundary impeding cross-shore flow and channeling (concentrating) flow in the longshore direction (Komar, 1976). This was represented in the comparison of morning and afternoon results. The fact that the dispersion in the cross-shore direction was impeded, largely regardless of the prevailing conditions, throughout the deployment period highlights the topography's influence.

Another significant contrast between the two sampling periods was the tidal regime. During the September deployments, semidiurnal spring tides of up to 2 m were observed, with significant implications for the nearshore beach morphology, as noted in Section 3.3.1. During the March deployments, the tidal regime was characterised by neap conditions whereby the tidal range initially was close to zero; however, over the course of the deployment period this increased to a range of approximately 1 m over a semi-diurnal period. Tidal oscillations are known to have several key impacts on the nearshore hydrodynamic regime. Specifically, tidal variances have been attributed to increases in rip currents and longshore currents (Simpson et al., 2005; Komar, 1976), particularly around low tide when water draining from the beach becomes trapped behind topographic features, such as shore

parallel sandbars. Flow in longshore currents and rips is enhanced as the water moves towards the breaks in the sandbar and then flows rapidly through these features in the offshore direction (Brander, 1999; Komar, 1976); as such, it is plausible that the tidal oscillations might have an effect on dispersion in the study area through tidally-induced currents producing turbulence and mixing in the water column (Xing and Davies, 2003).

During field experiments, the author spoke to several local residents who offered valuable information pertaining to the long-term behaviour of various aspects of the beach including seasonal variations in current patterns due to tidal oscillations. In particular, a resident of 40 years described drift netting for mullet during the 1970s in the nearshore zone between 50 and 200 m from shore. Specifically, the resident recalled watching the net, which was anchored at one end, rotate 90° from a position perpendicular to the shore to a position parallel to the shoreline. This was noted because the conditions under which the movement took place were completely calm, with no wind or waves observed; however, the tide was dropping during this period, suggesting the tidal outflow was sufficient to generate a longshore current capable of moving the net. While this description provides an interesting story, it is little more than circumstantial evidence.

Unfortunately, the effect of the tidal oscillations could not be readily obtained from the results presented in this study. This is because data were not collected over the entire tidal cycle; rather, sampling was opportunistic with results obtained from the same time period each day and hence relatively similar cycle stages. Additionally, the presence of other dominant factors, such as highly variable wind and wave conditions as well as topographic controls, as discussed previously, will tend to mask any values obtained through tidal oscillations. The dispersion magnitude directly induced by tidal processes affecting the nearshore spatial distribution and magnitude of currents was significantly smaller than the processes discussed previously due to the low-energy nature of tidal variations. However, it is also plausible that tidal movements interacting with other features may enhance dispersion. This is particularly true in the case of topographic features, such as sandbars, interacting with a low or falling tide. As the water level decreases, the number of waves breaking on the sandbar will increase owing to the shallower water. This leads to the definition of a new breaker line, which enhances effects on cross-shore and longshore dispersion associated with the boundary.

In order to determine the actual influence of the tides on nearshore dispersion, it would be necessary to deploy the drifters through entire tidal oscillation's various stages under completely calm conditions. This would ensure the effects of other forcing factors were removed from the obtained results.

Daily Variation (September 2004)

Significant variation was noted in the dispersion coefficient values determined across consecutive days in the same deployment period as well as under differing conditions throughout the duration of a single day. In order to determine the variability's influence in conditions between consecutive deployments, wind directions were taken into account during data processing. Dispersion coefficients determined in the total cross-shore and longshore directions for winds with a northerly and a southerly component, respectively, are shown in Table 5.5. This led to the derivation of markedly different dispersion coefficient values for the respective prevailing wind conditions. During the September deployments, it was found that $K = 0.16$ m²s^{-1} under prevailing winds with a southerly component, while $K = 0.03$ m²s^{-1} for winds with a prevailing northerly component. This was a significant variation, which was also seen in the longshore and cross-shore directions $K_x = 0.18$ m²s^{-1} and $K_y = 0.09$ m²s^{-1} for southerly prevailing winds, while $K_x = 0.03$ m²s^{-1} and $K_y = 0.02$ m²s^{-1} under northerly conditions.

These results may appear to be counter-intuitive when one notes the dominant direction of winds with a southerly component is southwesterly. This is congruous to the sea breeze described in the March deployments, which was associated with a significant retardation of mixing in the cross-shore direction. This was attributed to the sea breeze's enhancement of the onshore advective fluxes and the effect of the onshore winds in constraining the surf zone width. In this situation, however, cross-shore dispersion rates were larger under southwesterly conditions. This could be attributed to a combination of two factors, namely, the wind direction and velocity.

Table 5.5: Dispersion coefficient values calculated during the September 2004 deployments, taking into account whether the prevailing winds contained a northerly or southerly bias.

Date	Cluster	Wind Direction (°)	Wind Velocity (m/s)	Kx	R^2	Ky	R^2	K	R^2
1/09/2004	Cluster 1	230	4.61	-0.01	0.04	0.07	0.56	0.03	0.30
	Cluster 2	240	3.61	0.17	0.92	0.10	0.95	0.14	0.95
	Cluster 3	220	5.69	0.10	0.93	0.08	0.98	0.09	0.96
	Cluster 4	230	4.11	1.24	0.95	0.09	0.80	0.00	0.96
	Cluster 5	220	4.61	0.07	0.44	0.01	0.02	0.04	0.41
2/09/2004 (AM)	Cluster 1	360	1.5	0.00	0.64	0.01	0.67	0.01	0.77
	Cluster 2	30	1	0.01	0.80	0.00	0.00	0.00	0.28
	Cluster 3	330	0.5	0.04	0.80	0.02	0.41	0.03	0.78
	Cluster 4	250	4.61	0.19	0.93	0.59	0.84	0.39	0.87
2/09/2004 (PM)	Cluster 1	260	3.61	0.05	0.31	0.03	0.36	0.04	0.38
	Cluster 2	230	3.61	0.02	0.39	0.11	0.55	0.07	0.60
	Cluster 3	220	2.61	0.24	0.88	0.02	0.05	0.13	0.90
	Cluster 4	250	4.11	0.37	0.11	0.00	0.00	0.19	0.10
3/09/2004	Cluster 1	280	1.5	0.02	0.41	0.05	0.27	0.04	0.33
	Cluster 2	300	2.61	0.05	0.71	0.02	0.31	0.04	0.71
	Southerly Component	Mean		0.18	0.92	0.09	0.77	0.16	0.86
		Std Dev		0.06	0.03	0.02	0.20	0.13	0.15
		95% CI		0.06	0.03	0.02	0.18	0.11	0.13
	Northerly Component	Mean		0.03	0.74	0.02	0.42	0.03	0.65
		Std Dev		0.03	0.08	0.02	0.18	0.01	0.21
		95% CI		0.02	0.08	0.02	0.18	0.01	0.21

Data excluded due to high deviation from mean	Southerly component in wind
Data excluded due to low r^2	Northerly component in wind

The wind direction was a key factor in determining the seeming incongruity in the relationship between the sea breeze restricting dispersion in summer and similar conditions seemingly enhancing dispersion in winter. The key parameter was the level of wind energy that was transferred to waves incident upon the study area. Winds from the southwest direction produce waves which strike the Adelaide coastline obliquely, producing conditions optimal for the production of longshore currents (Longuet-Higgins, 1970). The production of turbulence in the nearshore surf zone through the action of wave breaking, and the longshore transport associated with the southwesterly winds ensures dispersion is relatively active.

In contrast, the prevailing wind direction with a northerly component during the September deployments was north-northeasterly. This was almost parallel to the study site's shoreline; as such, the direction of propagation ensured wind waves produced under these conditions did not transfer much energy into the surf zone. The reduced energy transfer into the surf zone implied that less turbulence was induced to drive dispersive processes when compared with southwesterly wind conditions.

The other factor influencing the relative rates of dispersion during the September deployments was the wind velocity. This applied in conjunction with the wind direction and served to reinforce the outcomes already obtained. Winds with a southerly component averaged 4.1 ms^{-1} during the September deployments, while winds from the north averaged just 1.42 ms^{-1}. As has already been addressed, the southwesterly conditions were optimal for the efficient transfer of wave energy into the surf zone and the promotion of the longshore current. The stronger winds experienced from the southwest direction added to this effect,

providing a higher amount of wind wave energy to facilitate the induction of turbulence and dispersion within the surf zone.

Conversely, the weak winds associated with the northerly direction provided restricted energy to the water surface, leading to limited wave energy being transferred into the surf zone. Of this limited potential supply, only a small proportion was effectively transferred into the surf zone, as the aspect of the beach relative to the winds was almost parallel. With little turbulence available within the nearshore zone, dispersion rates under northerly wind conditions were low in all directions, as there was no dominant force that had the effect of actively promoting turbulence in the water column and hence dispersion.

Consequently, it could be concluded that the dispersion coefficient's relative enhancement under wind conditions with a southerly component was due to a combination of wind velocity and direction. These factors govern the supply of wave energy into the surf zone and hence directly the affect the instigation of turbulence through the action of breaking waves. Turbulence diffusion is the key dispersive mechanism in the nearshore zone; thus, under more energetic and turbulent conditions, dispersion is enhanced. This is represented in the dispersion coefficient results calculated for the differing wind conditions. Under the influence of more energetic southerly winds associated with the efficient transfer of energy, dispersion rates were higher. In contrast, when low velocity northerly winds dominated and the level of turbulence in the nearshore zone was impeded, dispersion rates were lower.

Daily Variation (March 2005)

There was a significant variation noted in the prevailing conditions during the March deployments. During the first two days of deployment, the prevailing conditions were onshore with a strong sea breeze system operating during the afternoons. However, in the following two days, somewhat atypical conditions prevailed with offshore easterly winds dominating throughout the sampling period. This allowed the comparison of the prevailing wind conditions' effects, with easterly and westerly components, respectively, on the dispersion coefficient calculated values (represented in Table 5.6).

Table 5.6: Dispersion coefficient values calculated during the March 2005 deployments, taking into account whether the prevailing winds contained an easterly or westerly bias.

Date	Cluster	Wind Direction (°)	Wind Velocity (m/s)	Kx	R^2	Ky	R^2	K	R^2
20/03/2005	1	250	4.11	0.04	0.93	0.10	0.66	0.07	0.78
	2	245	4.37	0.01	0.40	0.04	0.67	0.03	0.73
	3	240	4.62	0.00	0.19	0.05	0.71	0.03	0.67
	4	230	5.14	0.01	0.39	0.15	0.60	0.08	0.67
	5	230	5.14	0.08	0.77	0.11	0.55	0.10	0.68
	6	220	5.65	0.05	0.87	0.02	0.21	0.04	0.66
21/03/2005	1	30	1.51	0.04	0.98	0.02	0.85	0.03	0.98
	2	320	2.05	0.02	0.82	0.18	0.93	0.10	0.94
	3	280	3.59	0.12	0.98	0.36	0.89	0.24	0.94
	4	240	7.2	0.01	0.75	0.00	0.72	0.00	0.76
22/03/2005	1	140	5.14	0.02	0.82	0.32	0.75	0.17	0.76
	2	150	6.68	0.11	0.87	0.83	0.59	0.10	0.87
	3	150	7.2	0.03	0.67	0.02	0.19	0.02	0.56
	4	150	7.2	0.08	0.83	0.06	0.71	0.71	0.80
23/03/2005	1	110	2.57	0.06	0.91	0.17	0.86	0.12	0.89
	2	100	4.11	0.01	0.23	0.34	0.67	0.17	0.67
	3	130	4.11	0.04	0.92	0.21	0.76	0.13	0.83
	4	140	4.11	0.01	0.41	0.32	0.86	0.17	0.87
	5	130	4.62	-0.02	0.52	0.03	0.58	0.01	0.17
	6	180	4.62	0.01	0.26	0.06	0.67	0.03	0.70
	7	160	5.14	0.03	0.49	0.02	0.28	0.03	0.44
	Westerly Component	Mean		0.05	0.85	0.13	0.72	0.08	0.76
		Std Dev		0.04	0.09	0.11	0.27	0.07	0.11
		95% C.I.		0.03	0.07	0.08	0.19	0.05	0.07
	Easterly Component	Mean		0.05	0.78	0.24	0.73	0.16	0.79
		Std Dev		0.03	0.24	0.24	0.11	0.20	0.12
		95% C.I.		0.03	0.19	0.14	0.06	0.11	0.07

Data excluded due to high deviation from mean	Westerly component in wind
Data excluded due to low r^2	Easterly component in wind

The values in Table 5.6 demonstrate a clear relationship between the wind direction and the dispersion rate. The total dispersion coefficient was measured as K = 0.16 m²s^{-1} under easterly conditions, while when westerly winds were prevailing, K = 0.08 m²s^{-1}. Similarly, under winds with an easterly component, the longshore dispersion coefficient K_y = 0.24 m²s^{-1} was significantly larger when compared with K_y = 0.14 m²s^{-1}, which was derived during periods of prevailing westerly conditions.

For the total dispersion coefficient K and the longshore dispersion coefficient K_y, a significant offset was observed between the easterly and westerly wind components. Specifically, an enhancement in the dispersion coefficient values in the order of 100% was observed in the easterly dominated results, relative to the values calculated under westerly conditions. This was in contrast to the dispersion coefficient values calculated in the cross-shore direction, where K_x = 0.05 m²s^{-1} for easterly and westerly prevailing wind conditions.

In contrast with the results obtained in September, the wind velocity did not vary significantly with the dominant direction, with an average velocity of 4.75 ms^{-1} recorded for winds with an easterly component compared with an average velocity of 4.65 ms^{-1} recorded for winds from the west.

The dominant factor in the relationship between wind conditions and dispersive rates is the wind direction. However, in the case of the cross-shore dispersion coefficient, it was evident there must have been different mechanisms influencing the dispersion rate, as clearly opposing wind regimes were associated with identical cross-shore dispersion coefficients. Addressing the cross-shore dispersion coefficient value demonstrated that under easterly and westerly wind conditions, dispersion was low.

This suggested that either cross-shore dispersion was being impeded, or there was only a limited amount of energy available to drive turbulence in the nearshore zone, thereby restricting the attainable cross-shore dispersion rates.

In the case of winds with a westerly component, it was unlikely dispersion rates were limited by the amount of wave energy entering the system. This was because the average wind speed was relatively high, reaching a maximum of 7.2 ms^{-1}, and the direction of average flow was almost directly onshore in a west-southwesterly direction. Under these conditions, the generation of wind waves within the Gulf of St Vincent was optimized, leading to the conclusion that the amount of energy available under the westerly prevailing conditions was sufficient to induce turbulence to drive more significant dispersion rates. Rather, the restriction of dispersion was due to the onshore sea breeze conditions' effects, as outlined in the seasonal comparison of data in Section 5.1.1.1. Namely, the onshore breeze and the associated waves had the effect of constraining the turbulent surf zone width in the cross-shore direction, thereby narrowing the domain over which cross-shore dispersion could occur, as the edge of the surf zone turbulence effectively acted as an offshore barrier to dispersion.

Under easterly prevailing winds, the restriction in the surf zone width through onshore winds was no longer a plausible cause for the relatively low values of cross-shore dispersion observed. Rather, as the wind blew from a predominantly south-southeast direction (bearing 130°), it could be assumed mixing in the cross-shore direction was low owing to a lack of turbulent energy in the surf zone driving dispersion. As the winds blew from the land, they did not create waves that were incident on the coastline within the study site. This ensured the dispersion coefficients in the cross-shore domain were low when winds with an easterly component were dominant.

It should be noted that the same topographic control to cross-shore dispersion applies under all wind conditions. Specifically, the shore parallel sandbar's presence, as discussed in Section 5.1.1.1, created an effective offshore boundary to dispersion, which was likely to enhance the effect of the sea breeze in restricting cross-shore dispersion. However, it was unlikely to influence dispersion coefficients under offshore wind conditions, as energy limitation is the key factor affecting dispersion, not a boundary to cross-shore flow.

The difference in the longshore dispersion coefficients calculated under differing wind regimes could also be justified through the prevailing wind conditions' direction. Winds with a westerly component were typically almost directly onshore, perpendicular to the coast, with an average bearing of 260°. These conditions are not optimal for generating longshore currents, as water is pushed directly onshore (as opposed to obliquely incident waves that generate longshore currents in the direction of the wind's longshore component (Section 2.3.2.1)). As there was no longshore component in the incident wave's direction, a uni-directional longshore current was unable to develop, and the longshore dispersion coefficient remained relatively low, as the separation of drifters was not affected by shear dispersion in the nearshore zone.

Comparatively, the average direction of the wind with an easterly component is south-southeasterly. These winds blow in a direction that is more parallel to the coast; so, while they do not generate waves that are incident upon the shoreline, they do generate a flow that moves parallel to the coast and is analogous with the longshore current (Komar, 1976). The longshore current increases the longshore dispersion coefficient through the impact of shear dispersion. Drifters were rapidly transported in the longshore direction as they entered the narrow region of relatively rapid flow typical of the longshore current. This led to an increase in the drifters' longshore separation, increasing K_y. Owing to the wind propagation's offshore orientation, the longshore current generated was not particularly strong and was not constrained to a narrow region. Therefore, the effect of shear dispersion associated with the longshore current was relatively minor.

Two prevailing wind regimes dominated the deployment period during March in roughly equal shares. These wind regimes were characterised by significant easterly and westerly directional components, respectively. Cross-shore dispersion was low under all conditions, which was attributed to restriction in the surf zone width through onshore advective processes during onshore westerly conditions, while when offshore easterly winds were dominant, the lack of cross-shore dispersion was attributed to a lack of energy driving turbulence and hence dispersion. It was also noted that during the March deployments, topographic controls applied because of the presence of an offshore submerged sandbar, which effectively formed a barrier to cross-shore dispersion under all prevailing wind conditions. In the longshore direction, enhancement of dispersion was observed while winds with an easterly component prevailed. This was attributed to the southerly bias in the wind's direction, which acted to promote longshore currents in the nearshore zone. These longshore currents acted to increase the observed dispersion by providing a mechanism through which shear dispersion was able to influence the separation of drifters in the longshore direction.

5.1.2 Accuracy of Results

The results presented in the previous sections, while as accurate as possible, are likely to contain various inaccuracies. These errors could be attributed to several factors, some of which were preventable and others that were inherent to the process and hence difficult to remove. They are best managed by reducing their impacts.

The most easily identified sources of measurement errors were due primarily to preventable causes. Specifically, errors in the field were caused when drifters moved into water that was too shallow, and the drifter casing, or the attached drogue, came into contact with the bottom. This resulted in an increase in the drag affecting the drifter and a subsequent decrease in its velocity. The effects of the drifter dragging on the bottom were difficult to eliminate from the data, as the change in drifter behaviour was subtle, with the variance in drifter behaviour occurring with increasing severity over time as the drag increased. The influence of drag on the drifters was difficult to identify, as it was possible dispersion could increase when the main cluster group moved away from the affected drifter, or conversely, decrease when the cluster group moved towards an affected drifter. This was often the case in situations where a 'lead' drifter would move into shallow water and become stuck while the remaining drifter group 'caught up'. Great efforts were devoted to removal of drag affected data from the analysis, both in the field, where dragging drifters were noted upon collection, and in the data analysis, where decreases in drifter velocity were noted in the proximity of the shoreline and known sandbars. However, it cannot be stated definitively that this process had a 100% success rate, particularly in situations where more than one drifter was affected. Similarly, other preventable errors present in the raw data included periods where the drifters were affected by breaking waves, known as surfing, and periods where the drifters were moved by hand. Both of these error sources were relatively rare owing to the study site's low wave energy nature and the field approach of not moving the drifters by hand until the end of a cluster deployment. Neither of these factors was likely to have significantly affected the processed data, as both effects were typified by short rapid motions usually associated with an obvious change in direction. The identification and removal of such events was relatively simple.

The more ingrained sources of data error stemmed from the unavoidable effects. From a technological perspective, measurement errors associated with the GPS system were present and induced significant scatter in the raw data; the removal of these effects was difficult. It was evident some data points were erroneous, as they were characterised by large deviations (up to 3.5 km) in the recorded position, for a short period, before returning to the 'real' position. However, at smaller scales, where the deviation was of the order of the actual drifter motion, it became difficult to distinguish measurement errors from actual data.

This problem was reduced to a large extent through the process of smoothing, which used a moving average routine to calculate the drifter's most likely position at each point in time. This process 'smoothed out' the effects of rapid short duration motions, creating a path for the drifter more representative of the underlying motion than suggested by the rapid short-term deviations. Thus, while the effects of GPS positioning errors were not simple to eliminate, their effects could be reduced in such a way they had little bearing on the final processed data.

The processed results' high variability was an area of concern that was reduced to the greatest extent possible by applying several procedures, as outlined in Section 3.4.1.2. Specifically, a 0.5 cut-off was applied for the coefficient of determination r^2 value when calculating the dispersion coefficient from the line of best fit on the graph of variance with time. This ensured the dispersion coefficient's calculated value was representative of the underlying data. In addition, results that did comply with the r^2 condition, but differed from the calculated mean by a factor of 10 or more, were removed. This second condition was applied to reduce the inherently erratic nature of turbulent dispersion in the nearshore zone.

While the conditions of homogeneity and isotropy in eddies responsible for turbulent diffusion must be respected (Johnson, 2004), it is also clear that different factors do influence dispersion in the surf zone and over different timescales. The same flow may be regarded as a mean motion at small scales of observation, while at larger scales it may be observed to form part of a complex turbulent flow (List et al., 1990). The period and scale of forces affecting the drifters would have an influence on the determined dispersion coefficients. In order to reduce these effects, values that were sufficiently detached from the mean were removed from further analysis.

While these methodologies were effective in reducing the recorded dispersion coefficients' variability, the size of the 95% confidence intervals relative to the coefficient values indicated the inherently erratic nature of dispersion itself as well as the factors influencing it. This had significant implications when analysing the trends obtained from a relatively small number of points—specifically, the analysis of daily variations in the March and September deployments. Ideally, more data points would have been available, leading to a greater level of confidence in average values upon which assumptions as to the dominant dispersive regime were based. However, it was possible to work only with the data that was available, and in some cases this meant the degree of certainty in the result was compromised to an extent by assuming a limited number of data points were accurate and representative of the underlying trends.

In the analysis of dispersion trends with varying wind conditions, it was necessary to attempt to identify some of the causal relationships between observed conditions and the associated dispersion rate. As this was based on a relatively limited number of data points, it is prudent to note the inherent variability in dispersion rates, and acknowledge this may impact on the interpreted relationships. In the same manner, it is important to acknowledge that while the primary factor affecting dispersion at the study site was wind conditions, the system is dynamic and subjected to ongoing changes in the tide, current, and wave regimes, which could also have a significant impact on dispersion.

5.1.3   Scale Dependence

The relationship between the dispersion coefficient and the drifter separation scale was addressed by finding the dispersion coefficient for 1 m bins of standard deviation.

The coefficients for the lines of best fit between K, K_x, and K_y and the length scales σ, σ_x, and σ_y, for each of the cluster releases during September 2004 are shown in Table 5.7.

When these data were used, it was possible to determine the power law relationships for the dispersion coefficient K:

$$K = 0.03\sigma^{1.40}$$
(2)

where, c_1 (0.03) and c_2 (1.40) fall within 95% confidence intervals of ±0.02 and ±0.26, respectively. Likewise, in the cross-shore direction, K_x was described by a power law with c_1 = 0.02±0.01 and c_2 = 1.46±0.38, and in the longshore direction, c_1 = 0.03±0.02 and c_2 = 1.35±0.48.

Table 5.7: Coefficients of the least squares lines of best fit, calculated for each of the drifter clusters released between the 1st and 3rd of September 2004, based on the values of K calculated for 1 m bins of standard deviations. Data omitted from the calculation of mean and confidence intervals are highlighted.

Date	Run	Drifters	Time (s)	TOTAL			Cross-shore			Long-shore		
				C1	C2	r²	C1	C2	r²	C1	C2	r²
1/09/2004	1	3	296	0.11	0.11	0.00	0.02	1.68	0.81	0.11	0.47	0.21
	2	4	47	0.09	1.85	1.00	0.12	0.83	0.32	0.07	0.69	1.00
	3	5	49	0.04	1.96	1.00	0.06	1.35	1.00	0.08	1.13	1.00
	4	5	381	0.17	0.43	0.10	0.15	0.43	0.28	0.06	0.91	0.33
	5	4	166	0.02	1.37	1.00	0.02	1.37	0.87	0.02	0.18	1.00
2/09/2004	1	5	742	0.01	-0.27	1.00	0.02	-0.45	0.33	0.00	1.54	0.97
	2	5	2212	0.01	0.18	0.02	0.01	0.88	0.54	0.01	-0.13	0.02
	3	5	713	0.06	0.22	0.03	0.03	0.70	0.24	0.08	-0.20	0.02
	4	5	954	0.01	1.56	0.89	0.01	1.45	0.64	0.03	1.38	0.81
2/09/2004	1	3	1025	0.01	2.02	0.76	0.01	2.25	0.72	0.01	1.49	0.60
	2	3	829	0.01	1.78	0.87	0.02	0.70	0.71	0.01	1.98	0.91
	3	3	569	0.05	0.91	0.63	0.04	1.36	0.45	0.04	0.93	0.65
	4	3	512	0.93	1.14	0.43	0.16	1.03	0.45	0.02	1.22	0.73
3/09/2004	1	5	539	0.00	3.54	0.85	0.01	2.14	0.78	0.00	2.99	0.81
	2	5	701	0.10	0.12	0.01	0.08	0.61	0.17	0.05	0.42	0.07
			Average	0.03	1.40	0.88	0.02	1.46	0.72	0.03	1.35	0.85
			Std dev	0.03	0.39	0.14	0.01	0.54	0.14	0.03	0.85	0.38
			95%CI	0.02	0.26	0.09	0.01	0.38	0.10	0.02	0.48	0.21

Data excuded due to high deviation from mean
Data excuded due to low r²

These values were lower than those Johnson (2004) calculated in his investigation of longshore flow. Johnson found power law exponents ranging between 1.57 and 2.38 in the cross-shore direction and between 1.91 and 2.41 in the longshore. The correlation was stronger with Johnson's (2004) data pertaining to dispersion through the rip head, in which power law exponents of 1.30 and 1.58 were determined in the cross-shore and longshore directions, respectively. The correlation was even closer when the data were compared with the results of Mariani (2005) who found power law exponents of 1.24, 1.36, and 1.33 in the total, cross-shore, and longshore directions, respectively. Mariani (2005) noted the correlation between his values and Richardson's (1926) 4/3rds power law, which relates the dispersion coefficient to the length scale separation of a number of marked particles. Mariani (2005) noted the apparent conflict between the conditions Richardson (1926) assumed of isotropic, homogenous, and unbounded flow and the surf zone's actual conditions. Johnson (2004) also noted this and suggested nearshore processes were rarely homogenous or isotropic, particularly in the cross-shore direction. Inhomogeneity in the nearshore turbulence means the dispersion of a pair of particles becomes dependent, not just upon their separation, but also their orientation and cross-shore position. This inhomogeneity can be attributed to the surf zone's changing depth profile. The changing depth profile offshore also has the effect of causing water columns to 'stretch' in the vertical direction when moving into deeper water in order to maintain continuity; this tends to induce negative dispersion in particles normally inclined to separate in a disorganised current field (Johnson, 2004; List et al., 1990).

Okubo (1971) first addressed the 4/3rds power law's unifying properties and noted that several theories of turbulent dispersion led to the same 4/3 power law. In particular, Okubo discussed the fact that other theories of turbulent dispersion were able to derive the same 4/3rds relationship without Richardson's (1926) and Batchelor's (1952) strict assumptions of classical analysis conducted. Okubo (1971) demonstrated this rule held for a remarkably large range of scales in oceanic dispersion, ranging from 10 m to 1000 km (Johnson, 2004), by plotting the dispersion coefficient K against the scale of diffusion represented by σ.

The derived power laws matched the exponent of Okubo's (1974) data closely; as such, the gradients observable in Figure 5.1 correlated closely with the 4/3rds law. However, a significant variation in magnitude was observed between the data range of Okubo (1974) and the derived values. List et al. (1990) noted a similar divergence of up to two orders of magnitude. They attributed this to the effects of coastal shear acting in addition to turbulent dispersion. While the oceanic scales of coastal shear are not directly comparable to the surf zone, it is likely the effects of shear dispersion increased the observed dispersion coefficients
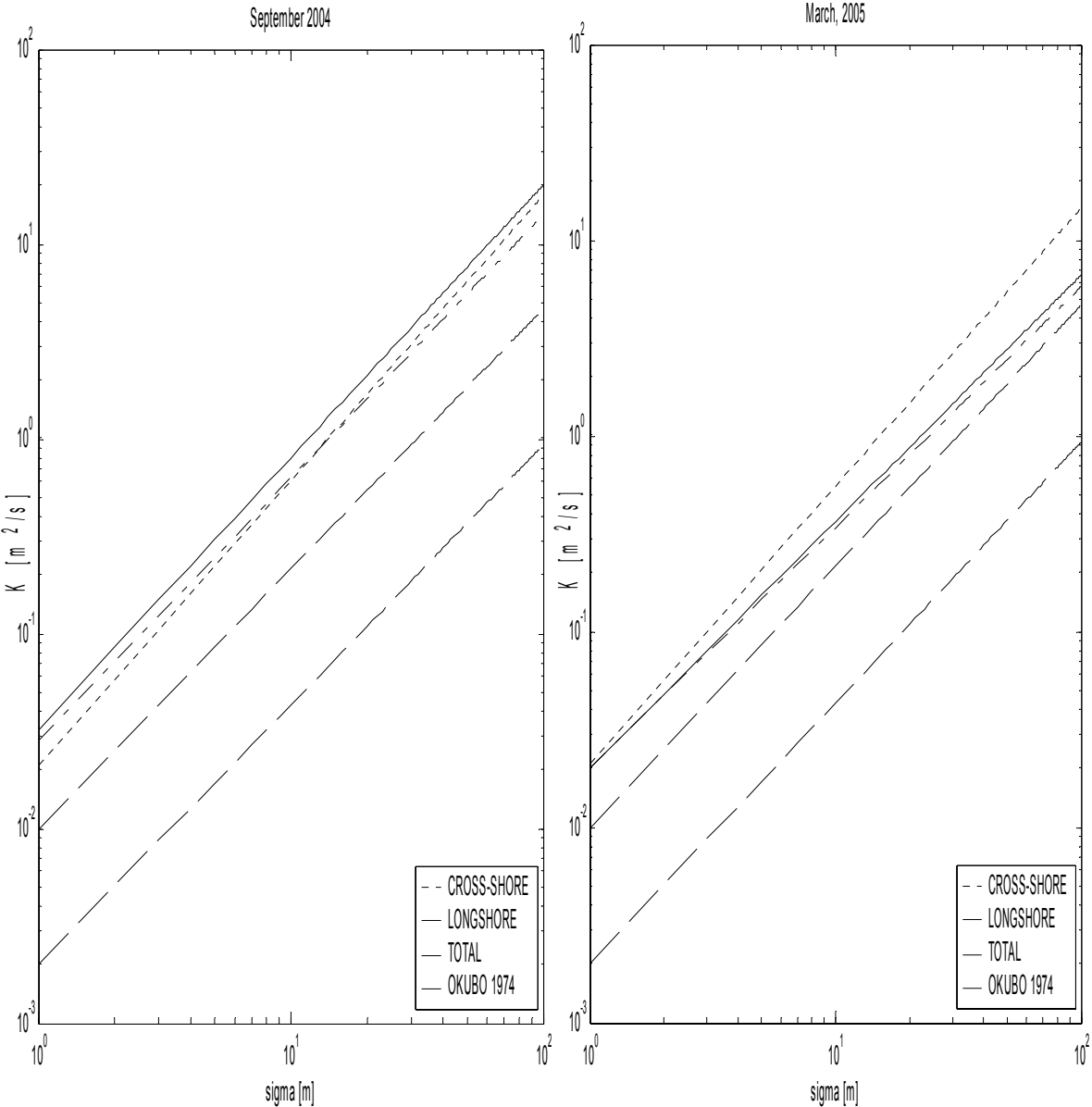
Figure 5.1: Comparison of the derived power laws with the data range of Okubo (1974).

Shear dispersion in the surf zone might be responsible for the deviation (noted in Figure 5.1) between the observed dispersion values and the effects of pure turbulent dispersion described by Okubo (1974) and the 4/3rds law. Tseng (2001) noted this and reasoned it was the apparent dispersion that was derived from Lagrangian modes of measurement; hence, the effect of shear flow must be removed to obtain the true turbulent diffusivity.

The coefficients for the lines of best fit between K, K_x, and K_y and the length scales σ, $σ_x$, and $σ_y$ for each of the cluster releases during March 2005 are shown in Table 5.8.

The values derived correlated relatively well with the results obtained from the September deployments. The dispersion coefficient K is described as:

$$K = 0.02\sigma^{1.26}$$
(22)

The confidence interval for these values was significant, with the 95% confidence interval of the exponent equal to ±0.18. Similar values were also determined in the cross-shore and longshore directions. In the cross-shore direction, the dispersion coefficient values are described by the power law with c_1 = 0.02±0.01 and c_2 = 1.23±0.32, and in the longshore domain, c_1 = 0.02±0.01 and c_2 = 1.42±0.17.

Table 5.8: Coefficients of the least squares lines of best fit, calculated for each of the drifter clusters released between the 20th and 23rd of March 2005, based on the values of K calculated for 1 m bins of standard deviation. Data omitted from the calculation of mean and confidence intervals are highlighted.

Date	Run	Drifters	Time (s)	TOTAL C1	TOTAL C2	TOTAL r²	Cross-shore C1	Cross-shore C2	Cross-shore r²	Long-shore C1	Long-shore C2	Long-shore r²
20/03/2005	1	5	1151	0.10	0.33	0.06	0.03	0.70	0.67	0.06	0.78	0.35
	2	5	989	0.03	0.70	0.19	0.02	0.66	0.11	0.02	1.12	0.50
	3	4	3271	0.01	1.27	0.58	0.01	0.60	0.26	0.01	1.43	0.60
	4	5	779	0.10	0.46	0.15	0.10	-0.10	0.01	0.05	0.92	0.55
	5	3	979	0.03	1.25	0.56	0.02	1.42	0.53	0.04	1.29	0.05
	6	4	906	0.03	0.77	0.33	0.06	0.46	0.10	0.03	0.87	0.43
21/03/2005	1	5	1113	0.02	0.56	0.82	0.02	0.79	0.61	0.01	1.19	0.85
	2	5	2994	0.01	1.22	0.73	0.01	1.10	0.70	0.02	1.17	0.65
	3	5	3349	0.02	1.00	0.89	0.04	0.68	0.57	0.02	1.16	0.85
	4	5	1569	0.00	0.75	0.25	0.01	0.63	0.13	0.00	1.74	1.00
22/03/2005	1	5	2033	0.01	1.80	0.74	0.06	-0.20	0.05	0.01	1.73	0.79
	2	5	1443	0.03	1.14	0.42	0.01	1.45	0.62	0.01	1.81	0.68
	3	5	1301	0.45	-0.84	0.29	0.06	0.19	0.03	0.25	-0.44	0.15
	4	5	2976	0.01	1.51	0.52	0.03	0.87	0.33	0.01	1.40	0.59
22/03/2005	1	5	1510	0.03	1.05	0.54	0.02	1.11	0.51	0.01	1.57	0.76
	2	5	1117	0.09	0.75	0.37	0.38	-1.17	0.41	0.07	1.01	0.55
	3	5	642	0.17	0.50	0.13	0.02	0.97	0.38	0.00	1.81	0.09
	4	5	792	0.04	1.02	0.61	0.13	-0.78	0.39	0.02	1.39	0.73
	5	5	776	0.03	0.43	0.09	0.03	0.46	0.14	0.00	2.16	0.73
	6	4	881	0.03	0.79	0.39	0.00	2.08	0.80	0.02	1.24	0.67
	7	5	918	0.07	0.35	0.03	0.06	0.26	0.08	0.01	1.73	0.85
			Mean	0.02	1.26	0.64	0.02	1.23	0.63	0.02	1.42	0.71
			Std Dev	0.01	0.28	0.13	0.01	0.47	0.10	0.02	0.34	0.14
			95% C.I.	0.01	0.18	0.09	0.01	0.32	0.01	0.01	0.17	0.07

Data excuded due to low r²

These values were of the same order of magnitude as the values derived during September, and correlated well with those of Mariani (2005) who performed field work under similar sea breeze dominated conditions. The observed cross-shore dispersion rates were significantly lower during March, which reduced the overall power law exponent. Mariani (2005) noted this and identified a relative enhancement in the longshore power law exponent, which he associated with 'drifters dispersing faster and more consistently' in the longshore direction.

Comparison with Mariani's results was significant, as it demonstrated a similar trend occurring under sea breeze conditions at two different study sites.

While Mariani (2005) was unable to offer an explanation for his 'enhancement' in longshore dispersion observations, the comparison of results from March and September, respectively, offered the insight that the observed deviation was due to restricted cross-shore dispersion rather than enhanced dispersion in the longshore direction.

During the September deployments, the power law exponents describing the relationship between the dispersion coefficient and separation scale were relatively stable in a narrow band between 1.35 and 1.46. In contrast, during March, the power law exponents ranged between 1.23 and 1.42, depending on direction. In particular, the cross-shore exponent decreased from 1.46 to 1.23, thus demonstrating that under sea breeze conditions the longshore dispersion coefficient remained relatively unchanged. This could be attributed to restriction in the turbulent surf zone width, which was promoted by sea breeze action. The sea breeze, through its generation of onshore directed wind waves with relatively large magnitudes (for a low-energy site, sheltered from large ocean swells), increases onshore advection and acts to restrict the offshore extent of turbulence (Bowen and Inman, 1974). Consequently the scale over which dispersion is able to occur in the cross-shore domain is restricted, thus reducing the power law exponent value describing K relative to σ in the cross-shore domain.

5.1.4   Implications

The calculated dispersion rates and the factors influencing them have significant implications for contaminant fate and transport in Adelaide's coastal waters. As discussed previously, the recorded dispersion rates in the nearshore zone were low when compared with more energetic settings, such as the surf zone and the offshore oceanic environment.

This outcome indicated that the dilution of contaminants entering the nearshore zone through the various rivers, storm water, and wastewater discharges along the Adelaide metropolitan coastline occurred at a slow rate. Johnson (2004) noted that there was little understanding of the net flux of material from the surf zone to the immediate offshore region due to horizontal currents, especially on longshore uniform beaches. The results obtained, however, suggested the effective boundary formed by the turbulent surf zone edge and the topographic control imposed by the longshore sandbar formation, combined to constrain the offshore extent over which dispersion of contaminants from the nearshore zone was able to occur. This created a bounded nearshore zone in which dispersion rates were low, and through which little matter was transported in the cross-shore direction. Effectively, any contaminants entering the nearshore zone would remain trapped in this narrow region, with the primary transportation occurring in the longshore direction.

5.2   Drifter Paths and Current Velocity

Extensive qualitative descriptions of the drifter behaviour in the nearshore and surf zones subsequent to release as clusters is included in the Approach section (Section 3.3) of this document. For this reason, the analysis of individual cluster deployments will not be addressed in detail in this section; rather, the focus will be on fundamental variations in drifter behaviour with specific consideration to the factors that instigate the largest variations in drifter velocities and paths.

5.2.1   Direction

Qualitatively, trends in drifter behaviour subsequent to release were highly dependent on prevailing wind conditions. Under prevailing wind conditions with a southerly component, drifters moved in a northerly direction. Conversely, with a northerly component in the prevailing conditions, drifters moved towards the south. Likewise, when winds contained an onshore (westerly) component, shoreward motion was enhanced, while during offshore conditions, drifters were observed to maintain their offshore position and, in some cases, moved offshore. Offshore motion was largely restricted to periods where minimal wave energy was incident on the coast, thus restricting the onshore advection associated with wave action, which tended to suppress the offshore motion induced purely by the prevailing winds.

These general trends are represented in Figure 5.2, where the drifter paths' plots under various prevailing wind conditions are compared. Inset A represents the drifter behaviour subsequent to deployment approximately 50 m offshore while winds from a bearing of ~30° were prevailing. As can be seen in the individual drifters' paths, which were averaged to determine the cluster centroid track, the centroid's motion was almost directly in a southeasterly direction. This could be attributed to the combined influence of the northerly breeze, which promoted the southerly drift, and wave activity noted during the deployment, which encouraged advective onshore transport (Dean and Dalrymple, 2002; Inman et al., 1971).

Inset C of Figure 5.2 represents drifter motion under southerly prevailing conditions. The contrast between Insets A and C is clear, with a directly northwards drifter path tracked during the prevailing southerlies. The cluster was deployed approximately 45 m offshore, and at the time of retrieval the centroid position was approximately 25 m offshore, thus representing a level of onshore transgression during the deployment. Again, the drifter motion's onshore component could be attributed to a wave-generated onshore mass flux. Similarly, insets B and D represent cluster deployments under westerly and easterly prevailing conditions, respectively. The drifters' enhanced onshore motion is evident in B, where the cluster was released approximately 100 m from shore, and the drifters (with the exception of Drifter 6) were washed ashore with only approximately 60 m of longshore transport. In the case of easterly conditions (represented in Inset D), the drifters, which were deployed approximately 35 m offshore, moved northwards, parallel to the coast, before being recovered approximately 60 m offshore. The lack of direct offshore motion under the easterly conditions could be attributed to the topography's constraining effects. The drifters were released in a channel inside a major shore-parallel sandbar, and were observed traveling northwards on the shoreward side of this feature for approximately 100 m before this feature became deeper, resulting in the enhancement of motion in the cross-shore domain. The impact of wave-based factors in this deployment was insignificant, as no wave activity was observed, thus reducing the potential influence of surf zone bounding effects.

These observations were unsurprising given the known relationship between wind speed and direction and surface currents, which was particularly enhanced in the absence of significant external perturbations, such as currents generated from non-locally generated waves (Horikawa (Ed.), 1988). This demonstrated the relationship between the prevailing wind conditions and the nearshore current system's spatial structure, under conditions where wind was the dominant influencing factor.

The drifters' directional behaviour could be compared to the current structure's vertical profile measured by ADCP. Consequently, the influence of changes in the wind and wave regime on the vertical current structure could also be investigated.

ADCP measurements were collected on 21 March 2005 and have been separated into three-hour sections, representing morning and afternoon conditions. The variation in the

deployment conditions is marked, with the respective average wind speed and directions presented in Table 5.9. This shows the dramatic increase in wind speed and change in direction to a southwesterly bearing typical of the sea breeze phenomenon.

Table 5.9: Average wind speed and directions for the ADCP deployment on the 21st of March 2005 (courtesy of the Bureau of Meteorology).

| Time	Speed (m/s)	Direction (°)
9:45-12:45	1.99	331.25
13:30-16:30	6.39	231.43

The associated changes in the current structure are represented in Figures 5.3 and 5.4, which represent the average current profiles in the longshore and cross-shore directions, respectively, under calm morning conditions and during vigorous sea breeze conditions in the afternoon.

The most marked change in the current profiles was observed in the longshore direction (Figure 5.3). During the morning, the wind conditions were relatively calm and from a northerly direction. This induced the weak southerly transport observed in Inset A, where the negative current velocity indicated a southerly direction. Inset A suggested that mixing through the water column was complete, as the entire velocity profile was constant— approximately 0.06 ms^{-1} from the seabed to the surface—except for a small section of flow approximately 1.3 m above the seafloor, which was typified by lower velocities of approximately 0.01–0.02 ms^{-1}.
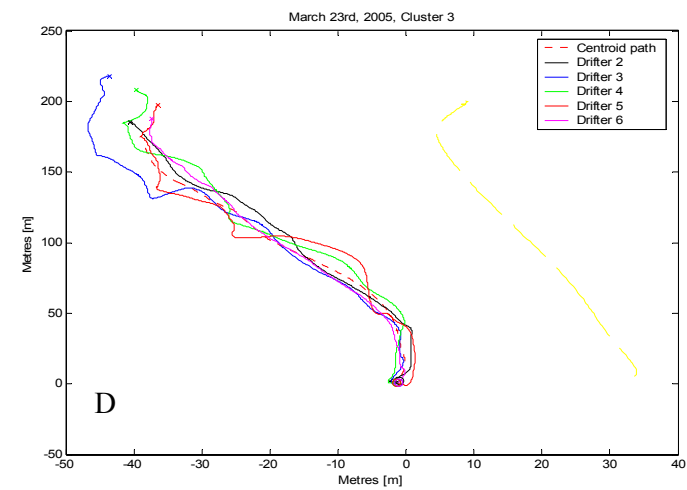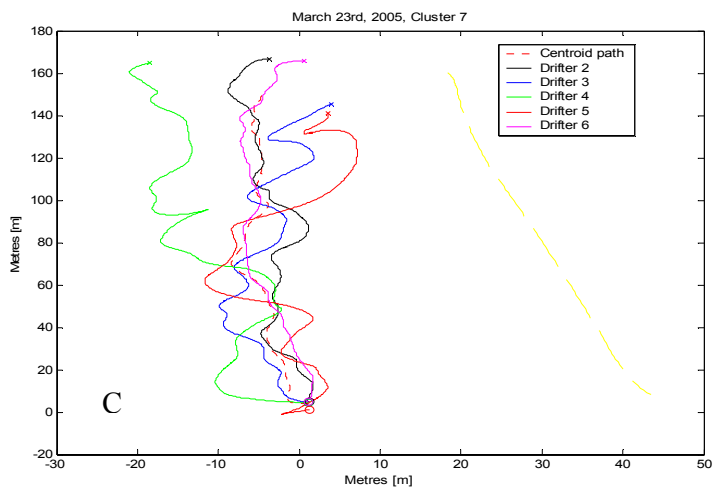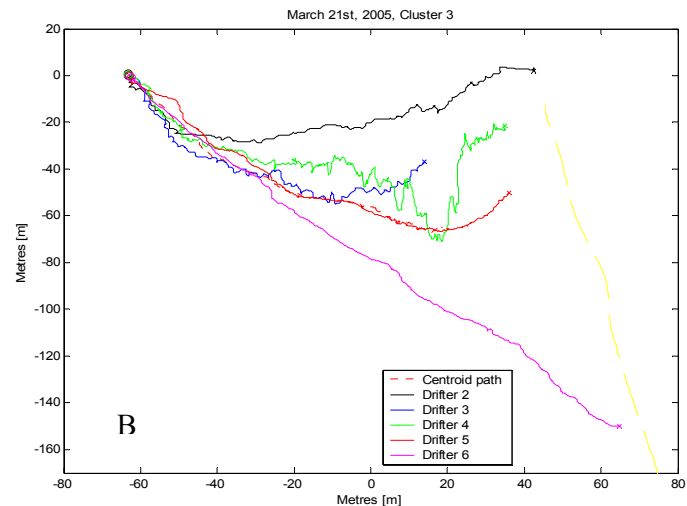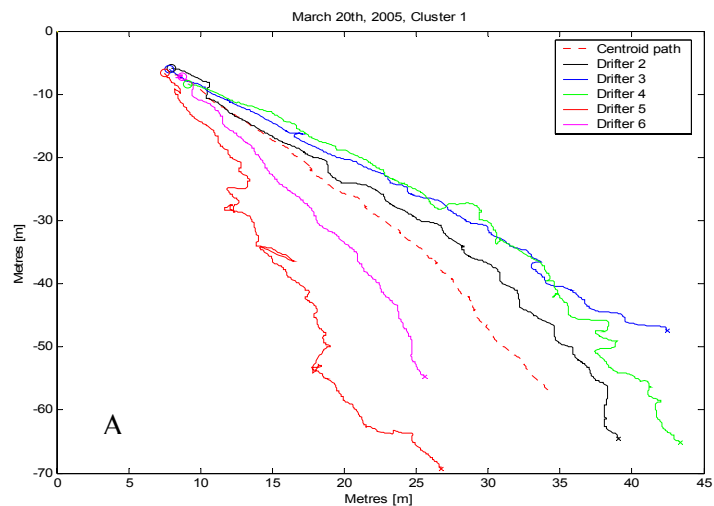
Figure 5.2: Graphical representation of the general trends exhibited in the drifter motion under northerly (A), westerly (B), southerly (C), and easterly (D) prevailing wind conditions.

The velocity profile changed markedly during the afternoon. Wind speeds were observed to increase by a factor of more than three. This increase in velocity was associated with a change in course, such that the direction of approach was southwesterly at a bearing of 230°'s, resulting in obliquely incident conditions along the north-south aligned coastline. Obliquely incident wind and wave conditions are optimal for generating northerly longshore currents (Komar, 1976; Horikawa, 1988; Mariani, 2005). The northerly flowing longshore current was clearly observed in the ADCP data (Inset B), where the surface current in a northerly direction was in the order of 0.10 ms^{-1}. The longshore current's surface enhancement was due to the increased frictional effect of wind close to the surface. In contrast with the morning conditions, the current velocity profile decreased rapidly with depth, showing a slight reversal in direction at the sea floor, and a depth averaged current of just 0.035 ms^{-1} compared with a surface velocity of 0.10 ms^{-1}.
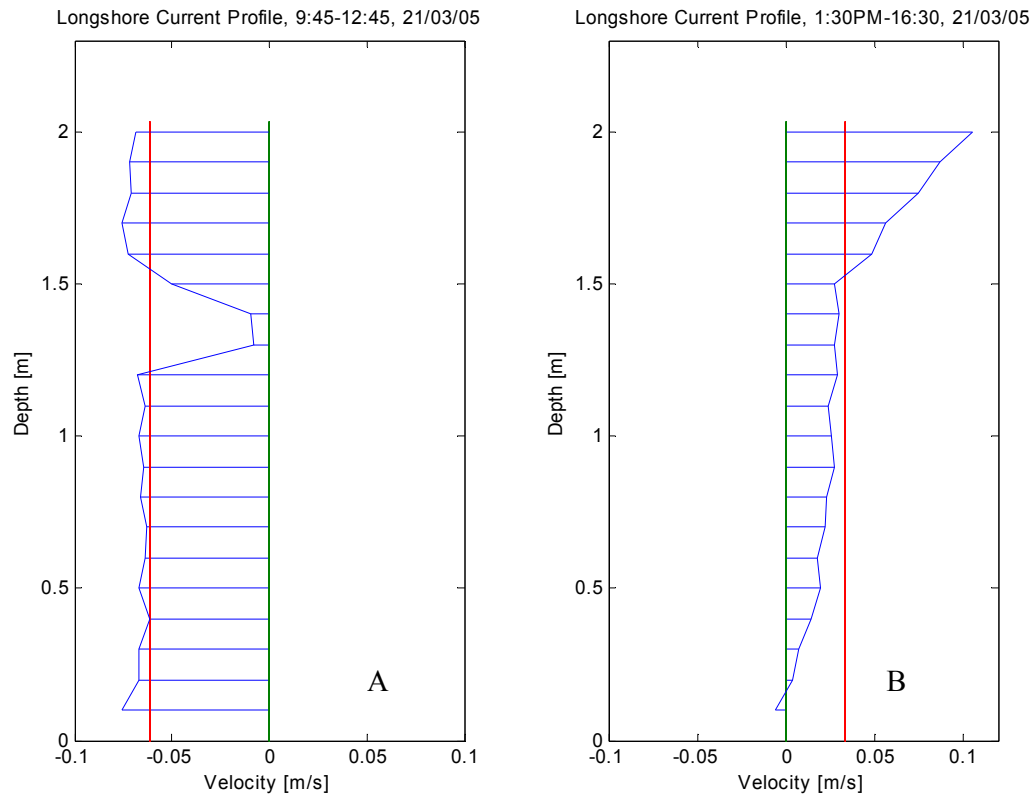

Figure 5.3: Longshore ADCP current profiles from the morning (A) and afternoon (B) of the 21st of March 2005. The green line represents a velocity of 0; the red line indicates the mean depth averaged velocity. The length of the lines indicates the average depth. (Negative velocity indicates southerly currents.)

The current profiles correlated strongly with the observed drifter paths, which followed southerly paths during the morning and were transported in a northerly direction during the afternoon. This was coincidental with the surface currents recorded by the ADCP, which were the dominant factors influencing drifter motion, as the casing's maximum depth was just 0.32 m and the total drogue depth was ~60 cm.

The current profile's cross-shore components also demonstrated significant variability due to their relationship to the prevailing wind and wave regime. During the morning, the observed current profile was offshore (westerly) at an average velocity of ~0.05 ms^{-1} (Figure 5.4—Inset A). This velocity was maintained at a relatively constant rate through the profile; however, a degree of intensification was noted in the center of profile and a slight reduction in velocity

was noted in the surface layers. This reduction in the offshore current in the surface layers might be attributed to the onshore motion of waves and the friction of the prevailing winds' westerly component. During the afternoon (Inset B), the average velocity increased to ~0.07 ms^{-1}, which was attributable to the intensification in observed wind conditions. This induced a greater level of mass transport into the nearshore zone, and hence led to an increase in the offshore directed flow.
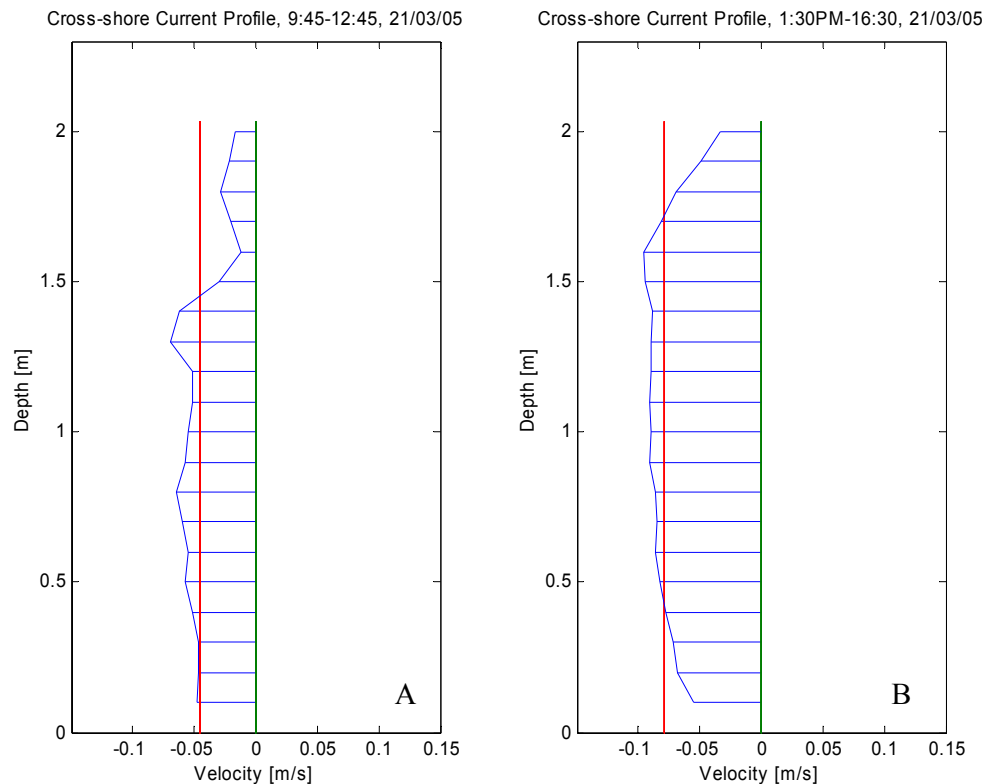
Figure 5.4: Cross-shore ADCP current profiles from the morning (A) and afternoon (B) of the 21st of March 2005. The green line represents a velocity of 0; the red line indicates the mean depth averaged velocity. The length of the lines indicates the average depth. (Negative velocity indicates westerly currents.)

Effectively, the dominant current that was measured in the cross-shore direction was the undertow, the return flow resulting from the onshore advection of mass occurring closer onshore because of breaking waves.

The current velocity profiles obtained in these low-energy conditions differed significantly from those Johnson (2004) obtained near an active, relatively high-energy surf zone. Johnson observed a clear deviation in the cross-shore flow vertical profile, with a large onshore component at velocities in the order of 30 cm/s noted in the water column higher levels, which was associated with the passage of breaking waves. The undertow was not uniformly distributed with depth because of the decrease in wave-induced stress with depth (Dean and Dalrymple, 2002) and was suppressed underneath the energetic onshore flow created by breaking waves. In the low-energy environment, however, the passage of wave bores was restricted to low frequency occurrences with most waves passing the ADCP location without breaking; as such, there was little onshore mass flux through the water column's surface layers and the offshore directed return flow was able to dominate.

5.2.2   Velocity

The velocity of drifter motions recorded in the nearshore zone is presented in Table 5.10. The values were relatively low, with a measured maximum average speed on a single day's deployment of 22 cm/s, and a minimum of 5 cm/s. Maximum momentary velocities were similarly low, with values ranging between 20 cm/s and 62 cm/s. These values illustrated the nearshore current regime's relatively low-energy nature when compared with the velocities obtained in several drifter experiments including:

- Johnson (2004), who found average longshore velocities of greater than 50 cm/s and maximum values in excess of 1.50 ms^{-1};
- Olsson (2004), who found average velocities in nearshore circulative cells located in the lee of coastal structures ranging between 0.44 ms^{-1} and 0.26 ms^{-1} and maximum velocities up to 2 ms^{-1};
- Mariani (2005), who determined longshore velocities ranging between 0.30 ms^{-1} and 1.0 ms^{-1}, depending on the sea breeze strength.

Table 5.10: Average wind and drifter velocities.

		Wind		Current	
				Max	*Mean*
		Speed	*Direction*	*Velocity*	*Velocity*
Date	*Clusters*	*(m/s)*	*(°)*	*(m/s)*	*(m/s)*
1-Sep	5	4.52	228	0.57	0.22
2-Sep	8	2.69	240	0.61	0.13
3-Sep	2	2.05	290	0.36	0.14
20-Mar	6	4.81	235	0.62	0.14
21-Mar	4	3.58	330	0.20	0.05
22-Mar	4	6.55	150	0.41	0.17
23-Mar	7	4.18	135	0.45	0.21

The relatively low magnitude of the nearshore current systems in this study could be attributed to the low incident wave energy at the study site, in contrast to the studies noted above, which were all undertaken at exposed locations on the Western Australian coastline, and reported incident significant swell heights up to 1.51 m (Olsson, 2004). As previously noted, however, the incident swell energy at the sheltered Adelaide study site was low, with the dominant energy source in the nearshore zone being the locally generated short period wind waves. Examination of the data supported this assertion, with a strong correlation observed between the wind speed and direction and the mean current velocities. The correlation was not as strong for the maximum velocities; however, given the momentary nature of these values they could have easily been affected by erratic random motions; as such, they were intended to act only as a guide to the relative magnitude of the largest currents relative to the mean.

The highest velocities were recorded under relatively strong prevailing winds, as demonstrated on 1 September, where the maximum average drifter velocity was recorded during wind speeds in excess of 4.5 ms^{-1}. However, the wind direction was also important, with onshore winds observed leading to larger velocities in the nearshore zone. The largest average wind velocity recorded over the seven day experimental period was 6.55 ms^{-1}; however, as the direction of this breeze was southeasterly, the generation of wind waves incident upon the nearshore zone was limited, and thus a relatively low magnitude nearshore current of 0.17 ms^{-1} was recorded by the drifters. In contrast, the lowest average wind speed recorded, 2.05 ms^{-1}, was associated with an average velocity of 0.14 ms^{-1}—only 0.03 ms^{-1} less than that recorded under the higher wind speed.

The direction of propagation, however, was almost directly onshore, ensuring the maximum level of wave energy was incident upon the shoreline.

The correlation between the ADCP data and the drifter-recorded velocities was relatively strong. The average drifter speed, recorded on 21 September, was just 5 cm/s, which correlated well with the depth averaged velocities recorded by the ADCP. In the cross-shore direction, velocities of 0.05 ms^{-1} were recorded in the morning compared to 0.072 ms^{-1} in the afternoon, while in the longshore direction, the morning depth averaged velocity was 0.057 ms^{-1} compared with 0.037 ms^{-1} in the afternoon. The drifter velocities were averaged over the entire day, aggregating the variations induced by changes in the prevailing conditions; however given the previously noted reduction in the ADCP's recorded surface current velocities, the values appeared highly congruous. Olsson (2004) investigated the level of coherency in the comparison of Lagrangian drifter measurements and Eulerian ADCP data and found the level of similarity was very strong, with a general underestimation in the order of 5% observed in the Eulerian data. Olsson (2004) noted the drifter velocities' high correlation with the Eulerian data could be attributed, in part, to the low water depth, whereby the surface current measured by the drifters did not vary significantly from the mean depth averaged current. This was because in the surf zone's shallow water, given enough time, these currents essentially combined to become a single non-differentiable water body.

It is important to note the significance of the state of the seas' development, as the nearshore current systems' velocity was dependent on the wave action in the nearshore zone. Winds change direction and intensity more rapidly than could be integrated by the wave regime, and hence there was a lag time between the wind speed being recorded and the seas reaching a state of development representative of the conditions. As such, reported current velocities will not always be fully representative of the wind conditions recorded at the same time, which explains some of the seeming contradictions in Table 5.10, where some (20 March) greater wind speeds were associated with current speeds that were lower than those recorded under lower wind speeds (1 September) from the same direction.

5.2.3   Flow Fields

Numerous deployments of the drifters from the same location on 3 September provided data suitable for the construction of a velocity field diagram (Figure 5.5) representing the flow's primary characteristics over a section of the study site. The ensemble plot of all the drifter paths, which were combined in the velocity field, is presented in Inset B. This demonstrates the drifter paths' relatively structured format, with relatively little variation noticeable in the paths of the 35 individual drifter tracks. The flow's general trend was northerly, with a limited offshore component attributable to the south easterly winds prevailing at an average velocity of 4.18 ms^{-1}.

Inset A represents the average velocity of drifters inside spatial bins of 5 m by 10 m dimension. As can be seen, the current regime's spatial pattern was relatively simple, with a clear channel of enhanced flow apparent in a northerly direction. The drifters were initially deployed in approximately 1.5 m water depth, inshore of a large sandbar formation. The drifter paths were observed moving inside of this feature into areas of slightly deeper water while progressing in a northerly direction. As the drifters moved into the channel inside the shore parallel sandbar feature, the average velocities were observed intensifying. This was related to the increased water depth allowing a region of enhanced flow to develop, which was evident in the significantly enhanced drifter velocities within the channel formation.
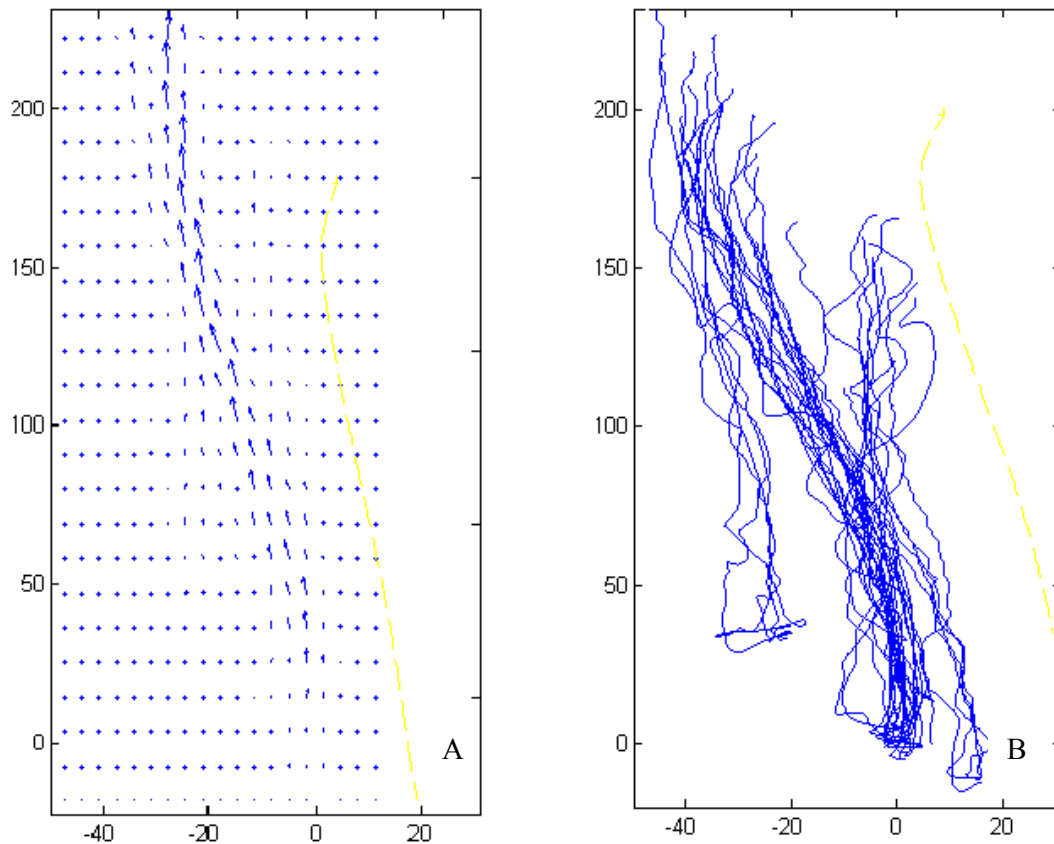
Figure 5.5: Velocity field diagram calculated from the drifter deployments of the 23rd of September. Inset A represents the average velocities and direction for each box on a 5 m by 10 m grid, where a 1 m/s current is equivalent to a distance of 15 m and 'dots' represent point were no velocities were recorded. Inset B represents the ensemble of all the individual drifter paths compiled in the calculation of the velocity field. The units of the vertical and horizontal axes are [m].

The channel flow could be observed closely tracking the shoreline, indicating the region of enhanced flow was a function of depth, thereby maintaining a close correlation with the offshore depth contours. It was evident that the magnitude of the observed flows decreased markedly in either direction cross-shore of the peak flow. In the onshore and offshore directions, respectively, this decrease in velocity could be attributed to the declining water depth firstly, moving towards the shoreline, and secondly, moving offshore, but into the shallower water associated with the elevated sandbar.

The most prevalent feature of the velocity vectors in Figure 5.5 is the longshore component's dominance, indicating the primary direction of drifter motion within the nearshore zone was in the longshore domain. This correlated with the calculated dispersion coefficient values (see Section 5.1), which demonstrated enhanced dispersion in the longshore domain through the effects of shear flow, while cross-shore dispersion was impeded through the bounding effects of topographic and hydrodynamic conditions. Figure 5.5 clearly represents this situation, where the dominant flow conditions were longshore in nature and drifter motion was extremely limited in the cross-shore dimension.

The current system's spatial structure (represented in Figure 5.5) was relatively simple, presenting a system with a relatively stable current regime dominated by a single primary flow feature.

It represents the consistency of the nearshore currents' spatial structure; as such, it could be interpolated that the underlying dispersive properties were similarly uniform for the given conditions. This is a significant result, as it allows the extrapolation of the derived dispersion data to the surrounding Adelaide metropolitan coastline through the demonstrated consistency of current structures over 200 m length within the study area.

6.   Conclusions

Field measurements of nearshore waves offshore Brighton Beach indicated that in the Adelaide coastal waters, the predominant wave direction, for swell and locally generated waves, was from the southwest between 230° and 250°. It also appeared only southwesterly wind had an influence in generating storm waves.

Mixing and dispersion rates in Adelaide coastal waters were measured using Lagrangian drifters. The results indicated that local meteorological conditions predominantly drove the process of turbulent diffusion responsible for dispersion. These conditions directly controlled the wave energy in the Gulf of St Vincent's sheltered waters. As such, the coastal waters' dispersive characteristics generally reflected the prevailing wind regime.

Dispersion rates in the study region were low, resulting in material discharged from terrestrial sources, such as rivers and storm water drains, remaining within the nearshore zone. This was enhanced by the surf zone bounding effects, whereby dispersion in the cross-shore direction was restricted by the presence of barriers in the form of shoreline and the breaker line, and in some cases the presence of an offshore bar. In contrast, transport in the longshore direction was not affected by any substantial boundaries. It could be concluded that materials discharged from terrestrial sources were confined to the nearshore region where limited mixing with offshore waters occurred. The longshore flow was the key factor determining the fate and transport of material discharged into the coastal zone.

References

Abbs, D. J. and Physick, W. L., 1992, 'Sea-breeze observations and modeling: a review', *Australian Meteorological Magazine*, 41, 7–19.

Adelaide Coastal Waters Study, 2004, *Adelaide Coastal Waters Study—Research Summary: Towards informed management of Adelaide's coastal waters*, [online], CSIRO, Available from: http://www.clw.csiro.au/acws/documents/ ACWS_Research_Summary2004.pdf   [3rd December 2004]

Bowen, A. J. and Inman, D. L., 1967, 'Rip currents 2: laboratory and field observations', *Journal of Geophysical* Research, 74, 5479–5490.

Bowles, P., Burns, R. H., Hudswell, F. and Whipple, R. T. P., 1958, 'Exercise mermaid', *UK Atomic Energy Authority, Harwell, Report Number AERE E/R 262,* published HMSO.

Brander, R. W., 1999, 'Field observations on the morphodynamic evolution of a low energy rip current system', *Marine Geology*, 157, 199–217.

Bureau of Meteorology, 2004, *What is the weather usually like: climate averages for Australian sites,* [online], Available from: <http://www.bom.gov.au/climate/averages/tables/cw_023034.shtml> [25th April 2005]

Chelton, D., Hussey, K., Parke, M., 1981, 'Global satellite measurements of water vapour, wind speed and wave height', *Nature*, 294, 529–532.

CSIRO Land and Water, 2004a, *Adelaide Coastal Waters Study*, [online], Available from: <http://www.clw.csiro.au/acws/>, [15th December 2004]

CSIRO Land and Water, 2004b, *Towards Informed Management of Adelaide's Coastal Waters, Adelaide Coastal Waters Study—Research Summary, 2004*, [online], Available from: <http://www.clw.csiro.au/acws/documents/ACWS_Research_Summary2004.pdf> [14th December, 2004]

De Silva Samarasinghe, J. R., Bode, L. and Mason, L. B., 2003, 'Modeled response of Gulf St Vincent (South Australia) to evaporation, heating and winds', *Continental Shelf Research*, Pergamon, 23, 1285–1313.

Dean, R. G. and Dalrymple, R. A., 2002, *Coastal Processes with Engineering Applications*, Cambridge University Press, Cambridge, UK.

Deans, J. and Smith, I., 1999, *Monitoring Sand Management at Glenelg and West Beach Harbours, Adelaide*, [online], Department for Environment and Heritage, South Australia, Available from: http://www.environment.sa.gov.au/coasts/pdfs/sandmgmt.pdf [4th December 2004]

Fischer, H. B., Imberger, J., List, J. E., Koh, R. C. Y. and Brooks, N. H., 1979, *Mixing in Inland and Coastal Waters*, Academic Press, Sydney.

Grzechnik, M., 2000, *Three-Dimensional Tide and Surge Modeling and Layered Particle Tracking Techniques Applied to Southern Australian Coastal Seas*, PhD thesis, Adelaide University.

Hemer, M. and Bye, J., 1999, 'The swell climate of the South Australia sea', *Transactions of the Royal Society of South Australia*, 123(3), 107–113.

Hofmann-Wellnhof, B. H., Lichtenegger, H. and Collin, J., 1997, *Global Positioning System: Theory and Practice*, 4th Ed, Springer-Verlag.

Horikawa, K. (ed), 1988, *Nearshore Dynamics and Coastal Processes*, University of Tokyo Press, Tokyo.

Inman, D. L., Tait, R. J. and Nordstrom, C. E., 1971, 'Mixing in the surf zone', *Journal of Geophysical Research*, 76(15), 3463–2514.

Johnson, D., 2004, *The Spatial and Temporal Variability of Nearshore Currents*, PhD Thesis, The University of Western Australia.

Johnson, D., Stocker, R., Head, R., Imberger, J., Pattiaratchi, C., 2003, 'A compact low-cost GPS drifter for use in the oceanic nearshore zone, lakes and estuaries', *Journal of Atmospheric and Oceanic Technology*, 20, 1880–1884.

Komar, P., 1976, *Beach Processes and Sedimentation*, Prentice Hall, United States.

List, E. J., Gartrell, G. and Winant, C. D., 1990, 'Diffusion and dispersion in coastal waters', *Journal of Hydraulic Engineering*, 116(10), 1158–1179.

Longuet-Higgins, 1970a, 'Longshore currents generated by obliquely incident waves', *Journal of Geophysical Research*, 75(33), 6778–6789.

Masselink, G. and Pattiaratchi, C. B., 1997, 'The effect of sea breeze on beach morphology, surf zone hydrodynamics and sediment resuspension', *Marine Geology*, 146, 115–135.

Munson, B. R., Young, D. F. and Okiishi, T. H., 2002, *Fundamentals of Fluid Mechanics*, John Wiley and Sons Inc, U.S.A.

Okubo, A., 1974, 'Some speculation on oceanic diffusion diagrams', *Rapp. R.-v. Reun. Cons. Int. Explor. Mer,* 167, 77–85.

Olsson, D., 2004, *Field Studies of Rip Currents in the Lee of Coastal Structures*, Engineering Honours Thesis, The University of Western Australia.

Oltman-Shay, J., Howd, P. A. and Birkenmeier, W. A., 1989, 'Shear instabilities of the mean-longshore current, 2. Field observations', *Journal of Geophysical Research*, 94(C12), 18,031–18,042.

Pal, K., Murthy, R., and Thomson, R., 1998, 'Lagrangian measurements in Lake Ontario', *Journal of Great Lakes Research*, 24(3), 681–697.

Pattiaratchi, C., Hegge, B., Gould, J. and Eliot, I., 1997, 'Impact of sea-breeze activity on nearshore and foreshore processes in southwestern Australia', *Continental Shelf Research*, 17(13), 1539–1560.

Pearson, J. M., Guymer, I., West, J. R. and Coates, L. E., 2002, 'Effect of wave height on cross-shore solute mixing', *Journal of Waterway, Port, Coastal and Ocean Engineering*, Jan/Feb 1281(10).

Petrusevics, P., 2004, *Currents in South Australian Shelf and Adjacent Waters*, [online], Available from: <http://www.users.bigpond.com/p.pet/erin/cisasaw1.htm> [17th December 2004].

Proehl, J. A., Lynch, D. R., McGillicuddy, D. J. and Ledwell, J. R., 2005, 'Modeling turbulent dispersion on the north flank of Georges Bank using Lagrangian particle methods', *Continental Shelf Research*, 25(7–8), 875–900.

Provis, D. and Steedman, K., 1985, 'Wave measurements in the Great Australian Bight', Paper presented at Australasian Conference on Coastal and Ocean Engineering, IEAust., Christchurch, NZ.

Recktenwald, G., 2000, *Numerical Methods with MATLAB, Implementation and Application*, Prentice Hall, Sydney.

Richardson, L., 1926, 'Atmospheric diffusion shown on a distance-neighbour graph', *Procceeds of the Royal Society*, A110, 709–727.

Riddle, A. M. and Lewis, R. E., 2000, 'Dispersion experiments in UK coastal waters', *Estuarine, Coastal and Shelf Science*, 51, 243–254.

Rodriguez, A., Sanchez-Arcilla, A., Redondo, J. M., Bahia, E. and Sierra, J. P., 1995, 'Pollutant dispersion in the nearshore region: modeling and measurements', *Water, Science and Technology,* 32(9–10), 169–178.

Sawford, B., 2001, 'Turbulent relative dispersion', *Annual Review of Fluid Mechanics*, 33, 289–317.

Simpson, J. H., Williams, E., Brasseur, L. H. and Brubaker, J. M., 2005, 'The impact of tidal straining on the cycle of turbulence in a partially stratified estuary', *Continental Shelf Research*, 25, 51–64.

South Australia Coastal Protection Board, 2000, *Monitoring Sand Movements along the Adelaide Coastline*, [online], Department for Environment and Heritage, South Australia, Available from: http://www.environment.sa.gov.au/coasts/pdfs/no32.pdf [6th December 2004].

South Australian Coastal Protection Board, 1993[a], *The Adelaide Metropolitan Coastline*, [online], Department for Environment and Heritage, South Australia, Available from: http://www.environment.sa.gov.au/coasts/pdfs/no27.pdf [6th December 2004].

South Australian Coastal Protection Board, 1993[b], *Maintaining the Adelaide Coastline*, [online], Department for Environment and Heritage, South Australia, Available from: <http://www.environment.sa.gov.au/coasts/pdfs/no28.pdf> [6th December 2004].

South Australian Coastal Protection Board, 2004, *The Management of Adelaide Metropolitan Beaches,* [online], Department for Environment and Heritage, South Australia, Available from: http://www.environment.sa.gov.au/coasts/pdfs/metro_beach_review.pdf [6th December 2004].

Svendsen, I. A. and Putrevu, U., 1996, 'Surf-zone hydrodynamics', in *Advances in Coastal and Ocean Engineering*, (ed) Liu, P. L-F., World Scientific, Singapore, pp1–78.

SWAN, 2004, *SWAN Cycle III version 40.31 User Manual*, Delft University of Technology, The Netherlands.

Takewaka, S., Misaki, S. and Nakamura, T., 2003, 'Dye diffusion experiment in a longshore, current field', *Coastal Engineering Journal*, World Scientific Publishing Company and Japan Society of Civil Engineers, 45(3), 471–487.

Tseng, R. S., 2001, 'On the dispersion and diffusion near estuaries and around Islands', *Estuarine Coastal and Shelf Science*, 54, 89–100.

U.S. Army Corps Coastal Engineering Research Center, 2002, *Coastal Engineering Manual,* Department of the Army, Washington D.C.

Verspecht, F., 2002, *Oceanographic Studies around the North West Cape, Western Australia*, Engineering Honours Thesis, The University of Western Australia.

Winant, C. D., 1983, 'Longshore coherence of currents along the southern California Shelf during summer', *Journal of Physical Oceanography*, 13, 54–64.

Xing, J. and Davies, A. M., 2003, 'A model study of tidally induced suspended sediment transport in the Iberian shelf region', *Estuarine, Coastal and Shelf Science*, 58, 321–333.